frontiers | Research Topics

Methods in gynecological oncology

Edited by
Federico Ferrari, Federica Perelli and Bala Audu

Published in
Frontiers in Oncology

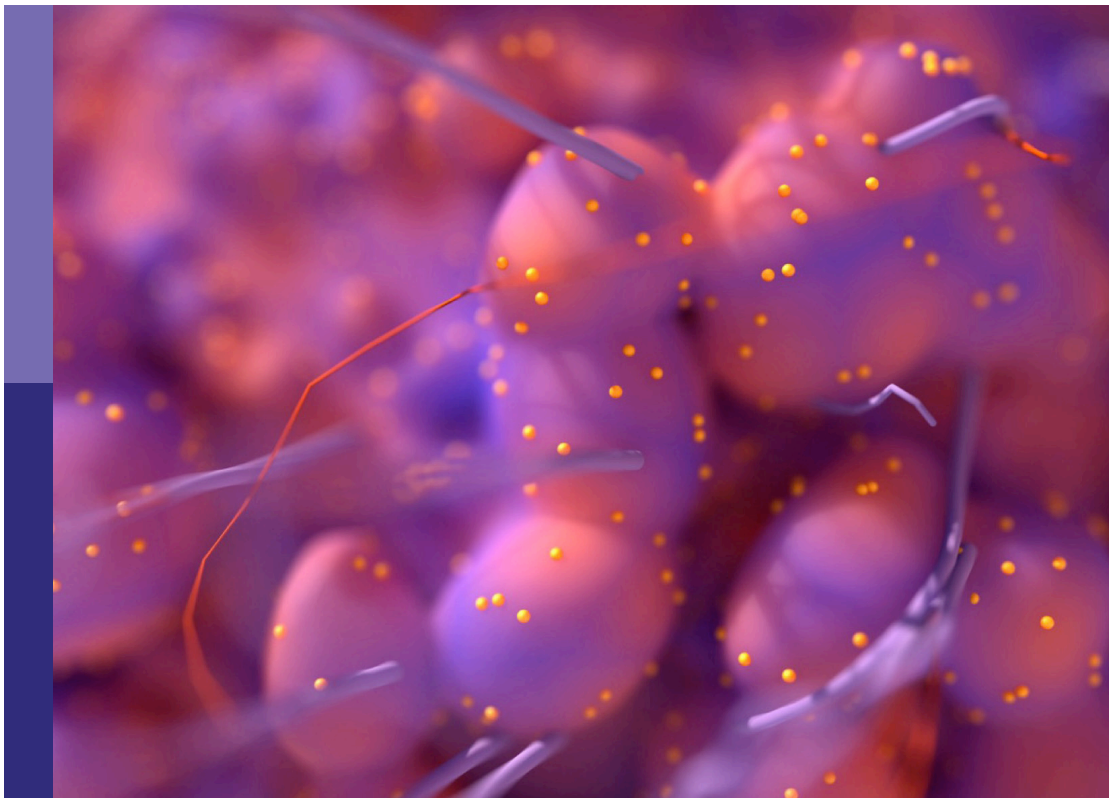

ISSN 1664-8714
ISBN 978-2-83251-993-6
DOI 10.3389/978-2-83251-993-6

About Frontiers

Frontiers is more than just an open access publisher of scholarly articles: it is a pioneering approach to the world of academia, radically improving the way scholarly research is managed. The grand vision of Frontiers is a world where all people have an equal opportunity to seek, share and generate knowledge. Frontiers provides immediate and permanent online open access to all its publications, but this alone is not enough to realize our grand goals.

Frontiers journal series

The Frontiers journal series is a multi-tier and interdisciplinary set of open-access, online journals, promising a paradigm shift from the current review, selection and dissemination processes in academic publishing. All Frontiers journals are driven by researchers for researchers; therefore, they constitute a service to the scholarly community. At the same time, the *Frontiers journal series* operates on a revolutionary invention, the tiered publishing system, initially addressing specific communities of scholars, and gradually climbing up to broader public understanding, thus serving the interests of the lay society, too.

Dedication to quality

Each Frontiers article is a landmark of the highest quality, thanks to genuinely collaborative interactions between authors and review editors, who include some of the world's best academicians. Research must be certified by peers before entering a stream of knowledge that may eventually reach the public - and shape society; therefore, Frontiers only applies the most rigorous and unbiased reviews. Frontiers revolutionizes research publishing by freely delivering the most outstanding research, evaluated with no bias from both the academic and social point of view. By applying the most advanced information technologies, Frontiers is catapulting scholarly publishing into a new generation.

What are Frontiers Research Topics?

Frontiers Research Topics are very popular trademarks of the *Frontiers journals series*: they are collections of at least ten articles, all centered on a particular subject. With their unique mix of varied contributions from Original Research to Review Articles, Frontiers Research Topics unify the most influential researchers, the latest key findings and historical advances in a hot research area.

Find out more on how to host your own Frontiers Research Topic or contribute to one as an author by contacting the Frontiers editorial office: frontiersin.org/about/contact

Methods in gynecological oncology

Topic editors

Federico Ferrari — University of Brescia, Italy

Federica Perelli — Santa Maria Annunziata Hospital, Italy

Bala Audu — University of Maiduguri, Nigeria

Citation

Ferrari, F., Perelli, F., Audu, B., eds. (2023). *Methods in gynecological oncology*. Lausanne: Frontiers Media SA. doi: 10.3389/978-2-83251-993-6

Table of contents

frontiers | Frontiers in Oncology

TYPE Editorial
PUBLISHED 09 March 2023
DOI 10.3389/fonc.2023.1167088

OPEN ACCESS

EDITED AND REVIEWED BY
Sarah M Temkin,
Office of Research on Women's Health,
National Institutes of Health NIH,
United States

*CORRESPONDENCE
Federica Perelli
federica.perelli@gmail.com

SPECIALTY SECTION
This article was submitted to Gynecological Oncology, a section of the journal Frontiers in Oncology

RECEIVED 15 February 2023
ACCEPTED 23 February 2023
PUBLISHED 09 March 2023

CITATION
Perelli F, Mattei A, Scambia G and Cavaliere AF (2023) Editorial: Methods in gynecological oncology.
Front. Oncol. 13:1167088.
doi: 10.3389/fonc.2023.1167088

Editorial: Methods in gynecological oncology

Federica Perelli[1]*, Alberto Mattei[1], Giovanni Scambia[2] and Anna Franca Cavaliere[3]

[1]Azienda USL Toscana Centro, Gynecology and Obstetric Department, Santa Maria Annunziata Hospital, Florence, Italy, [2]Department of Science of Woman, Child and Public Health, Fondazione Policlinico Universitario A. Gemelli IRCCS, Università Cattolica del Sacro Cuore, Rome, Italy, [3]Division of Gynecology and Obstetrics, Fatebenefratelli Isola Tiberina Gemelli Hospital, Rome, Italy

KEYWORDS

gynecological oncology, gynecological cancer, ovarian cancer, endometrial cancer, cervical cancer, vulvar cancer, vaginal cancer

Editorial on the Research Topic
Methods in gynecological oncology

Introduction

Gynecological oncology deals with the 360-degree management of the woman suffering from a neoplasm of the female genital tract. Its research field is oriented towards an improvement of diagnostic, therapeutic and prognostic techniques aimed at improving the survival and quality of life of women affected by gynecological cancers.

The correct staging and prognostic stratification of cancer patients is the basis for tracing an adequate treatment strategy at the same time radical enough to guarantee the cancer safety and minimally invasive to minimize the negative effects on the quality of life of cancer survivors.

This Research Topic aimed at widening the knowledges on the methods used for scientific advancement in the gynecological oncology field. The issue currently includes 9 papers on the diagnosis, prognostic stratification, treatment strategy of gynecological cancers patients. All contributions to this Research Topic focus on one or more of the research areas highlighted above, evidenced below by reference to the designated areas' letters.

The gynecological tumors affect female population with different incidences and features. Data from the National Cancer Institute Surveillance, Epidemiology and End Results Program (NCI SEER) reported that the more frequent gynecological malignancy is represented by uterine cancer with 65950 new cases in 2022 and a 5-year relative survival of 81.3%, followed by ovarian cancer with 19880 new cases in 2022 and a 5-year relative survival of 49.7%, cervical cancer with 14100 new cases in 2022 and a 5-year relative survival of 66.7%, vulvar cancer with 6330 new cases in 2022 and a 5-year relative survival of 70.3% (1). Primary vaginal cancer is very rare, showing a prevalence of approximately 1 in 100,000 women (typically of squamous cell histology) (2).

Ovarian tumors show the worst prognosis between gynecological cancers and they can be divided into epithelial, germ cell or sex cord-stromal tumors based on the type of cell from which they originate. Epithelial ovarian cancer (EOC) can be categorized according to their invasiveness and biological features into borderline or malignant.

Gynecological neuroendocrine tumors are rare, there are no clear guidelines for their clinical management and they can originate from cervical, endometrial and ovarian tissue. Ovarian neuroendocrine tumors account for about 2% of all gynecological tumors and they are divided into carcinoid, small cell neuroendocrine tumor (SCNET), and large cell neuroendocrine tumor (LCNET) (3).

Diagnostic methodology in gynecological oncology

This thematic issue aims to show current advances in diagnosis and screening of gynecologic malignancies.

Xu et al. proposed a radiomics nomogram to distinguish borderline ovarian cancer from malignant epithelial ovarian cancer (EOC). In classifying early-stage type I and type II EOC, the radiomics signature exhibited superior diagnostic performance over the clinical model, based on patient age, menopausal status, CA-125 level, bilaterality, MR-reported pelvic fluid, tumor configuration, and peritoneal involvement. Radiomics has recently emerged as a powerful approach for non-invasively capturing the inter-lesion heterogeneity that can be used to build an objective and accurate decision support systems for cancer patients. The diagnostic efficacy of the nomogram was the same as that of the radiomics model. Xu et al. used imaging features to characterize the properties of adnexal masses with the aim of improving the diagnostic characterization of EOC and providing to tailor specialized treatment plans on different patients. The authors concluded that the radiomics model and combined model had higher benefits than the clinical model to distinguish borderline from EOC.

Concerning diagnostic improvement to better characterize a pelvic mass suspected for malignancy Yang et al. reported a model based on the combination between the marker's value HE4 and the already proposed ADNEX (Assessment of Different NEoplasias in the adneXa) model proposed by Timmerman et al. in the research conducted by the IOTA (International Ovarian Tumor Analysis) (4–6). The authors concluded that the ADNEX model performs excellently to determine the benignity or malignancy of a ovarian tumor, with higher specificity when combined with HE4. This combination can improve the differential diagnosis ability and the sensitivity of an ovarian borderline tumor and a Stage II–IV OC.

Wang et al. reported a case of superficial myofibroblastoma (SMF) of the lower female genital tract, a relatively rare benign mesenchymal tumor, arose in a 71-year-old Chinese female patient with postmenopausal vaginal bleeding. The authors described a diagnostic path based on gynecological examination and colposcopic evaluation, color Doppler flow imaging, magnetic resonance and the final diagnosis by histopathological analysis. For the first time, colposcopy was used for auxiliary diagnosis and evaluation before surgery for SMF and revealed a lesion covered with normal squamous epithelium with a wide pedicle and a mushroom-like appearance.

Prognostic stratification in gynecological oncology

This section aims to underline the importance of prognostic classification of gynecological cancer patients in order to tailor them the more appropriate therapeutic and surveillance programme.

Xu et al. with their radiomics nomogram aimed at differentiate borderline ovarian cancer from malignant EOC identified a tool for imaging-based prognostic stratification of patients affected by ovarian malignancies.

Jiang et al. presented a nomogram based on clinical and non-clinical features that affect the prognosis of patients with cervical cancer to develop an accurate prognostic model that correlate with overall survival and cancer-specific survival. The authors constructed nomograms including the following factors: insurance status, grade, histology, chemotherapy, metastasis number, tumor size, regional node examination, LVSI, and radiation.

Pang et al. conducted a retrospective analysis of data from 469 patients affected by gynecologic LCNET to describe prevalence, survival outcomes, and associated factors with this rare neoplasm. Their analysis revealed that American Joint Committee on Cancer stage, lymph node metastasis, and chemotherapy were independent prognostic factors for overall survival and cancer-specific survival in patients with cervical LCNEC. Lymph node metastasis, surgery, and chemotherapy were independent prognostic factors for overall survival and cancer-specific survival in the ovarian group and for overall survival in the endometrial group. Lymph node metastasis and surgery were also independent prognostic factors for cancer-specific survival in the endometrial group.

Li and Cao developed nomograms to predict progression-free survival and overall survival in patients with ovarian clear cell carcinoma after primary treatment. Their analysis included several features studied on 358 Chinese patients. The most predictive nomogram for progression-free survival considered the following variables: thrombosis, the FIGO staging, residual of the tumor and distant metastasis. The most predictive nomogram for overall survival considered the following variables: thrombosis, lymph node metastasis, residual of the tumor, malignant ascites/washing, and platinum resistance.

Innovative therapeutic strategies in gynecological oncology

This thematic issue aims to propose new treatment strategies for women affected by a neoplasm of the female genital tract.

Pang et al. thanks to their retrospective analysis of data from 469 patients affected by gynecologic LCNET found that surgery alone may help to improve overall survival and cancer-specific survival in patients with early-stage cervical LCNET. In contrast, surgery+chemotherapy and surgery+radiotherapy may help to improve survival in those with early-stage ovarian and endometrial LCNET, respectively. Regardless of subtype, comprehensive treatment involving surgery, chemotherapy, and

radiotherapy should be considered to improve prognosis in patients with advanced-stage gynecologic LCNET.

Restaino et al. reported a brilliant and innovative treatment using human amniotic membrane for myocutaneous dehyscence after a radical surgical treatment for vulvar cancer. The authors described the first case of using human amniotic membrane to promote healing of a surgical wound in a patient with gynecological oncology. The implantation of amniotic membranes on surgical wounds appears to be safe, moreover, the psychological impact of the treatment on the patient was acceptable, with an improvement also in terms of pain.

Wang et al. showed the success of the surgical resection treatment of a patient affected by vaginal SMF.

Li et al. compared the survival outcomes among 590 stage IB3 cervical cancer patients who undergo abdominal radical hysterectomy +pelvic lymphadenectomy ± para-aortic lymph node dissection versus radiochemotherapy. The authors concluded that for FIGO 2018 stage IB3 cervical cancer patients, surgery based on abdominal radical hysterectomy and lymphadenectomy resulted in better overall survival and disease-free survival than radiochemotherapy.

Li et al. reported the successful surgical treatment of an ovarian SCNET patients, alive after two years from surgery who underwent laparoscopic total uterine double attachment resection, bilateral ovarian arteriovenous high ligation, abdominal catheterization and postoperative adjuvant chemotherapy.

Conclusion

In conclusion, this Research Topic provided several investigations focusing on relevant oncological aspects as diagnosis, prognostic stratification and therapeutic strategy of gynecological cancer patients.

Advances in oncological research provide the development of tools for conducting the patient counseling, her postoperative management, and her follow-up to tailor diagnostic, prognostic and therapeutic pathway on each different patient by multidisciplinary approach.

Some other aspects about methods in gynecological oncology should be addressed and deepened in future Research Topic, as the development of minimally invasive surgery techniques, the use of new radio and chemotherapy schemes, the fertility sparing surgical therapeutic pathways in young patients with gynecological cancer.

Author contributions

All authors listed have made a substantial, direct, and intellectual contribution to the work and approved it for publication.

Acknowledgments

We deeply thank all the authors and reviewers who have participated in this Research Topic.

Conflict of interest

The authors declare that the research was conducted in the absence of any commercial or financial relationships that could be construed as a potential conflict of interest.

Publisher's note

References

1. Available at: https://seer.cancer.gov/statfacts/ (Accessed February 15th 2023).

2. Gadducci A, Fabrini MG, Lanfredini N, Sergiampietri C. Squamous cell carcinoma of the vagina: Natural history, treatment modalities and prognostic factors. *Crit Rev Oncol Hematol* (2015) 93(3):211–24. doi: 10.1016/j.critrevonc.2014.09.002

3. Winer I, Kim C, Gehrig P. Neuroendocrine tumors of the gynecologic tract update. *Gynecol Oncol* (2021) 162(1):210–9. doi: 10.1016/j.ygyno.2021.04.039

4. Timmerman D, Planchamp F, Bourne T, Landolfo C, du Bois A, Chiva L, et al. ESGO/ISUOG/IOTA/ESGE consensus statement on preoperative diagnosis of ovarian tumors. *Ultrasound Obstet Gynecol* (2021) 58(1):148–68. doi: 10.1002/uog.23635

5. Timmerman D, Testa AC, Bourne T, Ferrazzi E, Ameye L, Konstantinovic ML, et al. Logistic regression model to distinguish between the benign and malignant adnexal mass before surgery: A multicenter study by the international ovarian tumor analysis group. *J Clin Oncol* (2005) 23(34):8794–801. doi: 10.1200/JCO.2005.01.7632

6. Timmerman D, Van Calster B, Testa A, Savelli L, Fischerova D, Froyman W, et al. Predicting the risk of malignancy in adnexal masses based on the simple rules from the international ovarian tumor analysis group. *Am J Obstet Gynecol* (2016) 214(4):424–37. doi: 10.1016/j.ajog.2016.01.007

frontiers | Frontiers in Oncology

ORIGINAL RESEARCH
published: 06 July 2022
doi: 10.3389/fonc.2022.933755

Survival Outcomes of Patients With Stage IB3 Cervical Cancer Who Undergo Abdominal Radical Hysterectomy Versus Radiochemotherapy

Zhiqiang Li[1‡], Qing Yang[2‡], Jianxin Guo[3‡], Guoqiang Liang[1‡], Hui Duan[1], Shaoguang Wang[4], Min Hao[5], Wentong Liang[6], Donglin Li[6], Xuemei Zhan[7], Qinghuang Xie[8], Jinghe Lang[1,9], Ping Liu[1] and Chunlin Chen[1*†]*

[1] Department of Obstetrics and Gynecology, Nanfang Hospital, Southern Medical University, Guangzhou, China, [2] Department of Obstetrics and Gynecology, Shengjing Hospital of China Medical University, Shenyang, China, [3] Department of Obstetrics and Gynecology, Daping Hospital, Army Medical University, Chongqing, China, [4] Department of Gynecology, Yantai Yuhuangding Hospital, Yantai, China, [5] Department of Gynecology, the Second Hospital of Shanxi Medical University, Taiyuan, China, [6] Department of Obstetrics and Gynecology, Guizhou Provincial People's Hospital, Guizhou, China, [7] Department of Gynecology, Jiangmen Central Hospital, Jiangmen, China, [8] Department of Gynecology, Foshan Women and Children Healthcare Hospital, Foshan, China, [9] Department of Obstetrics and Gynecology, Peking Union Medical College Hospital, Peking Union Medical College, Beijing, China

Objective: This study aimed to compare the survival outcomes among stage IB3 cervical cancer patients who undergo abdominal radical hysterectomy (ARH)+pelvic lymphadenectomy ± para-aortic lymph node dissection versus radiochemotherapy (R-CT).

Methods: Based on the large number of diagnoses and treatments for cervical cancer in the Chinese database, propensity score matching (PSM) was used to compare the 5-year overall survival (OS) and disease-free survival (DFS) rates of the ARH group and R-CT group.

Results: There were 590 patients with stage IB3 cervical cancer according to the FIGO 2018 staging system, with 470 patients in the ARH group and 120 patients in the R-CT group. The ARH and R-CT groups showed different 5-year OS and DFS rates in the total study population, and the 5-year OS and DFS rates in the R-CT group (n = 120) were lower than those in the ARH group (n = 470) (OS: 78.1% vs. 92.1%, $p < 0.001$; DFS: 71.6% vs. 90.3%, $p < 0.001$). R-CT was associated with a worse 5-year OS rate (hazard ratio [HR] = 3.401; 95% confidence interval [CI] = 1.875–6.167; $p < 0.001$) and DFS rate (HR = 3.440; 95% CI = 2.075–5.703; $p < 0.001$) by Cox multivariate analysis. After 1:3 PSM, the 5-year OS and DFS rates in the R-CT group (n = 108) were lower than those in the RH group (n = 280) (OS: 76.4% vs. 94.0%, $p < 0.001$; DFS: 69.3% vs. 92.6%, $p < 0.001$, respectively). R-CT was associated with a worse 5-year OS rate (HR = 4.071; 95% CI = 2.042–8.117; $p < 0.001$) and DFS rate (HR = 4.450; 95% CI = 2.441–8.113; $p < 0.001$) by Cox multivariate analysis.

OPEN ACCESS

Edited by:
Federica Perelli,
Santa Maria Annunziata Hospital, Italy

Reviewed by:
Carlo Ronsini,
Università degli Studi della Campania Luigi Vanvitelli
Italy
Abdelbaset Mohamed Elasbali,
Al Jouf University, Saudi Arabia

***Correspondence:**
Ping Liu
lpivy@126.com
Chunlin Chen
ccl1@smu.edu.cn

†ORCID:
Chunlin Chen
orcid.org/0000-0002-1708-3047

‡These authors have contributed equally to this work and share first authorship

Specialty section:
This article was submitted to Gynecological Oncology, a section of the journal Frontiers in Oncology

Received: 01 May 2022
Accepted: 31 May 2022
Published: 06 July 2022

Citation:
Li Z, Yang Q, Guo J, Liang G, Duan H, Wang S, Hao M, Liang W, Li D, Zhan X, Xie Q, Lang J, Liu P and Chen C (2022) Survival Outcomes of Patients With Stage IB3 Cervical Cancer Who Undergo Abdominal Radical Hysterectomy Versus Radiochemotherapy. Front. Oncol. 12:933755. doi: 10.3389/fonc.2022.933755

Conclusion: Our study found that for FIGO 2018 stage IB3 cervical cancer patients, ARH resulted in better OS and DFS than R-CT.

Keywords: cervical cancer, abdominal radical hysterectomy, radiochemotherapy, overall survival, disease-free survival, stage IB3 cervical cancer

INTRODUCTION

Cervical cancer is a common malignant tumor of the female genital tract and the fourth leading cause of cancer death among women worldwide, especially in developing countries (1). In 2018, FIGO updated their clinical classification system. The following main changes were incorporated: the use of any imaging modality and/or pathological findings for judging the stage. For stage IB disease, the width of the lesion is no longer taken into consideration. Stage IB now includes three subgroups based on tumor size increases of 2 cm: stage IB1 (≤2 cm), stage IB2 (>2 to ≤4 cm) and stage IB3 (>4 cm). The most relevant modification was the introduction of the lymph node (LN) status; indeed, LN involvement (*via* histological or radiological assessment) was specifically designated as stage IIIC disease (IIIC1 pelvic LN metastasis and IIIC2 para-aortic LN metastasis) (1, 2). As a result, a new problem has arisen—that is, whether stage IB2 treatment recommendations based on the old staging system are still suitable based on the new staging system. Based on the clinical diagnoses and treatments for cervical cancer in the Chinese (Four C) database, this paper compared ARH versus R-CT for stage IB3 cervical cancer patients based on the new FIGO 2018 staging system and explored appropriate treatment strategies for this patient population.

MATERIALS AND METHODS

Data Source

The establishment of the cervical cancer database was reviewed by the Ethics Committee of Nanfang Hospital, Southern Medical University (ethics number NFEC-2017-135), and written informed consent was waived by the ethics committee. The clinical trial identifier is CHiCTR1800017778 (International Clinical Trials Registry Platform Search Port, http://apps.who.int/trialsearch/). For the data collection methods and database establishment methods, please refer to the previously published articles by our team (3–7). General patient clinical data, surgery-related data, pathological information, and 315 other parameters were used for the standardized training of gynecologists and by the participating units after training for prognostic follow-up. Follow-up was mainly carried out *via* outpatient and telephone follow-up, and survival, recurrence, and other information were recorded. From 2004 to 2018, 63,926 cases of cervical cancer were collected across 47 hospitals in China.

Inclusion and Exclusion Criteria

In this study, the inclusion and exclusion criteria were as follows.

ARH with postoperative standard therapy group (ARH group) (1): aged ≥ 18 years old (2); FIGO (2018) stage IB3 (3); histological type of squamous cell carcinoma, adenocarcinoma, or adenosquamous carcinoma (4); primary treatment with open surgery (5); no use of neoadjuvant therapy (6); QM-B or QM-C hysterectomy + pelvic lymphadenectomy ± para-aortic lymph node resection; and (7) postoperative standard adjuvant treatment according to the pathological factors described by the guidelines.

R-CT group (1): aged ≥ 18 years old (2); FIGO (2018) stage IB3 (3); histological type of squamous cell carcinoma, adenocarcinoma, or adenosquamous carcinoma (4); primary treatment with R-CT; and (5) a radiotherapy dose ≥ 45 Gy.

The exclusion criteria were as follows (1): patients who did not meet the above inclusion criteria and (2) pregnant patients with cervical cancer, and patients with the accidental discovery of cervical cancer, stump cancer, or other types of malignant tumors.

Observation Indicators

The observation endpoints were overall survival (OS) and disease-free survival (DFS), and the cutoff point for long-term oncological outcomes was 5 years. OS was defined as the date of diagnosis until death from any cause or the last effective follow-up, and DFS was defined as the date of diagnosis until death, recurrence, or the last effective follow-up.

Statistical Methods

SPSS software (Version 22.0, SPSS Inc., Chicago, IL, USA) was used for statistical analysis, and the PSM extension of SPSS 22.0 software was used to perform propensity score matching (PSM). Measurement data are expressed as the mean ± standard deviation, and an independent sample t test was used for comparisons between groups. Count data are expressed as percentages (%), and the chi-square test was used to compare intergroup rates. Kaplan–Meier curves were drawn to analyze survival, and log-rank tests were used to compare differences in the survival curves. Multivariate Cox regression was used to analyze and determine the independent risk factors, relevant risks, and confidence intervals. In this study, $p < 0.05$ was considered statistically significant.

RESULTS

Case Screening Results

A total of 590 patients met the inclusion and exclusion criteria (470 in the RH group and 120 in the R-CT group) (**Figure 1**).

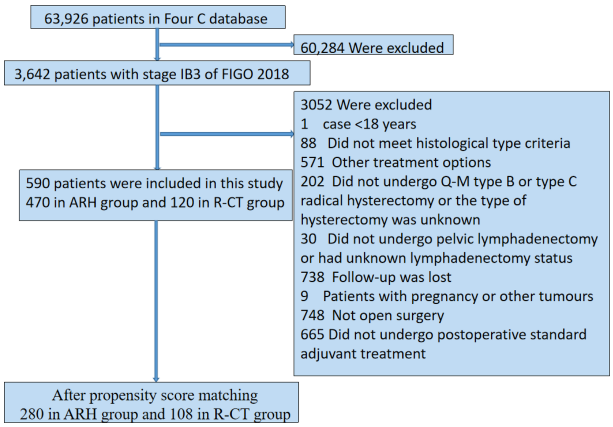

FIGURE 1 | Flow diagram of recruitment and exclusions. ARH, abdominal radical hysterectomy; R-CT, radio-chemotherapy.

Oncological Outcome Comparison of the ARH Group and the R-CT Group Before and After Matching

A total of 590 patients met the entry criteria: 470 were included in the ARH group, and 120 were included in the R-CT group. Baseline analysis showed that there were differences in the baseline parameter of age between the two groups (**Table 1**). Patients in the ARH group (47.11 ± 8.294 years) were younger than those in the R-CT group (50.54 ± 10.855 years) ($p < 0.001$). The baseline distribution of histological type and age was not balanced among the 590 patients who were included. To reduce the influence of confounding factors, we performed 1:3 PSM and then performed a survival analysis. After 1:3 PSM, 280 patients were included in the ARH group, and 108 patients were included in the R-CT group. The baseline analysis between the two groups was not statistically significant ($p > 0.05$) (**Table 1**). Among the total study population, the difference in survival outcomes was statistically significant between the ARH group (n = 470) and the R-CT group (n = 120) (OS 92.1% vs. 78.1%, $p < 0.001$; DFS 90.3% vs. 71.6%, $p < 0.001$) (**Figure 2**). Cox multivariate analysis indicated that the risk of death in the R-CT group was higher than that in the ARH group; for the R-CT group, the 5-year OS and DFS outcomes were independent risk factors (OS: HR = 3.401; 95% CI, 1.875–6.167; p = 0.001; HR = 3.440; 95% CI,

TABLE 1 | Data of the ARH group and R-CT group patients before and after matching.

Variables	Unmatched			Matched		
	ARH (n = 470)	R-CT (n = 120)	p-value	ARH (n = 280)	R-CT (n = 108)	p-value
Age (years)	47.11 ± 8.294	50.54 ± 10.855	<0.001	48.10 ± 8.003	48.59 ± 8.715	0.410
Histological type			0.142			0.838
Squamous cell carcinoma	411 (87.5%)	112 (93.4%)		258 (92.2%)	101 (93.5%)	
Adenocarcinoma	42 (8.9%)	7 (5.8%)		20 (7.1%)	6 (5.6%)	
adenosquamous carcinoma	17 (3.6%)	1 (0.8%)		2 (0.7%)	1 (0.9%)	

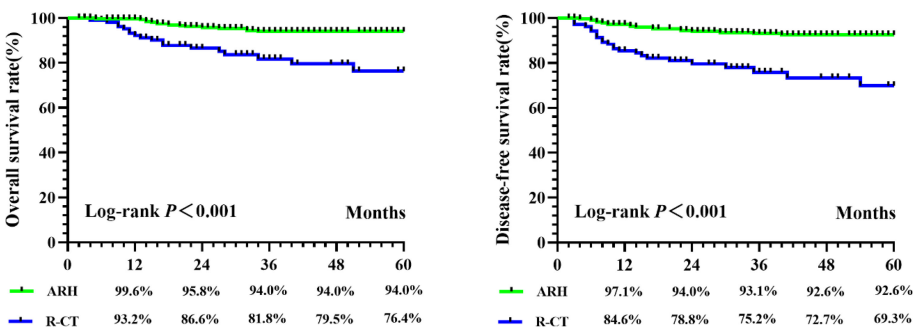

FIGURE 2 | The 5-year OS and DFS in ARH group and R-CT group before PSM.

TABLE 2 | COX Multivariate analysis of the overall study population according to group.

Variables	5-year OS				5-year OS			
Before matching	**p**	**HR**	**95% CI%**		**p**	**HR**	**95% CI**	
ARH group vs. R-CT group	<0.001	3.401	1.875	6.167	<0.001	3.710	2.219	6.204
Age	0.030	0.965	0.934	0.996	0.041	0.971	0.944	0.999
Histological type								
Squamous cell carcinoma	0.030				0.058			
Adenocarcinoma	0.948	1.040	0.320	3.385	0.310	1.554	0.663	3.641
Adenosquamous carcinoma	0.008	4.090	1.439	11.626	0.025	3.244	1.160	9.070

2.075–5.703, p < 0.001) **(Table 2)**. After 1:3 PSM, survival analysis showed that the 5-year OS and 5-year DFS in the ARH group were higher than those in the R-CT group (OS: 94.0% vs. 76.4%, p < 0.001; DFS: 92.6% vs. 69.3%, p < 0.001) **(Figure 3)**. Cox multivariate analysis indicated that for the R-CT group, the 5-year OS and DFS outcomes were independent risk factors (OS: HR = 4.071, 95% CI: 2.042–8.117, p < 0.001; DFS: HR = 4.450, 95% CI: 2.441–8.113, p < 0.001) **(Table 3)**.

DISCUSSION

The NCCN guidelines for stage IB3 cervical cancer recommend the first-choice treatment of concurrent radiotherapy and chemotherapy (evidence level 1) and the secondary-choice treatment of extensive hysterectomy PL ± PAL (evidence level 2B) (8, 9). Some controversy remains regarding neoadjuvant chemotherapy, and conflicting findings have been reported. The NCCN guidelines do not recommend neoadjuvant chemotherapy for cervical cancer (10) The FIGO guidelines also recommend that neoadjuvant chemotherapy be used only in areas lacking radiotherapy equipment and in clinical trials. Our study shows that patients with stage IB3 cervical cancer (FIGO 2018) treated with radical hysterectomy have good survival outcomes. Based on a sufficiently large sample size, long-term effective follow-up, and strict control of bias through tendency score matching in the analysis process, the analysis of this study has high credibility.

Although there are no studies discussing the survival outcomes of ARH versus R-CT in patients diagnosed based on the new 2018 FIGO stage IB3 classification system, previous research on patients diagnosed based on the 2009 FIGO stage IB2

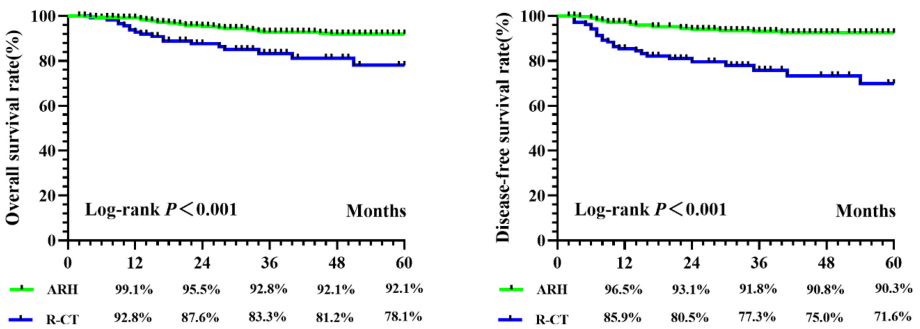

FIGURE 3 | The 5-year OS and DFS in ARH group and R-CT group after PSM.

TABLE 3 | COX multifactor analysis of matched patients.

Variables	5-year OS				5-yearDFS			
After matching	**p-value**	**HR**	**95% CI**		**p-value**	**HR**	**95% CI**	
ARH group vs. R-CT group	<0.001	4.071	2.042	8.117	<0.001	4.450	2.441	8.113
Age	0.005	0.940	0.900	0.982	0.035	0.951	0.925	0.997
Histological type								
Squamous cell carcinoma	0.090				0.159			
Adenocarcinoma	0.514	1.623	0.379	6.950	0.185	2.025	0.713	5.754
Adenosquamous carcinoma	0.032	9.317	1.205	72.049	0.140	4.541	0.609	23.876

classification system also has reference value. Stage IB2 (>4 cm) in the original staging system was changed to stage IB3 (>4 cm) in the 2018 system and did not include lymph node metastasis (11). Previous studies have shown that the 5-year OS rate of patients classified as having FIGO 2009 stage IB2 disease after ARH was 72% to 72.8% (12). The Melissa Bradbury study found that the OS rate of women with stage IB2 disease who underwent ARH during the 2009 FIGO staging period was higher than that of women who underwent R-CT (74.6%:60.0%, p = 0.05), which is consistent with the results of this study to some extent (13). The 5-year OS of patients with stage IB3 disease in this study was higher than that of patients with stage IB2 based on the previous (2009) staging system, which may explain the elimination of lymph node metastasis in the new staging system (14).

Considering time and economic costs, direct radical hysterectomy is preferred for FIGO 2018 stage IB3 disease, offering a new direction for the treatment of this patient population. Rocconi's cost–benefit analysis of the treatment of 2009 FIGO stage IB2 cervical cancer showed that, compared with primary radiotherapy or neoadjuvant chemotherapy, early radical hysterectomy is the most cost-effective strategy, followed by radical hysterectomy and adjuvant radiotherapy and chemotherapy (15). The current study also provides evidence to support this finding.

Compared with previous research reports and articles on the treatment of cervical cancer, this study has some advantages, but there is still a lack of international literature on treatment strategies for patients with FIGO 2018 stage IB3 disease. First, this is one of a few large, international real-world cervical cancer studies, contributing to a more complete clinical diagnosis and treatment database for cervical cancer. Second, due to the sufficient number of included patients, cervical cancer at each stage could be analyzed from many angles, levels, and directions. Third, we used the PSM method to balance baseline differences on the basis of real-world research methods, making the results more accurate. Fourth, only open-surgery cases were included because the LACC study found that laparoscopic surgery had worse oncological outcomes than open surgery (16), for possible reasons including tumor spillage, CO_2 circulation of tumor cells, and other factors (17). Our study was one of the first population-based studies to compare the 5-year OS and DFS rates between ARH and R-CT in stage IB3 cervical cancer patients. A strength of the present study was its large sample size. Our study analyzed a large cohort of cervical cancer patients across 47 hospitals over a 14-year period. This study may be the first to discuss the survival outcomes of FIGO 2018 stage IB3 cervical cancer patients who undergo ARH and R-CT.

However, our research inevitably has some limitations. First, this is a retrospective study that may have confounding factors and bias; for example, patients in the R-CT group were older than those in the ARH group. However, we tried to balance these differences by PSM. Second, although this study comprised 590 hospitalized patients with cervical cancer in China, it did not fully cover all regions of China; however, the database is still representative of the diagnoses and treatments of cervical cancer patients in China. Third, this study did not take into account preoperative cervical conization, which has been found to affect oncological outcomes (18).

In summary, the 5-year OS and DFS rates of patients with stage IB3 cervical cancer, according to the FIGO 2018 classification system, who underwent ARH were superior to those of patients who underwent R-CT, indicating that ARH may offer better oncologic outcomes to patients with cervical cancer. This finding is different from the radiotherapy recommendations described in the NCCN guidelines. More prospective clinical studies are needed to confirm the optimal treatment strategy for patients with FIGO 2018 stage IB3 cervical cancer.

DATA AVAILABILITY STATEMENT

The original contributions presented in the study are included in the article/supplementary material. Further inquiries can be directed to the corresponding authors.

ETHICS STATEMENT

This study was approved by the Ethics Committee of Nanfang Hospital affiliated with Southern Medical University (Guangzhou, China) (ethical number: NFEC-2017-135). Written informed consent for participation was not required for this study in accordance with the national legislation and the institutional requirements.

AUTHOR CONTRIBUTIONS

(I) Conception and design: CC, PL, JL; (II) administrative support: CC, PL; (III) provision of study materials or patients: XZ, DL, WL, MH, SW, HD, JL, PL, CC; (IV) collection and assembly of data: GL, JG, QY, ZL; (V) data analysis and interpretation: GL, ZL, QY, JG; (VI) manuscript writing: all authors. All authors contributed to the article and approved the submitted version.

FUNDING

This study received funding from the National Science and Technology Support Program of China (2014BAI05B03), the National Natural Science Fund of Guangdong (2015A030311024), and the Science and Technology Plan of Guangzhou (158100075).

ACKNOWLEDGMENTS

We thank Min Hao (The Second Hospital of ShanXi Medical University), Bin Ling (China-Japan Friendship Hospital), Lixin Sun and Hongwei Zhao (Shanxi Cancer Hospital), Jihong Liu

and Lizhi Liang (Sun Yat-sen University Cancer Center), Lihong Lin and Yu Guo (Anyang Tumor Hospital), Li Wang (The Affiliated Tumor Hospital of Zhengzhou University), Weidong Zhao (Anhui Provincial Cancer Hospital), Yan Ni (The Yuncheng Central Hospital of Shanxi Province), Wentong Liang and Donglin Li (Guizhou Provincial People`s Hospital), Xuemei Zhan and Mingwei Li (Jiangmen Central Hospital), Weifeng Zhang (Ningbo Women & Children's Hospital), Peiyan Du (The Affiliated Cancer Hospital and Institute of Guangzhou Medical University), Ziyu Fang (Liuzhou Workers' Hospital), Rui Yang (Shenzhen Hospital of Peking University), Long Chen (Qingdao Municipal Hospital), Encheng Dai and Ruilei Liu (Linyi People's Hospital), Yuanli He and Mubiao Liu (Zhujiang Hospital, Southern Medical University), Jilong Yao and Zhihua Liu (Shenzhen Maternity & Child Health Hospital), Xueqin Wang (The Fifth Affiliated Hospital of Southern Medical University), Anwei Lu (Maternal and Child Health Hospital of Guiyang Province), Shuangling Jin (Peace Hospital affiliated to Changzhi Medical College), Ben Ma (Guangzhou First People's Hospital), Zhonghai Wang (Shenzhen Nanshan People's Hospital), Lin Zhu (The Second Hospital of Shandong University), Hongxin Pan (The Third Affiliated Hospital of Shenzhen University), Qianyong Zhu (No. 153. Center Hospital of Liberation Army/Hospital No. 988 of the Chinese People's Liberation Army Joint Support Force), Dingyuan Zeng and Zhong Lin (Maternal and Child Health Care Hospital of Liuzhou), Xiaohong Wang (Laiwu People's Hospital/Jinan City People's Hospital), and Bin Zhu (The Affiliated Yiwu Women and Children Hospital of Hangzhou Medical College) for their contributions during the data collection.

REFERENCES

1. Bhatla N, Berek JS, Cuello Fredes M, Denny LA, Grenman S, Karunaratne K, et al. Revised FIGO Staging for Carcinoma of the Cervix Uteri. *Int J Gynecol Obstet* (2019) 145:129–35. doi: 10.1002/ijgo.12749
2. Bhatla N, Aoki D, Sharma DN, Sankaranarayanan R. Cancer of the Cervix Uteri. *Int J Gynecol Obstet* (2018) 143:22–36. doi: 10.1002/ijgo.12611
3. Liu P, Lin L, Kong Y, Huo Z, Zhu L, Bin X, et al. Comparison of Survival Outcomes Between Radio-Chemotherapy and Radical Hysterectomy With Postoperative Standard Therapy in Patients With Stage IB1 to IIA2 Cervical Cancer: Long-Term Oncological Outcome Analysis in 37 Chinese Hospitals. *BMC Cancer* (2020) 20:1–10. doi: 10.1186/s12885-020-6651-8
4. Zhang W, Chen C, Liu P, Li W, Hao M, Zhao W, et al. Staging Early Cervical Cancer in China: Data From a Multicenter Collaborative. *Int J Gynecol Cancer* (2019) 29:869–73. doi: 10.1136/ijgc-2019-000263
5. Zhang X, Li Z-Q, Sun L, Liu P, Li Z-H, Li P, et al. Cohort Profile: Chinese Cervical Cancer Clinical Study. *Front Oncol* (2021) 11:690275. doi: 10.3389/fonc.2021.690275
6. Zhang W, Chen C, Liu P, Li W, Hao M, Zhao W, et al. Impact of Pelvic MRI in Routine Clinical Practice on Staging of IB1-IIA2 Cervical Cancer. *Cancer Manag Res* (2019) 11:3603–9. doi: 10.2147/CMAR.S197496
7. Chen C, Wang W, Liu P, Li P, Wang L, Jin S, et al. Survival After Abdominal Q-M Type B Versus C2 Radical Hysterectomy for Early-Stage Cervical Cancer. *Cancer Manag Res* (2019) 11:10909–19. doi: 10.2147/CMAR.S220212
8. Abu-Rustum NR, Yashar CM, Bean S, Bradley K, Campos SM, Chon HS, et al. Cervical Cancer, Version 1.2020 Featured Updates to the NCCN Guidelines. *JNCCN J Natl Compr Cancer Netw* (2020) 18:660–6. doi: 10.6004/jnccn.2020.0027
9. Chen H, Liang C, Zhang L, Huang S, Wu X. Clinical Efficacy of Modified Preoperative Neoadjuvant Chemotherapy in the Treatment of Locally Advanced (Stage IB2 to IIB) Ervical Ancer: Randomized Study. *Gynecol Oncol* (2008) 110:308–15. doi: 10.1016/j.ygyno.2008.05.026
10. Katsumata N, Yoshikawa H, Kobayashi H, Saito T, Kuzuya K, Nakanishi T, et al. Phase III Randomised Controlled Trial of Neoadjuvant Chemotherapy Plus Radical Surgery vs Radical Surgery Alone for Stages IB2, IIA2, and IIB Cervical Cancer: A Japan Clinical Oncology Group Trial (JCOG 0102). *Br J Cancer* (2013) 108:1957–63. doi: 10.1038/bjc.2013.179
11. Havrilesky LJ, Leath CA, Huh W, Calingaert B, Bentley RC, Soper JT, et al. Radical Hysterectomy and Pelvic Lymphadenectomy for Stage IB2 Cervical Cancer. *Gynecol Oncol* (2004) 93:429–34. doi: 10.1016/j.ygyno.2004.01.038
12. Gadducci A, Sartori E, Maggino T, Zola P, Cosio S, Zizioli V, et al. Pathological Response on Surgical Samples Is an Independent Prognostic Variable for Patients With Stage Ib2-IIb Cervical Cancer Treated With Neoadjuvant Chemotherapy and Radical Hysterectomy: An Italian Multicenter Retrospective Study (CTF Study). *Gynecol Oncol* (2013) 131:640–4. doi: 10.1016/j.ygyno.2013.09.029
13. Bradbury M, Founta C, Taylor W, Kucukmetin A, Naik R, Ang C. Pathological Risk Factors and Outcomes in Women With Stage Ib2 Cervical Cancer Treated With Primary Radical Surgery Versus Chemoradiotherapy. *Int J Gynecol Cancer* (2015) 25:1476–83. doi: 10.1097/IGC.0000000000000513
14. Finan MA, DeCesare S, Fiorica JV, Chambers R, Hoffman MS, Kline RC, et al. Radical Hysterectomy for Stage IB1 vs IB2 Carcinoma of the Cervix: Does the New Staging System Predict Morbidity and Survival? *Gynecol Oncol* (1996) 62:139–47. doi: 10.1006/gyno.1996.0206
15. Rocconi RP, Estes JM, Leath CA, Kilgore LC, Huh WK, Straughn JM. Management Strategies for Stage IB2 Cervical Cancer: A Cost-Effectiveness Analysis. *Gynecol Oncol* (2005) 97:387–94. doi: 10.1016/j.ygyno.2005.01.028
16. Ramirez PT, Frumovitz M, Pareja R, Lopez A, Vieira M, Ribeiro R, et al. Minimally Invasive Versus Abdominal Radical Hysterectomy for Cervical Cancer. *N Engl J Med* (2018) 379:1895–904. doi: 10.1056/NEJMoa1806395
17. Ronsini C, Köhler C, De Franciscis P, La Verde M, Mosca L, Solazzo MC, et al. Laparo-Assisted Vaginal Radical Hysterectomy as a Safe Option for Minimal Invasive Surgery in Early Stage Cervical Cancer: A Systematic Review and Meta-Analysis. *Gynecol Oncol* (2022) 166:188–95. doi: 10.1016/j.ygyno.2022.04.010
18. Bizzarri N, Pedone Anchora L, Kucukmetin A, Ratnavelu N, Korompelis P, Carbone V, et al. Protective Role of Conization Before Radical Hysterectomy in Early-Stage Cervical Cancer: A Propensity-Score Matching Study. *Ann Surg Oncol* (2021) 28:3585–94. doi: 10.1245/s10434-021-09695-4

Conflict of Interest: The authors declare that the research was conducted in the absence of any commercial or financial relationships that could be construed as a potential conflict of interest.

frontiers | Frontiers in Oncology

TYPE Original Research
PUBLISHED 16 September 2022
DOI 10.3389/fonc.2022.949766

OPEN ACCESS

EDITED BY
Federico Ferrari,
University of Brescia, Italy

REVIEWED BY
Angelo Finelli,
ULSS2 Marca Trevigiana, Italy
Francesca Cisotto,
Spedali Civili Di Brescia, Italy

*CORRESPONDENCE
Jing Tang
33070728@qq.com

SPECIALTY SECTION
This article was submitted to Gynecological Oncology, a section of the journal Frontiers in Oncology

RECEIVED 21 May 2022
ACCEPTED 26 August 2022
PUBLISHED 16 September 2022

CITATION
Yang S, Tang J, Rong Y, Wang M, Long J, Chen C and Wang C (2022) Performance of the IOTA ADNEX model combined with HE4 for identifying early-stage ovarian cancer. *Front. Oncol.* 12:949766. doi: 10.3389/fonc.2022.949766

Performance of the IOTA ADNEX model combined with HE4 for identifying early-stage ovarian cancer

Suying Yang[1,2], Jing Tang[1,2*], Yue Rong[1,2], Min Wang[1,2], Jun Long[1,2], Cheng Chen[1,2] and Cong Wang[1,2]

[1]Department of Ultrasonography, Chongqing Health Center for Women and Children, Chongqing, China, [2]Department of Ultrasonography, Women and Children's Hospital of Chongqing Medical University, Chongqing, China

Objective: This work was designed to investigate the performance of the International Ovarian Tumor Analysis (IOTA) ADNEX (Assessment of Different NEoplasias in the adneXa) model combined with human epithelial protein 4 (HE4) for early ovarian cancer (OC) detection.

Methods: A total of 376 women who were hospitalized and operated on in Women and Children's Hospital of Chongqing Medical University were selected. Ultrasonographic images, cancer antigen-125 (CA 125) levels, and HE4 levels were obtained. All cases were analyzed and the histopathological diagnosis serves as the reference standard. Based on the IOTA ADNEX model post-processing software, the risk prediction value was calculated. We analyzed receiver operating characteristic curves to determine whether the IOTA ADNEX model alone or combined with HE4 provided better diagnostic accuracy.

Results: The area under the curve (AUC) of the ADNEX model alone or combined with HE4 in predicting benign and malignant ovarian tumors was 0.914 (95% CI, 0.881–0.941) and 0.916 (95% CI, 0.883–0.942), respectively. With the cutoff risk of 10%, the ADNEX model had a sensitivity of 0.93 (95% CI, 0.87–0.97) and a specificity of 0.73 (95% CI, 0.67–0.78), while combined with HE4, it had a sensitivity of 0.90 (95% CI, 0.84–0.95) and a specificity of 0.81 (95% CI, 0.76–0.86). The IOTA ADNEX model combined with HE4 was better at improving the accuracy of the differential diagnosis between different OCs than the IOTA ADNEX model alone. A significant difference was found in separating borderline masses from Stage II–IV OC (p = 0.0257).

Conclusions: A combination of the IOTA ADNEX model and HE4 can improve the specificity of diagnosis of ovarian benign and malignant tumors and increase the sensitivity and effectiveness of the differential diagnosis of Stage II–IV OC and borderline tumors.

KEYWORDS

ovarian cancer (OC), IOTA ADNEX model, human epididymis protein 4 (HE4), serum cancer antigen-125 (CA 125), receiver-operating characteristics (ROC) curve

Introduction

Ovarian cancer (OC), one type of gynecologic malignancy with a high mortality rate, has seriously threatened the life and health of women, whose incidence and mortality rate are gradually increasing over the years (1–4). The 5-year survival rate of advanced OC is about 30%, according to past reports. In contrast, postoperative survival rates of early-stage OC can reach 92.6%, while early diagnosis accuracy is just 16.3% (5). To enhance the accuracy of ovarian tumor ultrasound diagnosis, a number of prediction models have been developed by the International Ovarian Tumor Analysis (IOTA) group utilizing logistic regression analysis, which include the LR1, LR2, and IOTA ADNEX (Assessment of Different NEoplasias in the adneXa) models (6–8). As per related studies, the IOTA ADNEX model is the most effective in differentiating benign from malignant ovarian tumors.

Performing a suitable first surgical procedure is crucial for OC patients, which depends on the correct staging of the tumor before surgery. The IOTA group delivered the ADNEX model in 2014, which was the first to distinguish between benign ovarian tumors, borderline, invasive, and secondary metastatic cancers. An explanation of how to apply the ADNEX model from the IOTA group for discriminating between different subtypes of adnexal tumors was provided by Van Calster et al. (9). Related research shows that the model discriminated well between benign tumors and each of the four types of malignancy, with AUCs ranging between 0.85 and 0.99. Nevertheless, an ovarian borderline, a Stage I OC, or a metastatic ovarian tumor cannot be accurately differentiated with it (9–14). In addition, with regard to the IOTA ADNEX cutoff risk, the guidelines merely recommended the selection according to the type of center and the clinical characteristics of the patient, without an accurate value. A cutoff risk of 10% was mostly recommended in research, which has a high sensitivity (>90%) despite its low specificity (approximately 62%) (15, 16).

Detecting ovarian epithelial cancer at an earlier stage may be possible by combining tumor markers (17). Human epithelial protein 4 (HE4) is a highly recognized clinical marker for epithelial ovarian tumors after CA125 and usually applied in combination with CA125 to determine the benignity and malignancy of ovarian tumors. Specifically, it is superior to CA125 in detecting borderline and early-stage OC, and has been approved for evaluating follow-up and recurrence of OC patients (18–23).

At present, there is a lack of reports on the combined diagnosis of the IOTA ADNEX model and HE4. Therefore, this work proposed to combine the IOTA ADNEX model containing CA125 with HE4 to analyze its diagnostic efficacy and provide a reference for OC early detection.

Methods and materials

Setting of study and patients

An evaluation of diagnostic accuracy was conducted retrospectively in one hospital, a tertiary referral oncology center located in Chongqing, China, the Women and Children's Hospital of Chongqing Medical University. This study consecutively enrolled 405 women diagnosed with an adnexal mass *via* ultrasound from August 2017 to September 2020. The following were the inclusion criteria (1): patients were older than 14 years old (2); patients were all examined at the Women and Children's Hospital of Chongqing Medical University before surgery, and the serum CA125 and HE4 levels, ultrasound image workstation and report data were complete; and (3) patients' postoperative pathological diagnosis was definite. Exclusion criteria were patients with adnexal masses not derived from ovarian tissue. Ethics approval for research is provided by the Institutional Ethics Committee of Women and Children's Hospital of Chongqing Medical University.

Most of these patients have abdominal masses, abdominal pain, abdominal distension, and vaginal bleeding, while others are found accidentally during physical examinations. The examination was performed by a gynecologic ultrasonographer at the Women and Children's Hospital of Chongqing Medical University. Ultrasound machines used in the study were the GE Voluson E8 or E10 (GE Healthcare, Zipf, Austria), with transvaginal probes measuring 5.0–9.0 MHz and transabdominal probes measuring 2–7 MHz. For patients with no sexual history, transabdominal exploration was performed after filling the bladder, and transrectal ultrasonography was performed if necessary. Transvaginal ultrasonography was used for patients with a history of sexual intercourse. For larger

tumors, a combination of transcavitary and transabdominal ultrasound is used. According to the IOTA group's terminology and methods to evaluate the morphology of ultrasonographic tumors (24), if a patient has a number of adnexal masses, we choose the mass exhibiting the most complicated ultrasound morphology, and if masses are morphologically similar, the larger mass is used (15).

During the ultrasound examination, we collected the patient's age, menopausal status, and chemiluminescence measurements (Abbott i2000 analyzer, USA) of CA125 and HE4 before surgery.

ADNEX model

Cell phone applications for the IOTA ADNEX model are available. There are six ultrasound variables as well as three clinical variables in the model: age (years), referral center for an oncology or a non-oncology center, serum CA125 level (U/ml), maximum lesion diameter (mm), lesion diameter at its largest solid component (mm), cyst locules exceeding 10 (yes/no), amount of papillary projections (0, 1, 2, 3, or >3), ascites, or acoustic shadows present (yes/no). After inputting all the predictors objectively, as a result of the model, an absolute risk (in percentage terms) estimate is generated for five types of lesions in the adnexa. Furthermore, a malignancy risk estimate that incorporates all subtypes of malignancy is presented.

Reference standard

Reference standard was the histological pathological diagnosis results of the surgical specimens. These samples were examined by pathologists of our hospital and the ultrasound results were unknown. Tumors were classified based on guidelines of the World Health Organization for the classification of tumors (25). Stages of malignant tumors were determined by the new International Federation of Gynecology and Obstetrics criteria (26). A final diagnosis identified the five types of masses: benign, a borderline ovarian tumor (BOT), a Stage I OC, a Stage II–IV OC, and an ovarian metastatic cancer (Table 1).

Statistical analysis

MedCalc Statistical Software version 19.4.1 (MedCalc Software Ltd, Ostend, Belgium; https://www.medcalc.org; 2020) and IBM SPSS Statistics for Windows, Version 20.0 (Armonk, NY: IBM Corp) were used for statistical analysis. For statistical purposes, a borderline tumor was categorized as malignant.

An analysis of the ADNEX model and its combination with HE4 is based on receiver operating characteristic (ROC) curves. The area under the curve (AUC) with 95% confidence intervals (CIs) was calculated and the total risk of malignancy was used to distinguish benign from malignant tumors. AUC values of the different subclassification of malignant tumors were also calculated for analysis. The cutoff risks of 5%, 10%, and 15% of the ADNEX model were selected as the total risk of malignancy (for instance, calculate the risk of four different malignancies as a sum) in separating benign from malignant ovarian tumors, and the sensitivity and specificity, as well as the predictive values and likelihood ratios, were calculated. Additionally, DeLong's test was applied to compare the performance in identifying different subtypes of ovarian tumors when the ADNEX model was used alone or was combined with HE4.

In this work, tumor ultrasonographic characteristics, brief population statistics of patients, a description of the clinical features, and an analysis of tumor markers were conducted. If data are categorical, the chi-square test and Fisher's exact test should be used, and if data are continuous, the Mann–Whitney U test should be used. All comparisons were statistically significant at $p < 0.05$.

Results

Pathologic diagnosis and clinical findings

There were 405 patients with adnexal masses undergoing pre-operative ultrasound between August 2017 and September 2020. A total of 29 of these women were not included in this work because they were under 14 years old, the mass originated from the fallopian tube, insufficient clinical data, a broad ligament tumor on histology, failure to undergo surgery at our hospital, and they had not yet undergone surgery. Thus, 376 patients made up the final cohort (Figure 1).

Here is a listing of the histological results of the population studied in Table 1. Of these 376 women, 259 (68.9%) had benign ovarian tumors, whereas 117 (31.1%) had malignant ovarian tumors. There were 62 (16.5%) cases of BOT, 25 (6.6%) cases of Stage I OC, 26 (6.9%) cases of Stage II–IV OC, and 4 (1.1%) cases of metastatic ovary. Plasmacytoid cystadenoma and mucinous cystadenoma are the most commonly diagnosed benign tumors. On the other hand, clear cell carcinoma and serous high-grade carcinoma are the most common primary ovarian malignancies.

The clinical and ultrasonic characteristics of these women are summarized in Table 2. Those women with borderline tumors are younger than those with benign tumors, while their percentage in all malignant tumors is 52% (62/117). These findings showed that malignant tumors were slightly older than benign ones ($p = 0.074$). All patients were predominantly premenopausal ($p = 0.000$). Malignant tumors had a significantly higher maximum diameter, incidence of solid tissue, and incidence of papillary projections ($p < 0.05$ for all). More than triple the number of patients in the malignant group had more than 10 cyst locules ($p = 0.005$). A higher percentage of malignant patients had ascites than benign patients did ($p =$

TABLE 1 Pathological types of ovarian tumors in 376 patients.

Tumor pathology	*n* (%)
Benign	**259 (68.9)**
Mucinous cystadenoma	87 (23.0)
Serous cystadenoma	64 (17.0)
Cystadenofibroma	6 (1.6)
Seromucinous cystadenoma	12 (3.2)
Parovarian cyst	3 (0.8)
Endometriosis cyst	6 (1.6)
Serous adenofibroma	13 (3.5)
Serous surface papilloma	2 (0.5)
Theca cell tumor	11 (2.9)
Teratoma	35 (9.3)
Brenner tumor	2 (0.5)
Fibroma	7 (1.9)
Corpus luteum hematoma	1 (0.3)
Other ovarian benign lesion	10 (2.7)
Borderline ovarian tumor	**62 (16.5)**
Mucinous	23 (6.1)
Serous	35 (9.3)
Serous micropapillary type	1 (0.3)
Seromucinous	3 (0.8)
Primary ovarian malignant	**55 (14.6)**
Mucinous adenocarcinoma	3 (0.8)
Serous high-grade carcinoma	13 (3.5)
Clear cell carcinoma	8 (2.1)
Immature teratoma	2 (0.5)
Dysgerminoma	2 (0.5)
Endometrioid adenocarcinoma	4 (1.1)
Large cell neuroendocrine Carcinoma	1 (0.3)
Ovarian gonadal sex cord stromal tumor	1 (0.3)
Keratinizing squamous cell carcinoma	1 (0.3)
Granulosa-cell tumor	1 (0.3)
Yolk sac tumor	1 (0.3)
Poorly differentiated carcinoma	2 (0.5)
Carcinosarcoma	1 (0.3)
Seromucinous carcinoma	5 (1.3)
Adult granulose cell tumor	2 (0.5)
Rare primary invasive pathologies	4 (1.1)
Ovarian metastasis	**4 (1.1)**

0.031). We observed acoustic shadows only in one patient with malignant tumors.

Table 3 lists the results of analyzing serum CA125 and HE4 levels among different subtypes of ovarian tumors. For the CA125 level, the differences were statistically significant between benign and subtypes of malignant tumors except the ovarian metastasis ($p < 0.05$ for them), and between a Stage II–IV OC and an ovarian borderline tumor ($p = 0.019$). For the HE4 level, the differences were also statistically significant between the groups above except that between a benign tumor and an ovarian borderline tumor ($p = 0.075$). In addition, the differences in the HE4 level were also statistically significant between a Stage I OC and a Stage II–IV OC ($p = 0.011$), while no statistically significant differences were observed between an ovarian borderline tumor, a Stage I OC, and an ovarian metastasis tumor either in CA125 or in HE4 levels.

Assessing the differential diagnostic ability of the IOTA ADNEX model combined with HE4

Figure 2 shows that the AUC of the ADNEX model alone or combined with HE4 in predicting benign tumors and malignant OCs was 0.914 (95% CI, 0.881–0.941) and 0.916 (95% CI, 0.883–0.942). The differences between them were not significant ($p = 0.0925$).

As the cutoff risk increases, the specificity gradually increases and the sensitivity gradually decreases simultaneously when the ADNEX model was used alone (Table 4). The sensitivity (0.87) and specificity (0.86) were balanced at the cutoff risk of 30.8%. The specificity was 0.81 when the ADNEX model was combined with HE4, which was higher than that when the cutoff risk of ADNEX model was 10% (0.73) or 15% (0.78).

Results of the IOTA ADNEX model alone or combined with HE4 for discriminating between different subclassifications of ovarian tumors are listed in Table 5. Their performance in discriminating benign from the different subtypes of malignant tumors is excellent. The AUCs vary between 0.860 and 0.975 when the ADNEX model was combined with HE4 and between 0.841 and 0.977 when the ADNEX model was used alone. The difference between the groups above was not statistically significant ($p > 0.05$ for all). For the differential diagnosis ability between subclassifications of malignant tumors, the AUCs vary between 0.697 and 0.838 when ADNEX was used alone and increased to between 0.760 and 0.903 when the ADNEX model was combined with HE4. The difference in the differential diagnostic ability between an ovarian borderline tumor and a Stage II–IV OC was statistically significant ($p = 0.0257$). However, both of them have poor differential diagnostics for a Stage I OC and an ovarian metastasis, with an AUC of 0.71 and 0.76, respectively.

Regarding the differential diagnosis of an ovarian borderline tumor and a Stage II–IV OC, the AUC from 0.838 increased to 0.903 after the ADNEX model in combination with HE4, and the sensitivity increased from 0.73 to 0.85, while the specificity was maintained (Table 6).

Discussion

A correct and early diagnosis of OC can significantly increase the patient's chances of survival (27, 28). As

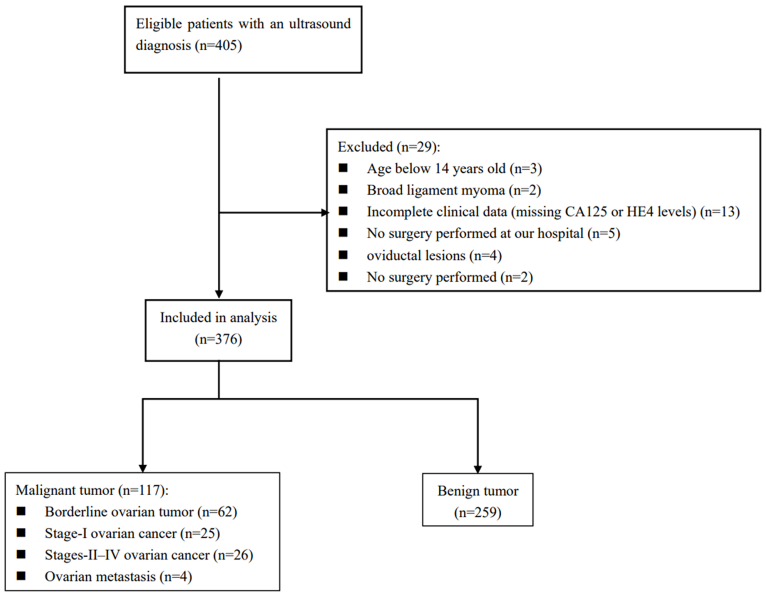

FIGURE 1
Diagram of how the study cohort was recruited from women diagnosed by ultrasound with adnexal masses based on the inclusion and exclusion criteria.

TABLE 2 General clinical and ultrasonographic features of 376 ovarian benign and malignant tumors.

Characteristic	Benign (*n* = 259)	Malignant (*n* = 117)					*p*
		Borderline (*n* = 62)	OC Stage I (*n* = 25)	OC Stages II–IV (*n* = 26)	Ovarian metastasis (*n* = 4)	Total (*n* = 117)	
Age (years)	38.00 (27.00, 49.00)	33.00 (27.75, 42.25)	48.00 (38.50, 53.00)	49.50 (46.00, 59.00)	54.00 (50.50, 58.25)	42.00 (30.00, 50.00)	0.074*
Menopausal status							0.000+
Premenopausal	216 (57.45)	56 (14.89)	17 (4.52)	16 (4.26)	1 (0.27)	90 (2.39)	
Postmenopausal	43 (11.44)	6 (1.60)	8 (2.13)	10 (2.66)	3 (0.80)	27 (7.18)	
Maximum diameter of lesion (mm)	76 (57, 102)	88 (59.50, 130.50)	117 (78, 146)	101 (76.50, 128.25)	84.5 (60, 107.50)	100 (66, 134)	0.000*
Solid tissue present	73 (19.41)	32 (8.50)	10 (2.66)	10 (2.66)	1 (0.27)	53 (14.10)	0.001+
Maximum diameter of largest solid component, if present (mm)	30 (14.50, 53.50)	63 (48.50, 93.00)	69 (38.75, 86.25)	34.50 (18.75, 54.25)	85 (75.00, 98.50)	52 (26.50, 75.00)	0.000*
Papillary projections present	47 (12.50)	40 (10.64)	8 (2.13)	6 (1.60)	0 (0)	54 (14.36)	0.000+
0	212 (56.38)	22 (5.85)	17 (4.52)	20 (5.32)	4 (1.06)	63 (16.76)	
1	27 (7.18)	16 (4.26)	1 (0.27)	1 (0.27)	0	18 (4.79)	
2	9 (2.39)	6 (1.60)	0	0	0	6 (1.60)	
3	3 (0.80)	5 (1.33)	2 (0.53)	2 (0.53)	0	9 (2.39)	
>3	8 (2.13)	15 (3.99)	5 (1.33)	3 (0.80)	0	23 (6.12)	

(Continued)

TABLE 2 Continued

Characteristic	Benign (*n* = 259)	Malignant (*n* = 117)					*p*
		Borderline (*n* = 62)	OC Stage I (*n* = 25)	OC Stages II–IV (*n* = 26)	Ovarian metastasis (*n* = 4)	Total (*n* = 117)	
>10 cyst locules	11 (2.93)	10 (2.66)	4 (1.06)	0	0	14 (3.72)	0.005^{+}
Acoustic shadows	23 (6.12)	0	1 (0.27)	0	0	1 (0.27)	0.002^{++}
Ascites	13 (3.46)	7 (1.86)	1 (0.27)	5 (1.33)	0	13 (3.46)	0.031^{+}

*For categorical data, n (%) is used, and for continuous data, the median (interquartile range) is used. The p-value for benign versus malignant groups is calculated with the following methods: *Mann–Whitney U test for continuous data, $^{+}$Chi-square test and $^{++}$Fisher exact test for categorical data. OC, ovarian cancer.

TABLE 3 Serum CA125 and HE4 level comparison between different subtypes of ovarian tumors.

Group	*n*	CA125	HE4
		Median (Q1, Q3)	Median (Q1, Q3)
Benign	259	17.30	36.00
		(11.5, 29.0)	(30, 43)
Borderline	62	46.75	41.00
		(26.13, 120.68)	(32.75, 53.0)
OC Stage I	25	57.8	47.00
		(18.15, 265.60)	(32.00, 104.50)
OC Stages II–IV	26	362.0	217.00
		(93.23, 751.98)	(42.10, 682.00)
Ovarian metastasis	4	126.55	58.5
		(29.55, 275.3)	(51.5, 88.0)
Z1		−4.26	−3.221
P1		0.000	0.013
Z2		−6.441	−2.674
P2		0.000	0.075
Z3		−8.022	−7.727
P3		0.000	0.000
Z4		−2.424	−2.721
P4		0.154	0.065
Z5		−0.129	1.251
P5		1.000	1.000
Z6		3.099	5.186
P6		0.019	0.000
Z7		−0.578	−1.924
P7		1.000	0.543
Z8		−2.707	−3.267
P8		0.068	0.011
Z9		−0.611	−1.293
P9		1.000	1.000
Z10		0.799	0.407
P10		1.000	1.000

We present the data as a median (interquartile range); P1–P10 represent the comparison between different subtypes of ovarian tumors using Mann–Whitney U test and Z-statistic calculated. P1, benign vs. Stage I OC; P2, benign vs. borderline; P3, benign vs. Stage II–IV OC; P4, benign vs. ovarian metastasis; P5, borderline vs. Stage I OC; P6, borderline vs. Stage II–IV OC; P7, borderline vs. ovarian metastasis; P8, Stage I OC vs. Stage II–IV OC; P9, Stage I OC vs. ovarian metastasis; P10, Stage II–IV OC vs. ovarian metastasis.

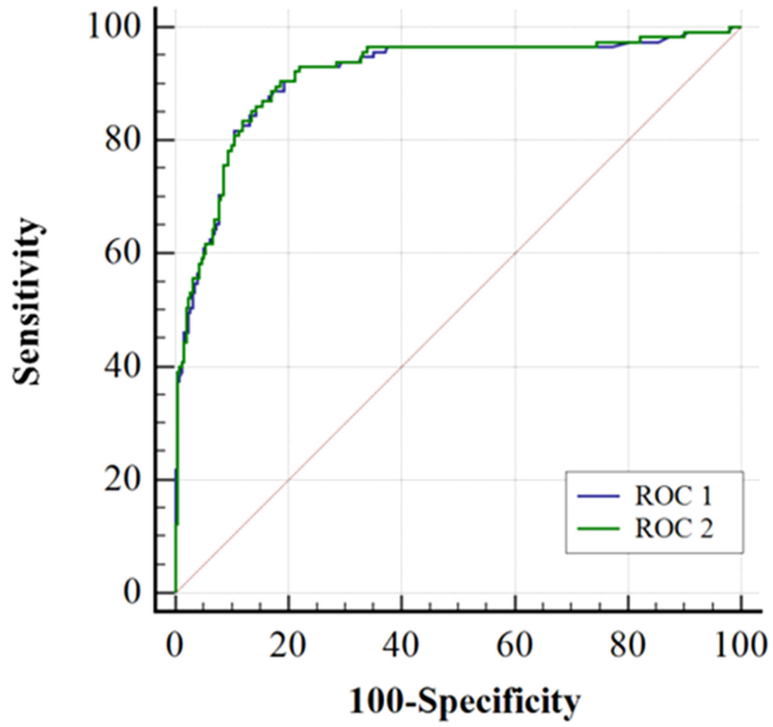

FIGURE 2
Receiver-operating characteristic curves (ROC) for the accuracy of ADNEX model alone (ROC 1) or in combination with HE4 (ROC 2) when separating malignant from benign ovarian tumors. The areas under ROC1 and ROC2 curves were 0.914 (0.881-0.941) and 0.916 (0.888-0.942), respectively. Comparing the AUC of the ROC 1 and the ROC 2 using DeLong's test (P=0.0925).

previously reported, the main models and scoring systems for diagnosing ovarian tumors were compared and analyzed. When diagnosing benign and malignant ovarian tumors, the ADNEX model had a higher AUC value and sensitivity (0.94 and 96.5%) than the risk of malignancy index (RMI) (0.85 and 89%), the risk of ovarian malignancy algorithm (ROMA) (0.84 and 91%), and the Copenhagen index (CPH-I) (0.81 and 69%) (29–32). The diagnostic performance of RMI and CPH-I is affected by the base rate of OC (33). The main limitations of the RMI are its lack of an estimated risk of malignancy, and its high reliance on serum CA125, which makes it relatively insensitive to borderline and early-stage invasive diseases, especially in women who are premenopausal (6, 34). In addition, a multicenter cohort study comparing six prediction models (RMI, LR2, Simple Rules, Simple Rules risk model, and the ADNEX model with or without CA125), conducted in 17 centers, demonstrated that the IOTA ADNEX model and the IOTA Simple Rules risk model were the best (6, 35). Furthermore, the ADNEX model is capable

TABLE 4 Efficacy of the IOTA ADNEX model alone or combined with HE4 to differentiate benign from malignant tumors.

ADNEX model	Cutoff	Sensitivity	Specificity	+LR	−LR	PPV	NPV
Benign vs. malignant	5%	0.97 (0.91–0.99)	0.55 (0.49–0.61)	2.16 (1.90–2.50)	0.06 (0.02–0.20)	0.49 (0.45–0.52)	0.97 (0.93–0.99)
	10%	0.93 (0.87–0.97)	0.73 (0.67–0.78)	3.39 (2.80–4.20)	0.10 (0.05–0.20)	0.60 (0.55–0.65)	0.96 (0.92–0.98)
	15%	0.93 (0.87–0.97)	0.78 (0.72–0.83)	4.15 (3.30–5.20)	0.09 (0.05–0.20)	0.65 (0.05–0.20)	0.96 (0.93–0.98)
	30.8%	0.87 (0.78–0.92)	0.86 (0.81–0.90)	6.03 (4.40–8.20)	0.16 (0.10–0.30)	0.73 (0.66–0.78)	0.93 (0.90–0.96)
Benign vs. malignant combining with HE4	0.171	0.90 (0.84–0.95)	0.81 (0.76–0.86)	4.88 (3.80–6.30)	0.12 (0.07–0.20)	0.68 (62.50–73.80)	0.95 (91.60–97.10)

The likelihood ratios are +LR and −LR. The predictive values are NPV and PPV.

TABLE 5 Comparison of the differential diagnostic ability of the IOTA ADNEX model alone or combined with HE4 in the identification of various types of ovarian tumors.

Discrimination	AUC (95% CI)		*p*
	ADNEX model combined with HE4	ADNEX model	
Benign vs. malignant	0.916 (0.883–0.942)	0.914 (0.881–0.941)	0.0925
Benign vs. BOT	0.860 (0.817–0.896)	0.841 (0.796–0.879)	0.2885
Benign vs. Stage I OC	0.955 (0.924–0.976)	0.948 (0.915–0.971)	0.2183
Benign vs. Stage II–IV OC	0.975 (0.949–0.990)	0.977 (0.952–0.991)	0.6051
Benign vs. metastasis	0.933 (0.896–0.960)	0.937 (0.901–0.963)	0.3517
BOT vs. Stage I OC	0.813 (0.714–0.890)	0.758 (0.653–0.844)	0.1200
BOT vs. Stage II–IV OC	0.903 (0.820–0.956)	0.838 (0.743–0.909)	0.0257
BOT vs. metastasis	0.821 (0.705–0.905)	0.773 (0.651–0.868)	0.3336
Stage I OC vs. Stage II–IV OC	0.812 (0.678–0.908)	0.734 (0.592–0.848)	0.0823
Stage I OC vs. metastasis	0.760 (0.566–0.898)	0.710 (0.513–0.862)	0.1587
Stage II–IV OC vs. metastasis	0.885 (0.715–0.972)	0.697 (0.503–0.850)	0.2960

The area under receiver operating characteristic curve (AUC) of the IOTA ADNEX model alone or in combination with HE4 is compared using DeLong's test. BOT is borderline ovarian tumor; OC is ovarian cancer.

of classifying subtypes of ovarian malignancies. Therefore, the ADNEX model is currently the most research-valued diagnostic model.

At our Gynecological Oncology Center, the IOTA ADNEX model is effective at differentiating benign from malignant ovarian tumors, which is in line with the research of domestic and foreign scholars (35). As far as the IOTA ADNEX cutoff value is concerned, 10% was usually selected as the cutoff point in current studies, although the sensitivity (varying from 93.3% to 98%) is high and specificity is low (varying from 62% to 77.8%). Therefore, some scholars have proposed to use 15% as the cutoff point to ensure that its sensitivity is >90%, and its specificity can be increased (varying from 72.7% to 83.7%) (15, 29, 36–39). In our study, when the IOTA ADNEX model was combined with HE4, the sensitivity of differentiating benign from malignant ovarian tumors was 90.43%, and the specificity could be increased to 81.47%. It can reduce the number of false positives, optimize resource allocation, and reduce treatment cost due to its high specificity.

Currently, ultrasound-based predictive models for the preoperative correct detection of an ovarian borderline tumor, a Stage I OC, and a metastatic tumor remain a challenge (40, 41). Previous studies have shown that almost one-half of all borderline tumors are incorrectly diagnosed or classified by subjective ultrasound evaluation, and diagnostic problems associated with difficult borderline tumors cannot be solved by logistic regression models (42). In comparison to the IOTA ADNEX model, the simple rules of IOTA and non-IOTA models perform poorly when it comes to identifying BOTs and Stage I OCs (43, 44). Consistent with previous studies (44, 45), the IOTA ADNEX performed excellently in terms of detecting most types of adnexal masses in this work (an AUC of 0.697 to 0.977 was observed). Nevertheless, the model performed poorly at distinguishing between an ovarian borderline tumor and a Stage I OC (AUC, 0.758), between an ovarian borderline and a metastatic tumor (AUC, 0.773), between a Stage I OC and a metastatic tumor (AUC, 0.710), between a Stage I OC and a Stage II–IV OC (AUC, 0.734), and between a Stage II–IV OC and a metastatic tumor (AUC, 0.697). The results were similar to or lower than previous studies (29, 37).

In order to enhance early OC detection, we combined the IOTA ADNEX model with HE4 for the first time. Serum CA125 was a clinical indicator in the ADNEX model that may be impacted by infections and pregnancy, having a lower sensitivity and a high false-positive rate (30, 46–49). Serum HE4, an important supplementary indicator of CA125, had a similar sensitivity and a higher specificity, especially for asymptomatic patients with Stage I OC, and had been

TABLE 6 An assessment of the IOTA ADNEX model combined with HE4 to differentiate an ovarian borderline tumor from a Stage II–IV OC.

ADNEX model	Sensitivity	Specificity	+LR	−LR	PPV	NPV	Cutoff	Youden index	*p*
Borderline vs. Stage II–IV OC	0.73 (0.52, 0.88)	0.90 (0.80, 0.96)	7.31 (3.3, 16.2)	0.3 (0.2, 0.6)	0.76 (0.60, 0.88)	0.89 (0.80, 0.94)	31.4	0.631	0.0257
Borderline vs. Stage II–IV OC combined with HE4	0.85 (0.65, 0.96)	0.90 (0.80, 0.96)	8.46 (3.9, 18.4)	0.17 (0.07, 0.4)	0.79 (0.63, 0.89)	0.93 (0.85, 0.97)	0.195	0.746	

NPV represents the negative predictive value; PPV represents the positive predictive value. The likelihood ratios are positive (+LR) or negative (−LR).

recommended as a potential biomarker (50). Our results showed that the ADNEX model, whether combined with HE4 or not, was excellent for the differential diagnosis of benign and malignant ovarian tumors (AUC of 0.916 and 0.914, respectively). The specificity of the combined diagnosis of the ADNEX model and HE4 is greater than that of the 10% cutoff risk in the ADNEX model, while the sensitivities are both greater than 90%. The differential diagnosis ability improved after the ADNEX model was combined with HE4 compared with the ADNEX model used alone in distinguishing between most of the different types of ovarian malignancies, with the AUC varying between 0.697 and 0.838 and increased to between 0.760 and 0.903. However, it was still ineffective at distinguishing between Stage I OC and metastasis tumor (AUC of 0.760 and 0.710, respectively). Most of the differences above were not statistically significant ($p > 0.05$ for them) except for an ovarian borderline tumor vs. a Stage II–IV OC ($p = 0.0257$), which may be related to the non-obvious expression of serum CA125 and HE4 levels that was significantly different between borderline, Stage I OC, and metastatic OC groups (as shown in Table 3) or may be related to the limited number of cases in our study. Therefore, further research should be conducted for biomarkers targeting early diagnosis of OC. Some researchers have proposed ovarian tumor stem cell-specific biomarkers such as CA24, CD44, CD133, and SSEA, and others have proposed the unique peritoneal microbial profile of OC patients. Perhaps, these biomarkers have important biological and clinical significance in terms of the early detection rate of OC (51, 52).

Our study has shortcomings. First, this work was conducted in one hospital, with limited data collection. Second, the feasibility was not verified either in internal or in external gynecological oncology centers with new data. We will gradually overcome these problems in a follow-up research.

In conclusion, the ADNEX model, alone or combined with HE4, performs excellently to determine the benignity or malignancy of an ovarian tumor, while the specificity was higher when combined with HE4. The ADNEX model combined with HE4 can improve the differential diagnosis ability and the sensitivity of an ovarian borderline tumor and a Stage II–IV OC.

Data availability statement

The original contributions presented in the study are included in the article/supplementary material. Further inquiries can be directed to the corresponding author.

Ethics statement

The studies involving human participants were reviewed and approved by Institutional Ethics Committee of Women and Children's Hospital of Chongqing Medical University. Written informed consent to participate in this study was provided by the participants' legal guardian/next of kin. Written informed consent was obtained from the individual(s), and minor(s)' legal guardian/next of kin, for the publication of any potentially identifiable images or data included in this article.

Author contributions

JT: project development. JT and SY: data collection, data analysis, and manuscript writing. YR, MW, JL, CC, and CW: data collection and manuscript writing. All authors contributed to the article and approved the submitted version.

Funding

The study was supported by the Technological Innovation and Application Development Project of Chongqing (cstc2019jscx-msxmX0235).

Conflict of interest

The authors declare that the research was conducted in the absence of any commercial or financial relationships that could be construed as a potential conflict of interest.

Publisher's note

References

1. Bray F, Ferlay J, Soerjomataram I, Siegel RL, Torre LA, Jemal A. Global cancer statistics 2018: GLOBOCAN estimates of incidence and mortality worldwide for 36 cancers in 185 countries. *CA Cancer J Clin* (2018) 68(6):394–424. doi: 10.3322/caac.21492

2. Sung H, Ferlay J, Siegel RL, Laversanne M, Soerjomataram I, Jemal A, et al. Global cancer statistics 2020: GLOBOCAN estimates of incidence and mortality worldwide for 36 cancers in 185 countries. *CA Cancer J Clin* (2021) 71(3):209–49. doi: 10.3322/caac.21660

3. Stewart C, Ralyea C, Lockwood S. Ovarian cancer: An integrated review. *Semin Oncol Nurs* (2019) 35(2):151–6. doi: 10.1016/j.soncn.2019.02.001

4. Webb PM, Jordan SJ. Epidemiology of epithelial ovarian cancer. *Best Pract Res Clin Obstet Gynaecol* (2017) 41:3–14. doi: 10.1016/j.bpobgyn.2016.08.006

5. *Cancer stat facts: Ovarian cancer* (2020). Available at: https://seer.cancer.gov/statfacts/html/ovary.html.

6. Timmerman D, Planchamp F, Bourne T, Landolfo C, du Bois A, Chiva L, et al. ESGO/ISUOG/IOTA/ESGE consensus statement on preoperative diagnosis of ovarian tumors. *Ultrasound Obstet Gynecol* (2021) 58(1):148–68. doi: 10.1002/uog.23635

7. Timmerman D, Testa AC, Bourne T, Ferrazzi E, Ameye L, Konstantinovic ML, et al. Logistic regression model to distinguish between the benign and malignant adnexal mass before surgery: a multicenter study by the international ovarian tumor analysis group. *J Clin Oncol* (2005) 23(34):8794–801. doi: 10.1200/JCO.2005.01.7632

8. Timmerman D, Van Calster B, Testa A, Savelli L, Fischerova D, Froyman W, et al. Predicting the risk of malignancy in adnexal masses based on the simple rules from the international ovarian tumor analysis group. *Am J Obstet Gynecol* (2016) 214(4):424–37. doi: 10.1016/j.ajog.2016.01.007

9. Calster BV, Hoorde KV, Froyman W, Kaijser J, Wynants L, Landoldo C, et al. Practical guidance for applying the ADNEX model from the IOTA group to discriminate between different subtypes of adnexal tumors. *Facts Views Vis Obgyn* (2015) 7(1):32–41.

10. Qian L, Du Q, Jiang M, Yuan F, Chen H, Feng W. Comparison of the diagnostic performances of ultrasound-based models for predicting malignancy in patients with adnexal masses. *Front Oncol* (2021) 11:673722. doi: 10.3389/fonc.2021.673722

11. He P, Wang JJ, Duan W, Song C, Yang Y, Wu QQ. Estimating the risk of malignancy of adnexal masses: validation of the ADNEX model in the hands of nonexpert ultrasonographers in a gynaecological oncology centre in China. *J Ovarian Res* (2021) 14(1):169. doi: 10.1186/s13048-021-00922-w

12. Peng XS, Ma Y, Wang LL, Li HX, Zheng XL, Liu Y. Evaluation of the diagnostic value of the ultrasound ADNEX model for benign and malignant ovarian tumors. *Int J Gen Med* (2021) 14:5665–73. doi: 10.2147/IJGM.S328010

13. Tug N, Yassa M, Akif Sargin M, Dogan Taymur B, Sandal K, Ertnuc M. Preoperative discriminating performance of the IOTA-ADNEX model and comparison with risk of malignancy index: an external validation in a non-gynecologic oncology tertiary center. *Eur J Gynaecol Oncol* (2020) 41(2)::200–7. doi: 10.31083/j.ejgo.2020.02.4971

14. Nohuz E, De Simone L, Chene G. Reliability of IOTA score and ADNEX model in the screening of ovarian malignancy in postmenopausal women. *J Gynecol Obstet Hum Reprod* (2019) 48(2):103–7. doi: 10.1016/j.jogoh.2018.04.012

15. Meys EMJ, Jeelof LS, Achten NMJ, Slangen BFM, Lambrechts S, Kruitwagen R, et al. Estimating risk of malignancy in adnexal masses: external validation of the ADNEX model and comparison with other frequently used ultrasound methods. *Ultrasound Obstet Gynecol* (2017) 49(6):784–92. doi: 10.1002/uog.17225

16. Joyeux E, Miras T, Masquin I, Duglet PE, Astruc K, Douvier S. Before surgery predictability of malignant ovarian tumors based on ADNEX model and its use in clinical practice. *Gynecol Obstet Fertil* (2016) 44(10):557–64. doi: 10.1016/j.gyobfe.2016.07.007

17. Capriglione S, Luvero D, Plotti F, Terranova C, Montera R, Scaletta G, et al. Ovarian cancer recurrence and early detection: may HE4 play a key role in this open challenge? a systematic review of literature. *Med Oncol* (2017) 34(9):164. doi: 10.1007/s12032-017-1026-y

18. Moore RG, Jabre-Raughley M, Brown AK, Robison KM, Miller MC, Allard WJ, et al. Comparison of a novel multiple marker assay vs the risk of malignancy index for the prediction of epithelial ovarian cancer in patients with a pelvic mass. *Am J Obstet Gynecol* (2010) 203(3):228.e1–6. doi: 10.1016/j.ajog.2010.03.043

19. Lin J, Qin J, Sangvatanakul V. Human epididymis protein 4 for differential diagnosis between benign gynecologic disease and ovarian cancer: a systematic review and meta-analysis. *Eur J Obstet Gynecol Reprod Biol* (2013) 167(1):81–5. doi: 10.1016/j.ejogrb.2012.10.036

20. Moore RG, Brown AK, Miller MC, Skates S, Allard WJ, Verch T, et al. The use of multiple novel tumor biomarkers for the detection of ovarian carcinoma in patients with a pelvic mass. *Gynecol Oncol* (2008) 108(2):402–8. doi: 10.1016/j.ygyno.2007.10.017

21. Melo A, Verissimo R, Farinha M, Martins NN, Martins FN, . Discriminative value of CA-125, HE4, risk of(RMI-II) and risk of malignancy algorithm (ROMA) in the differential diagnosis of pelvic masses: conclusions from a referral centre in Portugal. *J Obstet Gynaecol* (2018) 38(8):1140–5. doi: 10.1080/01443615.2018.1457632

22. Molina R, Escudero JM, Auge JM, Filella X, Foj L, Torne A, et al. HE4 a novel tumour marker for ovarian cancer: comparison with CA 125 and ROMA algorithm in patients with gynaecological diseases. *Tumour Biol* (2011) 32(6):1087–95. doi: 10.1007/s13277-011-0204-3

23. Scaletta G, Plotti F, Luvero D, Capriglione S, Montera R, Miranda A, et al. The role of novel biomarker HE4 in the diagnosis, prognosis and follow-up of ovarian cancer: a systematic review. *Expert Rev Anticancer Ther* (2017) 17(9):827–39. doi: 10.1080/14737140.2017.1360138

24. Timmerman D, Valentin L, Bourne TH, Collins WP, Verrelst H, Vergote I. Terms, definitions and measurements to describe the sonographic features of adnexal tumors: a consensus opinion from the international ovarian tumor analysis (IOTA) grop. *Ultrasound Obstet Gynecol* (2000) 16:500–5.

25. Meinhold-Heerlein I, Fotopoulou C, Harter P, Kurzeder C, Mustea A, Wimberger P, et al. The new WHO classification of ovarian, fallopian tube, and primary peritoneal cancer and its clinical implications. *Arch Gynecol Obstet* (2016) 293(4):695–700. doi: 10.1007/s00404-016-4035-8

26. Prat JOncology FCoG. Staging classification for cancer of the ovary, fallopian tube, and peritoneum. . *Int J Gynaecol Obstet* (2014) 124(1):1–5. doi: 10.1016/j.ijgo.2013.10.001

27. Jacobs IJ, Menon U, Ryan A, Gentry-Maharaj A, Burnell M, Kalsi JK, et al. Ovarian cancer screening and mortality in the UK collaborative trial of ovarian cancer screening (UKCTOCS): a randomised controlled trial. *Lancet* (2016) 387(10022):945–56. doi: 10.1016/s0140-6736(15)01224-6

28. Huang Y, Ming X, Li B, Li Z. Histological characteristics and early-stage diagnosis are associated with better survival in young patients with epithelial ovarian cancer: A retrospective analysis based on surveillance epidemiology and end results database. *Front Oncol* (2020) 10:595789. doi: 10.3389/fonc.2020.595789

29. Van Calster B, Van Hoorde K, Valentin L, Testa AC, Fischerova D, Van Holsbeke C, et al. Evaluating the risk of ovarian cancer before surgery using the ADNEX model to differentiate between benign, borderline, early and advanced stage invasive, and secondary metastatic tumours: prospective multicentre diagnostic study. *BMJ* (2014) 349:g5920. doi: 10.1136/bmj.g5920

30. Lycke M, Kristjansdottir B, Sundfeldt K. A multicenter clinical trial validating the performance of HE4, CA125, risk of ovarian malignancy algorithm and risk of malignancy index. *Gynecol Oncol* (2018) 151(1):159–65. doi: 10.1016/j.ygyno.2018.08.025

31. Minar L, Felsinger M, Cermakova Z, Zlamal F, Bienertova-Vasku J. Comparison of the Copenhagen index versus ROMA for the preoperative assessment of women with ovarian tumors. *Int J Gynaecol Obstet* (2018) 140(2):241–6. doi: 10.1002/ijgo.12371

32. Poonyakanok V, Tanmahasamut P, Jaishuen A, Wongwananuruk T, Asumpinwong C, Panichyawat N, et al. Preoperative evaluation of the ADNEX model for the prediction of the ovarian cancer risk of adnexal masses at siriraj hospital. *Gynecol Obstet Invest* (2021) 86(1-2):132–8. doi: 10.1159/000513517

33. Rolfsen ALD, Dahl AA, Pripp AH, Dorum A. Base rate of ovarian cancer on algorithms in patients with a pelvic mass. *Int J Gynecol Cancer* (2020) 30(11):1775–9. doi: 10.1136/ijgc-2020-001416

34. Timmerman D, Van Calster B, Jurkovic D, Valentin L, Testa AC, Bernard JP, et al. Inclusion of CA-125 does not improve mathematical models developed to distinguish between benign and malignant adnexal tumors. *J Clin Oncol* (2007) 25(27):4194–200. doi: 10.1200/JCO.2006.09.5943

35. Van Calster B, Valentin L, Froyman W, Landolfo C, Ceusters J, Testa AC, et al. Validation of models to diagnose ovarian cancer in patients managed surgically or conservatively: multicentre cohort study. *BMJ* (2020) 370:m2614. doi: 10.1136/bmj.m2614

36. Westwood M, Ramaekers B, Lang S, Grimm S, Deshpande S, de Kock S, et al. Risk scores to guide referral decisions for people with suspected ovarian cancer in secondary care: a systematic review and cost-effectiveness analysis. *Health Technol Assess* (2018) 22(44):1–264. doi: 10.3310/hta22440

37. Chen H, Qian L, Jiang M, Du Q, Yuan F, Feng W. Performance of IOTA ADNEX model in evaluating adnexal masses in a gynecological oncology center in China. *Ultrasound Obstet Gynecol* (2019) 54(6):815–22. doi: 10.1002/uog.20363

38. Huang X, Wang Z, Zhang M, Luo H. Diagnostic accuracy of the ADNEX model for ovarian cancer at the 15% cut-off value: A systematic review and meta-analysis. *Front Oncol* (2021) 11:684257. doi: 10.3389/fonc.2021.684257

39. Hiett AK, Sonek JD, Guy M, Reid TJ. Performance of IOTA simple rules, simple rules risk assessment, ADNEX model and O-RADS in differentiating between benign and malignant adnexal lesions in north American women. *Ultrasound Obstet Gynecol* (2022) 59(5):668–76. doi: 10.1002/uog.24777

40. Campos C, Sarian LO, Jales RM, Hartman C, Araujo KG, Pitta D, et al. Performance of the risk of malignancy index for discriminating malignant tumors in women with adnexal masses. *J Ultrasound Med* (2016) 35(1):143–52. doi: 10.7863/ultra.15.01068

41. Van Holsbeke C, Van Calster B, Bourne T, Ajossa S, Testa AC, Guerriero S, et al. External validation of diagnostic models to estimate the risk of malignancy in adnexal masses. *Clin Cancer Res* (2012) 18(3):815–25. doi: 10.1158/1078-0432.CCR-11-0879

42. Valentin L, Ameye L, Jurkovic D, Metzger U, Lecuru F, Van Huffel S, et al. Which extrauterine pelvic masses are difficult to correctly classify as benign or malignant on the basis of ultrasound findings and is there a way of making a correct diagnosis? *Ultrasound Obstet Gynecol* (2006) 27(4):438–44. doi: 10.1002/uog.2707

43. Timmerman D, Testa AC, Bourne T, Ameye L, Jurkovic D, Van Holsbeke C, et al. Simple ultrasound-based rules for the diagnosis of ovarian cancer. *Ultrasound Obstet Gynecol* (2008) 31(6):681–90. doi: 10.1002/uog.5365

44. Araujo KG, Jales RM, Pereira PN, Yoshida A, de Angelo Andrade L, Sarian LO, et al. Performance of the IOTA ADNEX model in preoperative discrimination of adnexal masses in a gynecological oncology center. *Ultrasound Obstet Gynecol* (2017) 49(6):778–83. doi: 10.1002/uog.15963

45. Sayasneh A, Ferrara L, De Cock B, Saso S, Al-Memar M, Johnson S, et al. Evaluating the risk of ovarian cancer before surgery using the ADNEX model: a multicentre external validation study. *Br J Cancer* (2016) 115(5):542–8. doi: 10.1038/bjc.2016.227

46. Soletormos G, Duffy MJ, Othman Abu Hassan S, Verheijen RH, Tholander B, Bast RCJr., et al. Clinical use of cancer biomarkers in epithelial ovarian cancer: Updated guidelines from the European group on tumor markers. *Int J Gynecol Cancer* (2016) 26(1):43–51. doi: 10.1097/IGC.0000000000000586

47. Cramer DW, Vitonis AF, Welch WR, Terry KL, Goodman A, Rueda BR, et al. Correlates of the preoperative level of CA125 at presentation of ovarian cancer. *Gynecol Oncol* (2010) 119(3):462–8. doi: 10.1016/j.ygyno.2010.08.028

48. Babic A, Cramer DW, Kelemen LE, Kobel M, Steed H, Webb PM, et al. Predictors of pretreatment CA125 at ovarian cancer diagnosis: a pooled analysis in the ovarian cancer association consortium. *Cancer Causes Control* (2017) 28 (5):459–68. doi: 10.1007/s10552-016-0841-3

49. Johnson CC, Kessel B, Riley TL, Ragard LR, Williams CR, Xu JL, et al. The epidemiology of CA-125 in women without evidence of ovarian cancer in the prostate, lung, colorectal and ovarian cancer (PLCO) screening trial. *Gynecol Oncol* (2008) 110(3):383–9. doi: 10.1016/j.ygyno.2008.05.006

50. Cao H, You D, Lan Z, Ye H, Hou M, Xi M. Prognostic value of serum and tissue HE4 expression in ovarian cancer: a systematic review with meta-analysis of 90 studies. *Expert Rev Mol Diagn* (2018) 18(4):371–83. doi: 10.1080/14737159.2018.1457436

51. Miao R, Badger TC, Groesch K, Diaz-Sylvester PL, Wilson T, Ghareeb A, et al. Assessment of peritoneal microbial features and tumor marker levels as potential diagnostic tools for ovarian cancer. *PloS One* (2020) 15(1):e0227707. doi: 10.1371/journal.pone.0227707

52. Muinao T, Deka Boruah HP, Pal M. Diagnostic and prognostic biomarkers in ovarian cancer and the potential roles of cancer stem cells - an updated review. *Exp Cell Res* (2018) 362(1):1–10. doi: 10.1016/j.yexcr.2017.10.018

frontiers | Frontiers in Oncology

TYPE Case Report
PUBLISHED 23 September 2022
DOI 10.3389/fonc.2022.954289

OPEN ACCESS

EDITED BY
Federico Ferrari,
University of Brescia, Italy

REVIEWED BY
Ceren Canbey,
Bagcilar Education and Research Hospital, Turkey
Marco Montella,
Università della Campania Luigi Vanvitelli, Italy

*CORRESPONDENCE
Ying Zhang
zhangying5413@126.com

SPECIALTY SECTION
This article was submitted to Gynecological Oncology, a section of the journal Frontiers in Oncology

RECEIVED 27 May 2022
ACCEPTED 02 September 2022
PUBLISHED 23 September 2022

CITATION
Li YY, Wu Y, Zhang Y and Li X (2022) Case report: Strategies for improving outcomes in patients with primary ovarian small-cell neuroendocrine carcinoma. *Front. Oncol.* 12:954289. doi: 10.3389/fonc.2022.954289

Case report: Strategies for improving outcomes in patients with primary ovarian small-cell neuroendocrine carcinoma

YingYing Li[1,2], Yueling Wu[1,2], Ying Zhang[1]* and Xiaofang Li[3]

[1]Department of Obstetrics and Gynecology, Affiliated Hospital of Guangdong Medical University, Zhanjiang, China, [2]Graduate School of Guangdong Medical University, Zhanjiang, China, [3]Department of Pathology, Affiliated Hospital of Guangdong Medical University, Zhanjiang, China

Small-cell neuroendocrine carcinoma (SCNEC) of the ovary is a gynecological malignancy characterized by rapid progression and poor prognosis. SCNEC is divided into primary and metastatic tumor. Primary ovarian neuroendocrine cancer is extremely rare and has a low 5-year survival rate. This paper reports the clinical manifestations of a 58-year-old patient with primary ovarian Small-cell neuroendocrine carcinoma and the prognosis after surgical adjuvant chemotherapy. The prevailing literature on this carcinoma is also reviewed and summarized. Our analysis reveals that histopathological examination is the standard diagnostic tool for ovarian SCNEC. We also highlight the importance of comprehensive imaging evaluation, early pathological diagnosis and comprehensive aggressive treatment to the prognosis of patients.

KEYWORDS

ovarian cancer, small cell neuroendocrine tumor, case report, metastatic disease, pulmonary type

Background

Neuroendocrine tumors are a group of heterogeneous tumors that originate from different neuroendocrine organs or stem cells. These tumors produce bioactive amines and polypeptide hormones. They usually occur in gastrointestinal pancreas, cervix or ovary (1). Gynecological neuroendocrine tumors are rare and there are no clear guidelines for their clinical management. For instance, ovarian neuroendocrine tumors account for about 2% of all gynecological tumors. Six percent of women have neuroendocrine cells in the ovarian stroma, and these cells contribute to the development primary ovarian neuroendocrine tumors. To date, the origin of neuroendocrine tumors is not clear. These tumors are divided into carcinoid, small cell neuroendocrine tumor, and large cell neuroendocrine tumor (2). Here, we report a patient with primary ovarian Small-cell neuroendocrine carcinoma with brain metastasis.

The clinical manifestation, diagnosis, and treatment of the patient are discussed. The patient gave written informed consent to the use of her clinical data for research. The study was approved by the Ethics Committee of the affiliated Hospital of Guangdong Medical University.

Case presentation

Basic information

A 58-year-old female patient who underwent brain surgery was suspected to have left frontal metastatic neuroendocrine carcinoma through postoperative pathology (Figure 1). After surgery, a pelvic MRI examination revealed a solid mass of about 2.4 cm * 3.5 cm * 3.4 cm on the right side of the pelvic region (Figure 2).

Auxiliary examinations

Gynecologic ultrasound showed irregular hypoecho mass (measuring 4.0 cm * 2. 7 cm) adjacent to the internal iliac arteriovenous vein in the right lower pelvis. Pelvic CTA demonstrated right pelvic cystic-solid mass; the lesion was supplied by blood from the right ovarian artery. In addition, pelvic MRI (Figure 2) showed a pelvic right solid mass, measuring about 2.4cm * 3.5cm * 3.4cm, with a clear boundary, local like linear signal connected to the uterus and potential right appendage source of malignant tumor lesions. Tests for serum tumor markers were negative.

Treatment

The patients received laparoscopic total uterine double attachment resection, bilateral ovarian arteriovenous high ligation, abdominal catheterization and postoperative adjuvant chemotherapy (chemotherapy regimen is shown in Table 1).

Postoperative pathological examination

Postoperative routine pathology showed an intact bilateral ovarian neuroendocrine carcinoma that was confined to the ovary (Figure 3). Immunohistochemistry analyses showed CD56 (+), CgA (+) Ki-67 index of about (30% -40%), PAX-8 (-), Syn (+), Vimentin (-) and WT-1 (-).

Prognosis and follow-up

The patient was still alive at a follow-up performed two years after surgery. There were no signs of recurrence during the follow-up period. However, the patient showed progressive memory decline, recent memory loss, loss of consciousness, behavioral regression, intermittent convulsions which could stop by themselves, and typical brain symptoms.

Discussion

Primary ovarian small cell carcinoma is a highly malignant gynecological tumor characterized by rapid progression and recurrence. Moreover, it has a low 5-year survival rate, with the 1- and 5- year survival rate being 50% and 10%, respectively (3). According to WHO 2017 Tumors of Female Genital Classification, small cell carcinoma of ovary are classified into Ovary-hypercalcemic Type (SCCOHT) and the Ovary-pulmonary Type (SCCOPT). SCCOPT was first reported by Eichhorn et al. (4) in 1992 (11 cases). However, According to the new WHO classification of Female Genital tumors (5), The concept of SCCOPT no longer exists. But the nomenclature concerning this clinical disorder has been ambiguous and highly

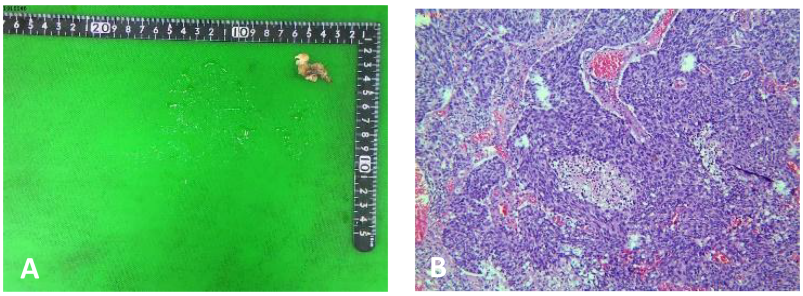

FIGURE 1
Pathology of brain surgery **(A)** A soft and grey brain solid mass tissue, 2.5 cm * 1.0 cm * 0.5 cm. **(B)** postoperative pathology:left frontal metastatic neuroendocrine carcinoma.

FIGURE 2
Pelvic magnetic resonance images showing a solid mass of about 2.4 cm * 3.5cm * 3.4cm on the right side of the pelvic region (arrow).

depended on histological features. We believe that this case is more consistent with SCCOPT in the old classification, Therefore, we continue to use the old term SCCOPT. In fact, less than 20 cases have been reported on SCCOPT in the past five years. We reviewed and analyzed previous data on ovarian small cell carcinoma as shown in Table 2.

Analysis of data on all the cases of lung-type small cell carcinoma generated in the past 5 years showed that all patients were similar in terms of age of onset, clinical symptoms, blood calcium level, pathological characteristics, and prognosis after treatment. However, in 75% of patients with lung small cell carcinoma, bilateral ovaries are involved and are often complicated with other gynecological tumors (5). However, the patient in our study had unilateral ovary carcinoma, with no other gynecological tumors. The patient was a postmenopausal 58-year-old woman who was diagnosed with a pelvic mass without any symptoms after brain surgery. The diagnosis of this condition is based on pathological examination. Previous data have shown that, histopathologically, most SCCOPT cases exhibit an inconspicuous sheet structural pattern, with monomorphic tumor cells showing spotted chromatin, inconspicuous or absent nucleoli, and reduced cytoplasm with nuclear atypia. The tumor cells may be arranged into rosettes in a few cases of SCCOPT. Consistently, our study demonstrates that the tumor cells had a uniform size, nested arrangement, slightly less cytoplasm, high ratio nucleoplasma, less obvious nucleoli, deep-stained cells and follicular space, which is different from features of the high calcium type small cell carcinoma (6).

Immunohistochemical characteristics of ovarian neuroendocrine tumors vary according to the type of tumor. Tumor cells in SCCOPT were cytoplasmically positive for neuroendocrine markers such as chromogranin, neuron-specific enolase, synaptophin and CD56 (membranous). Although chromogranin is the most specific marker, it has low sensitivity. For small cell neuroendocrine carcinoma, it has a positivity rate of about 50%. On the other hand, CD56 has been shown to be the most sensitive marker of neuroendocrine differentiation (62%), followed by CGA (39%) and SYN (26%) (7). These markers show positive results for epithelial cell membrane antigens and may be focal positive for vimentin and cytokeratin. In the present case, CD56 (+), CgA (+), Ki-67 index (30% - 40%), and Syn (+) results were consistent with those reported in previous studies and all of them predict good prognosis.

Clinically, SCCOPT must be distinguished from metastasis of lung and thymic small cell carcinoma to the ovary (8). The two are morphologically indistinguishable, with similar staining results of immune marker. They have neuroendocrine characteristics and can express specific neuroendocrine markers, such as chromogranin and chromopin A. Currently, differential diagnosis of SCCOPT is mainly based on pulmonary primary lesions and clinical history. In a previous study, cytokeratin 20 immunohistochemical findings showed that SCCOPT are perinuclear positive, while lung metastasis cancer show negative CK20 staining, which may provide a useful basis for the authentication and discrimination between SCCOPT and lung metastasis cancer (9). Although immunohistochemical tests did not show whether CK20 was positive, the patient had no history of smoking, chest discomfort or obvious abnormalities in chest CT. Therefore, lung small cell carcinoma was ruled out.

TABLE 1 Postoperative chemotherapy.

Period	Drug and dose	Side effect
1	Eetoposide 185mg + cisplatin 60mg	III leukocytes、II thrombocytopenia
2-5	Binding albumin paclitaxel 300mg + cisplatin 55mg	III leukopenia 、numbness of the hands and feet
6	Illinotecan 200mg + apatinib	III leukopenia
7-8	Carrelizumab 200mg + apatinib	/

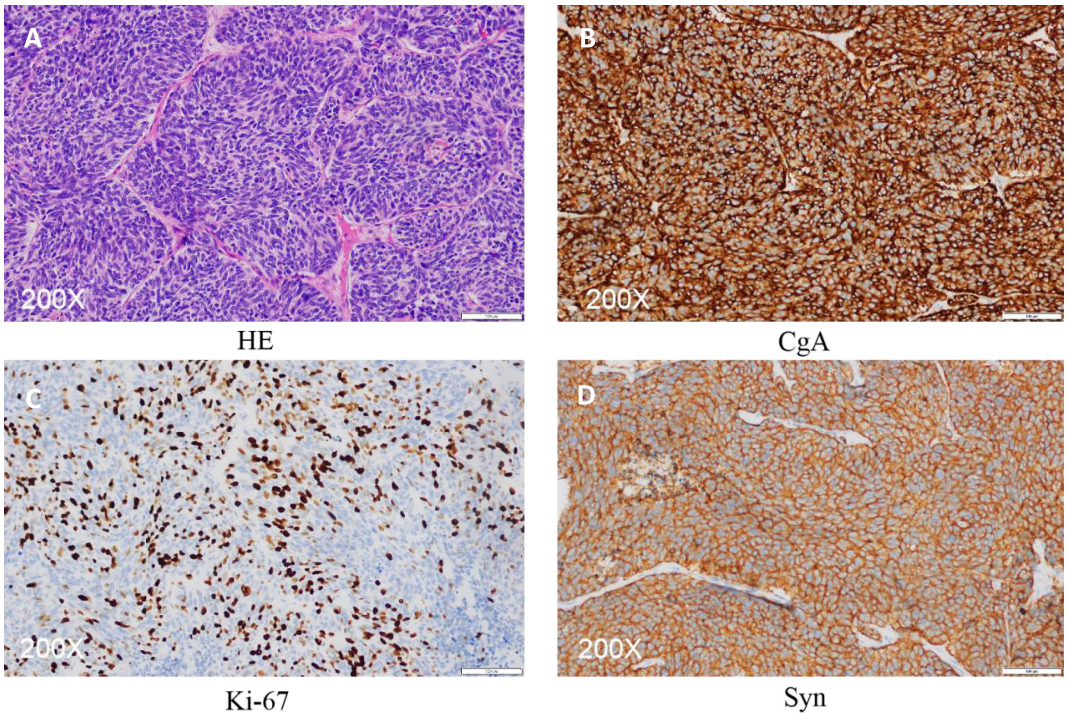

FIGURE 3
Pathology of ovarian surgery **(A)** HE stain. **(B–D)** Immunohistochemistry images showing the expression of CgA (+), ki-67 index about (30%-40%) and Syn (+).

Notably, the role of CK20 (+) in distinguishing ovarian primary SCCOPT from lung metastatic small cell carcinoma remains controversial.

Ovarian small cell carcinoma is mainly treated with surgical adjuvant chemotherapy. However, there is no standard chemotherapy regimen. Some studies have proposed that patient sensitivity to platinum drugs is dependent on disease stage, and these drugs may benefit patients with the early stage of the disease. However, of the currently used treatments are not effective. In 2020, Parikshaa Gupta et al. (6) analyzed three patients with stage IV lung small cell cancer who underwent tumor reduction surgery. Two patients received 6 cycles of TC regimen chemotherapy, and one experienced relapse after 1 month and no recurrence was reported after 30 months. The remaining one patient received six cycles of cisplatin plus etoposide chemotherapy plus 2 vaginal brachytherapy after 12

TABLE 2 Summary of published small cell carcinoma of the ovary.

Study	Age	n	Type	FIGO Stage	Outcome (follow-up period)
Syed A. Mannan et al.	21	1	SCCOPT(Left) and MOC	IC	DOD(10 months)
Eric M. Sieloff et al.	53	1	SCCOPT (Right)	Unstage	N/A
Parikshaa Gupta et al.	median 20	4	3 SCCOPT (bilateral) 1 SCCOPT (Right) and UEA	IV	1 N/A 1 NED (12 months) 2 AWD (12 months and 30 months)
Parikshaa Gupta et al.	44	1	SCCOPT(Right)	Unstage	N/A
D.Tsolakidis et al.	55	1	SCCOPT (Left)	IIIC	NED(21 months)
Lei Yin et al.	46	1	SCCOPT (bilateral) and UEA	Unstage	DOC(7 months)
Lin LI et al.	median 53	3	2 SCCOPT (Right) 1 SCCOPT (bilateral)	IC/IIIC/IV	2 NED(7 months and 30 months) 1 DOD(12 months)

UEA, Uterine Endometrioid Adenocarcinoma; MOC, Mucinous Ovarian Cancer; SCCOPT, SCCO of pulmonary type; AWD, alive with disease; DOD, dead of disease; DOC, dead of other courses; N/A, not available; NED, noevidence of disease.

months of follow-up. In 2021, Syed A. Mannan et al (10) performed tumor reduction plus 1 cycle of cisplatin + etoposide chemotherapy in one stage IC patient, who died after 10 months of follow-up. These data demonstrate that a combination of multiagent chemotherapy regimen and paclitaxel can prolong the survival time of patients in the stage of the disease or who develop postoperative recurrence.

In this case, the patient received surgical adjuvant chemotherapy and postoperative chemotherapy regimen (Table 1). Irinotecan specifically inhibits DNA topoisomerase I and interferes with DNA replication and cell division, which results in cytotoxicity. In comparison, apatinib is an orally targeted small-molecule anti-angiogenesis drug whereas carilizumab is a humanized anti-PD-1 monoclonal antibody with high affinity.

Chunyan Lan et al. (11) used a low dose of apatinib and carizumab in 10 patients with advanced Cervical Cancer, and obtained an objective remission rate of 55.6% (95% CI, 40.0% to 70.4%), as well as the median progression-free survival was 8.8 months (95% CI, 5.6 months to not estimable). Since the patient in our case had granulocytopia and other symptoms during the first 4 cycles of chemotherapy, it was replaced with second-line therapy. Follow-up data showed that the patient survived for more than 2 years after surgery but developed typical brain symptoms. In conclusion, the use of surgical adjuvant chemotherapy in this case prolonged the survival time of patients. Besides, platinum drugs were also effective for patients with small cell cancer, and their sensitivity was dependent on the disease stage. In summary, patients with small cell carcinoma of ovarian lung type require comprehensive treatment approach regardless of the stage.

Conclusion

In conclusion, SCCOPT is extremely rare. This cancer is common in postmenopausal women and has no specific clinical manifestations. The pathological and immunological examination of tumor tissues are the main diagnostic tools for this cancer. Positive expression of neuroendocrine markers; CD56, CgA, Syn, and negative results of Vimentin can confirm the diagnosis of SCCOPT. There is no effective treatment for patients with degree of malignancy and risk of relapse. The combination of surgical adjuvant multi-drug chemotherapy and platinum drugs can improve the prognosis of patients. Therefore, comprehensive imaging examination, early pathological diagnosis, and comprehensive treatment are important strategies to improve patient outcomes.

Data availability statement

The original contributions presented in the study are included in the article/supplementary material. Further inquiries can be directed to the corresponding author.

Ethics statement

The studies involving human participants were reviewed and approved by the Hospital Ethics Committee of the Affiliated Hospital of Guangdong Medical University. The patients/participants provided their written informed consent to participate in this study. Written informed consent was obtained from the individual(s) for the publication of any potentially identifiable images or data included in this article.

Author contributions

YL wrote the manuscript. YW contributed substantial advice help to polish the language. YZ conducted the project and revised the whole manuscript. XL was involved in preparing the pathological pictures. All authors contributed to the article and approved the submitted version.

Funding

This work was supported by the Natural Science Foundation of Guangdong Province (2017A030313559).

Conflict of interest

The authors declare that the research was conducted in the absence of any commercial or financial relationships that could be construed as a potential conflict of interest.

Publisher's note

References

1. Winer I, Kim C, Gehrig P. Neuroendocrine tumors of the gynecologic tract update. *Gynecol Oncol* (2021) 162(1):210–9.

2. Yin L, Li J, Wei Y, Ma D, Sun Y, Sun Y. Primary ovarian small cell carcinoma of pulmonary type with coexisting endometrial carcinoma in a breast cancer patient receiving tamoxifen: A case report and literature review. *Med (Baltimore)* (2018) 97(23):e10900.

3. Nasioudis D, et al. Small cell carcinoma of the ovary: A rare tumor with a poor prognosis. *Int J Gynecol Cancer* (2018) 28(5):932–8.

4. Eichhorn JH, Young RH, Scully RE. Primary ovarian small cell carcinoma of pulmonary type. a clinicopathologic, immunohistologic, and flow cytometric analysis of 11 cases. *Am J Surg Pathol* (1992) 16 (10):926–38.

5. McCluggage WG, Singh N, Gilks CB. Key changes to the World Health Organization (WHO) classification of female genital tumours introduced in the 5th edition. *Histopathology* (2022) 80(5):762–78.

6. Gupta P, et al. Small cell carcinoma of the ovary: Clinicopathologic and immunohistochemical analysis of 7 new cases of a rare malignancy. *Int J Surg Pathol* (2021) 29(3):236–45.

7. Zhu Y, et al. Clinicopathologic characteristics and survival outcomes in neuroendocrine carcinoma of the ovary. *Int J Gynecol Cancer* (2020) 30(2):207–12.

8. Oneda E, et al. Differential diagnosis of small cell carcinoma of the ovary or ovarian metastases of small cell carcinoma of the lung: A case report and review of the literature. *Case Rep Oncol* (2020) 13(2):822–8.

9. Rund CR, Fischer EG. Perinuclear dot-like cytokeratin 20 staining in small cell neuroendocrine carcinoma of the ovary (pulmonary-type). *Appl Immunohistochem Mol Morphol* (2006) 14(2):244–8.

10. Mannan SA, et al. A rare presentation of dual ovarian pathologies: Small cell carcinoma of the ovary and mucinous ovarian cancer. *Cureus* (2021) 13(11):e19468.

11. Lan C, et al. Camrelizumab plus apatinib in patients with advanced cervical cancer (CLAP): A multicenter, open-label, single-arm, phase II trial. *J Clin Oncol* (2020) 38(34):4095–106.

frontiers | Frontiers in Oncology

TYPE Case Report
PUBLISHED 23 September 2022
DOI 10.3389/fonc.2022.1009884

OPEN ACCESS

EDITED BY
Federico Ferrari,
University of Brescia, Italy

REVIEWED BY
Vito Andrea Capozzi,
University Hospital of Parma, Italy
Francesco Marasciulo,
Civil Hospital of Brescia, Italy

*CORRESPONDENCE
Lorenza Driul
lorenza.driul@uniud.it

SPECIALTY SECTION
This article was submitted to Gynecological Oncology, a section of the journal Frontiers in Oncology

RECEIVED 02 August 2022
ACCEPTED 31 August 2022
PUBLISHED 23 September 2022

CITATION
Restaino S, Paparcura F, Giorgiutti C, Trojan D, Montagner G, Pengo G, Pividore G, Albanese R, Rampino E, Dogareschi T, Bove T, Titone F, Trovò M, Garganese G, Parodi PC, Scambia G, Driul L and Vizzielli G (2022) Human amniotic membrane for myocutaneous dehiscence after a radical surgical treatment of vulvar cancer: A case report. *Front. Oncol.* 12:1009884. doi: 10.3389/fonc.2022.1009884

Human amniotic membrane for myocutaneous dehiscence after a radical surgical treatment of vulvar cancer: A case report

Stefano Restaino[1], Federico Paparcura[2], Cristina Giorgiutti[2], Diletta Trojan[3], Giulia Montagner[3], Giancarlo Pengo[4], Grazia Pividore[5], Roberta Albanese[6], Emanuele Rampino[6], Teresa Dogareschi[7], Tiziana Bove[2,7], Francesca Titone[8], Marco Trovò[8], Giorgia Garganese[9,10], Pier Camillo Parodi[6], Giovanni Scambia[10,11], Lorenza Driul[2]* and Giuseppe Vizzielli[2]

[1]Department of Maternal and Child Health, Obstetrics and Gynecology Clinic, University Hospital of Udine, Udine, Italy, [2]Medical Area Department (Dipartimento di Area Medica, DAME), Università degli Studi di Udine, Udine, Italy, [3]Fondazione Banca dei tessuti di Treviso Onlus, Treviso, Italy, [4]Surgical Video Production & Multimedia Medical – Azienda Sanitaria Universitaria Friuli Centrale, Udine, Italy, [5]Piwimed s.r.l., Udine, Italy, [6]Dipartimento di Scienze Chirurgiche, Clinica di Chirurgia Plastica Ricostruttiva, Università degli Studi di Udine, Udine, Italy, [7]Department of Anesthesia and Intensive Care, University Hospital of Udine, Udine, Italy, [8]Radiation Oncology Department, University Hospital of Udine, Udine, Italy, [9]Gynecology and Breast Care Center, Mater Olbia Hospital, Olbia, Italy, [10]Dipartimento di Scienze della Vita e Sanità Pubblica, Università Cattolica del Sacro Cuore, Roma, Italy, [11]Dipartimento per la salute della Donna e del Bambino e della Salute Pubblica, Fondazione Policlinico Universitario Agostino Gemelli IRCCS, Unità Operativa Complessa Ginecologia Oncologica, Roma, Italy

Background: The application of the amniotic membrane could have a favourable effect on tissue repair and regeneration. We report the first case of implant of an amniotic membrane in a patient affected by myo-cutaneous dehiscence, after a radical surgical treatment for vulvar cancer.

Methods: We describe a case of a 74-years-old patient affected by vulvar cancer. After radiotherapy, the patient underwent to an anterior pelvic exenteration with uretero-ileo-cutaneostomy by Wallace, bilateral pelvic lymphadenectomy, omental biopsies, omental flap, bilateral inguinal lymphadenectomy, resection of ulcerated left inguinal lesion, reconstruction with left gracilis muscle flap and locoregional V-Y advancement flap. The patient developed a myo-cutaneous dehiscence. Two months after the surgery, following an accurate curettage of the wound and negative pressure therapy, a patch of human amniotic membrane was implanted.

Results: The surgical procedure was easy, feasible and did not require long operating room times. No intraoperative or postoperative complications occurred. The results obtained were encouraging with a marked improvement in the surgical wound.

10.3389/fonc.2022.1009884

Conclusion: the use of amniotic membranes was safely and easily performed to promote the healing of complicated surgical wounds.

KEYWORDS

amniotic membrane, case report, allograft, vulvar cancer, dehiscence

Introduction

Vulvar cancer is one of most rare gynecological tumors, in fact, it accounts for only 2-5% of the cases (1). Squamous cell carcinoma (SCC) of the vulva, the most common subtype, has traditionally been considered a disease of postmenopausal women, although the average age of incidence has decreased in recent years due to the increase in HPV infections worldwide (1–4). The treatment of vulvar cancer depends mainly on histology and staging (1, 2), other variables influencing the management are age, coexistence of comorbidities and the patient's performance status. Treatment is predominantly surgical, particularly for SCC, although concomitant chemoradiation is an effective alternative, particularly for advanced tumors and those where pelvic exenteration would be necessary to obtain adequate surgical edges (1–5). The most severe and common postoperative complications of vulvar cancer surgery are lymphedema, lymphocele, and wound dehiscence. In particular, en bloc surgery raised complications and wound dehiscence to 70-90% of cases (6, 7). The use of negative pressure therapy is an option for the conservative management of large wounds dehiscence (8). Human amniotic membrane (HAM) has been reported as a versatile graft in many surgical interventions. The first clinical application of HAM dates back to 1910 (9) and since then several studies reports its efficacy, especially as a biological dressing for chronic wounds (10, 11), but also in gynecological surgery (12, 13). In fact, HAM promotes cell migration and proliferation; it has anti-inflammatory and antimicrobial properties without prompting immunoreaction in the recipient (14–17). We describe the first case of implantation of HAM in a patient affected by vulvar cancer with a myocutaneuos dehiscence.

Case description

We report the case of a 74-year-old female patient with previous bilateral salpingo-oophorectomy and hysterectomy for uterine fibromatosis. She had a clinical history of hypertension and dyslipidaemia and a silent family history. The patient came to our attention due to the development of itching and vulvar oedema associated with leucoxantorrhoea. A gynaecological examination under narcosis with multiple biopsies was performed. Histological examination diagnosed unrelated HPV infiltrating squamous cell carcinoma cT3 N2 MX. Staging MRI and PET-CT were subsequently performed, which confirmed vulvar neoplasia with locoregional infiltration and bilateral lymph node localisation. Imaging also revealed the presence of a lung abdensation, which was biopsied and diagnosed as adenocarcinoma with pulmonary primitivity. The lung tumour underwent radiotherapy treatment, with complete response. On the subsequent PET-CT scan it was no longer described.

For the vulvar neoplasm, the patient underwent radiotherapy treatment for a total of 35 sessions. From 13th July 2021 to 28th September 2021, we performed exclusive radiotherapy treatment of vulvar neoplasm and loco-regional lymph node drainage (total dose 54 Gy in 35 sessions). Three months after radiotherapy treatment, we observed a persistent of the disease confirmed also by PET-CT scan examination. For this reason, the patient was submitted on 27th January 2022 to an anterior pelvic exenteration with uretero-ileo-cutaneostomy packing by Wallace (18), bilateral pelvic lymphadenectomy, omental biopsies, omental flap, bilateral inguinal lymphadenectomy, resection of ulcerated left inguinal lesion, reconstruction with left gracilis muscle flap and locoregional V-Y advancement flap. Two days after surgery, the gracilis muscle flap was distressed with subsequent dehiscence of the surgical wound (Figure 1). For this reason, we decided to apply negative pressure therapy at the dehiscence site. Considering the difficulties in healing on 11th April 2022 we decided to implant amniotic membrane on surgical wound because of its anti-inflammatory and antimicrobial properties (Figures 2A, B). The human amniotic membrane was provided by Treviso Tissue Bank Foundation, a non-profit health organization accredited by the National Transplant Centre. The placenta is collected from donors undergoing caesarean delivery, after their consent for the donation. Donors areselected and screened according to Italian requirement, that includes serological and molecular tests. The placenta is processed in a Good Manufacturing Practice (GMP) compliant facility, shortly after retrieval. The amniotic membrane is carefully detached from the chorion and rinsed with sterile saline solution to remove residual blood. Subsequently, amniotic membrane is immersed in a cocktail of antibiotics validated for tissue decontamination

FIGURE 1
Myo-cutaneous dehiscence.

(19, 20). After the removal of blood and spongy residues, amniotic membrane is cut in patches of desired sizes, that are positioned on filters in contact with the stromal side, to keep the orientation. Amniotic membrane is then stored in vapor phase liquid nitrogen, immersed in a cryopreserving solution made up with Base medium (Alchimia Srl, Italy), DMSO (WAK-Chemie, Germany) and human albumin (Kedrion, Italy). On that date, the patient still had a continuous solution between the

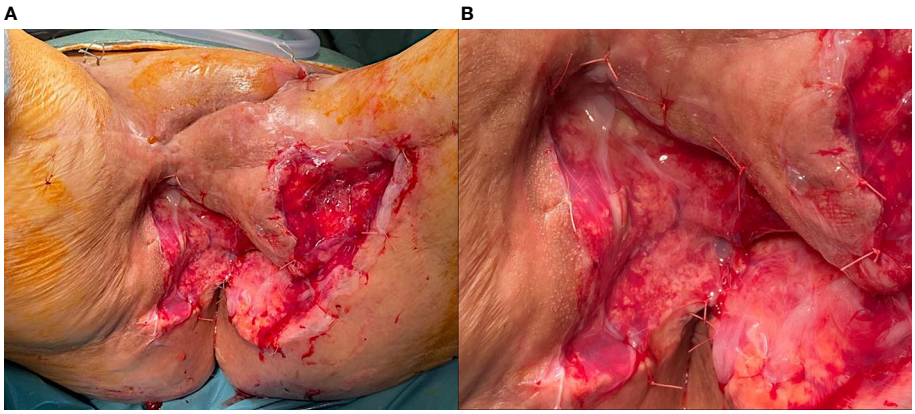

FIGURE 2
(A) Human amniotic membrane application. **(B)** Human amniotic membrane detail.

myocutaneous gracilis flap and the root of the right thigh, about 5-6 cm in longitudinal diameter, which deepened by about 2 cm. There was also a further continuous solution at the level of the root of the left thigh, the myocutaneous flap and the inguinal root, approximately 3 cm in maximum diameter and 1-2 cm deep, which was in continuity with the previous one at the level of the anal margin.

Surgical procedure

Under general anaesthesia, the patient was placed in the lithotomy position. We removed the negative pressure therapy. Following an accurate curettage of the vulvar scar with a curette to remove the granulation tissue, the tract was prepared for the implant of the HAM. The cryopreserved HAM resting on a filter was thawed in the operating room by immersion in a bath of saline solution at 40°C, without removing the packaging. It was subsequently washed twice in saline solution at 25°C; finally, one side of the square HAM was transfixed with a resorbable suture (2-0 Vicryl^{TM}, Ethicon Endo-Surgery, Inc., Cincinnati, OH, USA). Attention was paid to place the epithelial side of the HAM outward, to face the dehiscence wound (Figures 2A, B). The temporal timeline of the clinical case is showed in Figure 3.

Results

No intraoperative or postoperative complications occurred. Stool softeners and analgesics were prescribed as needed. We continued to use negative pressure therapy at the wound site, changing the dressing weekly. Within 10 days of the amniotic membranes being placed, the wounds had significantly reduced (Figure 4). On 23rd April 2022 the patient died for other circumstances unrelated to the surgical procedure. However, the results obtained were encouraging with a marked improvement in the surgical wound.

Discussion

The implantation of amniotic membranes on surgical wounds appears to be safe; moreover, the psychological impact of the treatment on our patient was acceptable, with an improvement also in terms of pain and thus quality of life. HAM has already been used in several sites of the gastrointestinal tract, such as the duodenum, colon and rectovaginal fistula (21, 22). The use of HAM is also a widespread clinical practice in other fields of medicine such as eye surgery and the treatment of an increasing number of ocular surface diseases (23).

To our knowledge, this is the first case of using HAM to promote healing of a surgical wound in a patient with gynecological oncology. The benefits of amniotic membrane placement in difficult-to-heal surgical wounds could be related to its anti-inflammatory and antimicrobial properties and low immunogenicity (14–17). In fact, no immunosuppression therapy was administered to the patients and no immune reaction was triggered by the HAM, analogously to other published clinical application of this graft (24–27).

Due to sudden death, it was not possible to evaluate the long-term outcome of this procedure, but the results obtained seemed encouraging, considering the progression of healing achieved in the first two weeks after application of the amniotic membrane.

-.1This is an isolated case of the application of HAM, with a follow-up that is too limited to establish their real effectiveness.

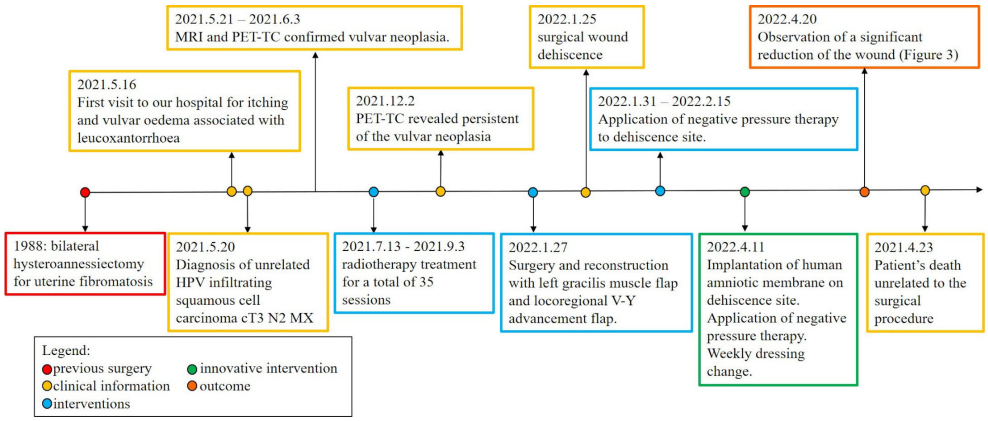

FIGURE 3
Timeline of the clinical case.

FIGURE 4
Effect of human amniotic membrane after two weeks.

Within the limits of this case report, a promising suggestion has been made regarding the use of HAM for gynecological surgery.

Conclusion

Taking into account the high risk of dehiscence in vulvar cancer patients undergoing radical surgery, the use of HAMs could be a weapon to be considered. Case series providing longer follow-up should be encouraged, in order to provide useful data for increased use of this technique. In particular, future clinical studies could aim at comparing the efficacy of HAM versus traditional techniques.

Data availability statement

The raw data supporting the conclusions of this article will be made available by the authors, without undue reservation.

Ethics statement

Ethical review and approval was not required for the study on human participants in accordance with the local legislation and institutional requirements. The patients/participants provided their written informed consent to participate in this study. Written informed consent was obtained from the individual(s) for the publication of any potentially identifiable images or data included in this article.

Author contributions

SR: Conceptualization and original draft preparation; FP: data curation and methodology; CG: data curation; GM and DT were involved in the drafting and revision of the manuscript. GP: software; GP: visualization; RA: supervision; ER: supervision; TD: methodology; TB: supervision; GG: validation; PP: validation; GS: validation; LD: validation; GV: Conceptualization and supervision. All authors contributed to the article and approved the submitted version.

Acknowledgments

We thank Dr Morandini Marzia, Dr Barbui Elisa, Dr Spampinato Angelina, all nursing personnel and operating room staff of the Obstetrics and Gynecology Unit.

Conflict of interest

Author GPi was employed by Piwimed s.r.l.

The remaining authors declare that the research was conducted in the absence of any commercial or financial relationships that could be construed as a potential conflict of interest.

Publisher's note

References

1. Rogers LJ, Cuello MA. Cancer of the vulva. *Int J Gynaecol Obstet* (2018) 143 Suppl 2:4–13. doi: 10.1002/ijgo.12609

2. Kang YJ, Smith M, Barlow E, Coffey K, Hacker N, Canfell K. Vulvar cancer in high-income countries: Increasing burden of disease. *Int J Cancer* (2017) 141:2174–86. doi: 10.1002/ijc.30900

3. Hacker NF, Eifel PJ, van der Velden J. Cancer of the vulva. *Int J Gynecol Obstet* (2015) 131(Suppl 2):S76–83. doi: 10.1016/j.ijgo.2015.06.002

4. Koh WJ, Greer BE, Abu-Rustum NR, Campos SM, Cho KR, Chon HS, et al. Vulvar cancer, version 1.2017, NCCN clinical practice guidelines in oncology. *J Natl Compr Canc Netw* (2017) 15(1):92–12. doi: 10.6004/jnccn.2017.0008

5. Rao YJ, Chin RI, Hui C, Mutch DG, Powell MA, Schwarz JK, et al. Improved survival with definitive chemoradiation compared to definitive radiation alone in squamous cell carcinoma of the vulva: A review of the national cancer database. *Gynecol Oncol* (2017) 146(3):572–9. doi: 10.1016/j.ygyno.2017.06.022

6. Rahm C, Adok C, Dahm-Kähler P, Bohlin KS. Complications and risk factors in vulvar cancer surgery - a population-based study. *Eur J Surg Oncol* (2022) 48 (6):1400–6. doi: 10.1016/j.ejso.2022.02.006

7. Gitas G, Proppe L, Baum S, Kruggel M, Rody A, Tsolakidis D, et al. A risk factor analysis of complications after surgery for vulvar cancer. *Arch Gynecol Obstet* (2021) 304(2):511–9. doi: 10.1007/s00404-020-05949-w

8. Norman G, Shi C, Goh EL, Murphy EM, Reid A, Chiverton L, et al. Negative pressure wound therapy for surgical wounds healing by primary closure. *Cochrane Database Syst Rev* (2022) 4(4):CD009261. doi: 10.1002/14651858.CD009261.pub7

9. Davis JW. Skin transplantation with a review of 550 cases at the johns Hopkins hospital. *Johns Hopkins Med J* (1910) 15:307. doi: 10.1097/00000658-190909000-00022

10. Valiente MR, Nicolás FJ, García-Hernández AM, Fuente Mora C, Blanquer M, Alcaraz PJ, et al. Cryopreserved amniotic membrane in the treatment of diabetic foot ulcers: A case series. *J Wound Care* (2018) 27(12):806–15. doi: 10.12968/jowc.2018.27.12.806

11. Mermet I, Pottier N, Sainthillier JM, Malugani C, Cairey-Remonnay S, Maddens S, et al. Use of amniotic membrane transplantation in the treatment of venous leg ulcers. *Wound Repair Regener* (2007) 15(4):459–64. doi: 10.1111/j.1524-475X.2007.00252.x

12. Bleggi-Torres LF, Werner B, Piazza MJ. Ultrastructural study of the neovagina following the utilization of human amniotic membrane for treatment of congenital absence of the vagina. *Braz J Med Biol Res* (1997) 30(7):861–4. doi: 10.1590/S0100-879X1997000700007

13. Fotopoulou C, Sehouli J, Gehrmann N, Schoenborn I, Lichtenegger W. Functional and anatomic results of amnion vaginoplasty in young women with Mayer-Rokitansky-Küster-Hauser syndrome. *Fertil Steril* (2010) 94(1):317–23. doi: 10.1016/j.fertnstert.2009.01.154

14. Wassmer CH, Berishvili E. Immunomodulatory properties of amniotic membrane derivatives and their potential in regenerative medicine. *Curr Diabetes Rep* (2020) 20(8):31. doi: 10.1007/s11892-020-01316-w

15. Hao Y, Ma DH, Hwang DG, Kim WS, Zhang F. Identification of antiangiogenic and antiinflammatory proteins in human amniotic membrane. *Cornea* (2000) 19(3):348–52. doi: 10.1097/00003226-200005000-00018

16. Adinolfi M, Akle CA, McColl I, Fensom AH, Tansley L, Connolly P, et al. Expression of HLA antigens, beta 2-microglobulin and enzymes by human amniotic epithelial cells. *Nature* (1982) 295(5847):325–7. doi: 10.1038/295325a0

17. Akle CA, Adinolfi M, Welsh KI, Leibowitz S, McColl I. Immunogenicity of human amniotic epithelial cells after transplantation into volunteers. *Lancet* (1981) 2(8254):1003–5. doi: 10.1016/S0140-6736(81)91212-5

18. Wallace DM. Ureteric diversion using a conduit: a simplified technique. *Br J Urol* (1966) 38(5):522–7. doi: 10.1111/j.1464-410X.1966.tb09747.x

19. Montagner G, Trojan D, Cogliati E, Manea F, Vantini A, Paolin A. Stability analysis of the antibiotic cocktail used by treviso tissue bank foundation for tissues decontamination. *Cell Tissue Banking* (2018) 19(4):721–6. doi: 10.1007/s10561-018-9725-y

20. Serafini A, Riello E, Trojan D, Cogliati E, Palù G, Manganelli R, et al. Evaluation of new antibiotic cocktails against contaminating bacteria found in allograft tissues. *Cell Tissue Banking* (2016) 17(4):619–28. doi: 10.1007/s10561-016-9581-6

21. Niknejad H, Peirovi H, Jorjani M, Ahmadiani A, Ghanavi J, Seifalian AM. Properties of the amniotic membrane for potential use in tissue engineering. *Eur Cell Mater* (2008) 15:88–99. doi: 10.22203/eCM.v015a07

22. Hosseini SV, Haghpanah Aski M, Al-Hurry AMAH, Hassan A-RK, Khazraei H, Zabangirfard Z, et al. Simultaneous application of human amniotic membrane and tachosil® in the repair of recto-vaginal fistula in an animal model. *Comp Clin Path* (2017) 26:405–9. doi: 10.1007/s00580-016-2391-1

23. Paolin A, Cogliati E, Trojan D, Griffoni C, Grassetto A, Elbadawy HM, et al. Amniotic membranes in ophthalmology: long term data on transplantation outcomes. *Cell Tissue Bank* (2016) 17(1):51–8. doi: 10.1007/s10561-015-9520-y

24. Frigerio I, Bannone E, Trojan D, Montagner G, Bergamaschi G, Butturini G. Implantation of amniotic membrane over pancreatic anastomosis after pancreaticoduodenectomy: report of the first case. *J Surg Case Rep* (2019) 2019 (5):rjz097. doi: 10.1093/jscr/rjz097

25. Ragazzo M, Val M, Montagner G, Trojan D, Fusetti S, Guarda Nardini L. Human amniotic membrane: an improvement in the treatment of medication-related osteonecrosis of the jaw (MRONJ)? a case-control study. *Cell Tissue Bank* (2022) 23(1):129–41. doi: 10.1007/s10561-021-09922-y

26. Grossi U, Romano M, Rossi S, Gallo G, Picciariello A, Felice C, et al. Anal fistula human amniotic membrane endosealing (F-HAME): A proof of concept study. *Front Surg* (2022) 9:869923. doi: 10.3389/fsurg.2022.869923

27. Ratto C, Parolini O, Marra AA, Orticelli V, Parello A, Campennì P, et al. Human amniotic membrane for the treatment of cryptoglandular anal fistulas. *J Clin Med* (2022) 11(5):1350. doi: 10.3390/jcm11051350

frontiers | Frontiers in Oncology

TYPE Original Research
PUBLISHED 06 October 2022
DOI 10.3389/fonc.2022.961678

OPEN ACCESS

EDITED BY
Federico Ferrari,
University of Brescia, Italy

REVIEWED BY
Carlo Ronsini,
Università degli Studi della Campania "Luigi Vanvitelli", Italy
Jun Wang,
Fourth Hospital of Hebei Medical University, China

*CORRESPONDENCE
Yanqing Li
liyanqing1017@163.com
Lianyin Jia
jlianyin@163.com

SPECIALTY SECTION
This article was submitted to Gynecological Oncology, a section of the journal Frontiers in Oncology

RECEIVED 05 June 2022
ACCEPTED 21 September 2022
PUBLISHED 06 October 2022

CITATION
Jiang K, Ai Y, Li Y and Jia L (2022) Nomogram models for the prognosis of cervical cancer: A SEER-based study. *Front. Oncol.* 12:961678. doi: 10.3389/fonc.2022.961678

Nomogram models for the prognosis of cervical cancer: A SEER-based study

Kaijun Jiang[1], Yiqin Ai[2], Yanqing Li[2*] and Lianyin Jia[1*]

[1]Yunnan Key Laboratory of Artificial Intelligence, Kunming University of Science and Technology, Kunming, China, [2]Department of Radiation Therapy, The Third Affiliated Hospital of Kunming Medical University, Kunming, China

Background: Cervical cancer (CC) is one of the most common cancers in women. This study aimed to investigate the clinical and non-clinical features that may affect the prognosis of patients with CC and to develop accurate prognostic models with respect to overall survival (OS) and cancer-specific survival (CSS).

Methods: We identified 11,148 patients with CC from the SEER (Surveillance, Epidemiology, and End Results) database from 2010 to 2016. Univariate and multivariate Cox regression models were used to identify potential predictors of patients' survival outcomes (OS and CSS). We selected meaningful independent parameters and developed nomogram models for 1-, 3-, and 5-year OS and CSS *via* R tools. Model performance was evaluated by C-index and receiver operating characteristic curve. Furthermore, calibration curves were plotted to compare the predictions of nomograms with observed outcomes, and decision curve analysis (DCA) and clinical impact curves (CICs) were used to evaluate the clinical effectiveness of the nomograms.

Results: All eligible patients (n=11148) were randomized at a 7:3 ratio into training (n=7803) and validation (n=3345) groups. Ten variables were identified as common independent predictors of OS and CSS: insurance status, grade, histology, chemotherapy, metastasis number, tumor size, regional nodes examined, International Federation of Obstetrics and Gynecology stage, lymph vascular space invasion (LVSI), and radiation. The C-index values for OS (0.831 and 0.824) and CSS (0.844 and 0.841) in the training cohorts and validation cohorts, respectively, indicated excellent discrimination performance of the nomograms. The internal and external calibration plots indicated excellent agreement between nomogram prediction and actual survival, and the DCA and CICs reflected favorable potential clinical effects.

Conclusions: We constructed nomograms that could predict 1-, 3-, and 5-year OS and CSS in patients with CC. These tools showed near-perfect accuracy and clinical utility; thus, they could lead to better patient counseling and personalized and tailored treatment to improve clinical prognosis.

KEYWORDS

cervical cancer, nomogram, overall survival, cancer-specific survival, SEER database

Introduction

Cervical cancer (CC) is one of the most commonly occurring cancers in women. Despite being one of the most preventable cancers through screening, cervical cancer caused the death of 4138 women in the US in 2018, the equivalent of 11 women per day, one-half of whom were aged ≤58 years at death (1). Although the overall incidence of CC has been declining for decades, rates of the distant-stage disease and cervical adenocarcinoma, which are often undetected by cytology, are increasing; this increase is largely driven by trends in young women (2). These findings underscore the need for more targeted efforts to increase both human papillomavirus (HPV) vaccination among all individuals aged ≤26 years and primary HPV testing or HPV/cytology co-testing every 5 years in women from the age of 25 years, as recommended by the American Cancer Society in updated guidelines published in 2020 (3, 4). The clinical stage is a reliable and widely accepted indicator that can be used to evaluate the prognosis of patients with CC (5). At the end of April 2022, there were two main clinical staging schemes: the American Joint Committee on Cancer (AJCC) Staging Seventh Edition and the International Federation of Obstetrics and Gynecology (FIGO) 2009 Guidelines. FIGO staging is mainly based on clinical characteristics, but few studies have considered the impact of non-clinical parameters on its clinical utility and net benefit in patients with CC (6–9). Clinical staging is mainly based on cervical tumor size or extent of pelvic disease, with less weight given to other important prognostic factors such as age, race, and treatment modality. Therefore, clinical staging alone is insufficient to predict the prognosis of patients with CC, and a more complete prognostic assessment protocol is required. Herein, we revised the TNM stage according to the FIGO classification (2009 version) and explored the use of nomogram models for prognosis prediction in patients with CC in terms of overall survival (OS) and cancer-specific survival (CSS) in combination with clinical and non-clinical indicators.

The nomogram model is a simple visualization tool based on multivariate Cox proportional hazard regression, which is becoming increasingly popular in oncology as a means of predicting and quantifying the probability of an individual patient's survival (10). Our data were based on the Surveillance, Epidemiology, and Outcomes Database (SEER), which collects data on cancer diagnosis, treatment, and survival, covering approximately 35% of the US population (11). This widely used resource collects demographic, clinical, and outcome information on all types of cancer and makes it freely available to researchers (11).

In this retrospective study, we developed nomogram models to provide a simple graphical representation of clinical events and generate numerical probabilities (12), and derived and validated prognostic profiles to predict OS and CSS in patients with CC enrolled in the SEER database from 2010 to 2016. We expect these nomograms to have applications in supporting clinical decision-making and ongoing work. Compared with other studies evaluating survival prognosis in patients with CC using nomograms (6–9), the sample of patients with more complete patient parameters enrolled in our study enabled us to use more real-time data (13). Importantly, we predicted CSS and OS and evaluated our model internally and externally using five approaches: the C-index (Harrell protocol index), receiver operating characteristic (ROC) curves, calibration plots, decision curve analysis (DCA) and clinical impact curves (CICs), making our study more complete and reliable compared with previous studies.

Material and methods

Patients and endpoints

The study used the database of the SEER National Cancer Institute (https://seer.cancer.gov/), a free US cancer registry. We gained access to SEER database files, and all authors followed SEER database policies throughout the search process. Individual informed consent was not required because no personal data were used in this study.

Information on patients newly diagnosed with CC between 2010 and 2016 was extracted from the SEER-18 database using the SEER*Stat software version 8.3.9.2. As information on site-specific metastases was only available from 2010 in the SEER database, we limited the scope of the analysis to the period 2010–2016. Patients with CC were considered eligible to be enrolled in this study if they had only one primary malignancy, an end date of active surveillance, and complete clinical and pathological information (e.g., age, race, FIGO stage, tumor grade, and treatment). Variables for each patient included age, race, marital status, insurance, primary site, TNM status, pathological type, histological grade, distant metastasis, treatment strategy, vital status, and survival time. The exclusion criteria in this study were as follows: (a) unknown AJCC 6th TNM stage; (b) unknown marital status; (c) unknown race; (d) regional median family income; (e) unknown laterality of the tumor; (f) unknown tumor size; (g) unknown histological grade; (h) unknown radiotherapy and chemotherapy records; and (i) unknown survival months. In our study, TNM status was classified according to FIGO (2009 edition). Distant metastases were diagnosed in the lymph nodes, liver, lung, bone, and brain. We added a variable of "metastasis numbers", which was classified according to the transfer of organs. Local treatment of primary tumors was mainly by surgery or radiation therapy. The surgical approach was characterized by three variables: radiation sequence with surgery (RSS), primary site surgery, and regional lymph node surgery (RLNS). Radiation was

classified into four types: beam radiation, brachytherapy, combination of beam with brachytherapy (BRB), and no/unknown treatment. The primary endpoints of this study were OS and CSS of patients with CC.

Statistical analysis

All eligible patients were randomized in a 7:3 ratio into training and validation groups. Chi-square test was used to compare clinical and pathological characteristics between the training and validation groups. The nomograms were developed in the training cohort as follows. First, univariate Cox analysis was used to evaluate the ability of each variable to predict OS. Second, variables that reached statistical significance in the univariate Cox analysis were fitted in the multivariate Cox analysis. To identify independent variables that had significant impact on patient outcomes, an adverse selection procedure using Akaike information criterion (AIC) scores for variable selection was introduced. Finally, the remaining variables were used in the construction of the nomograms. The primary endpoints of the nomograms were 1-, 3-, and 5-year OS and CSS.

The nomograms were validated in the training cohort and the validation cohort. To assess the predictive accuracy of the nomogram, we used the C-index, ROC curves (14), and calibration curves (with 1000 bootstrap resamples) to visually differentiate the predicted and actual values for 1-, 3-, and 5-year OS and CSS. Furthermore, DCA and CICs were used to assess the clinical value of the nomogram (15). Kaplan–Meier analysis and log-rank test were used to investigate the differences in survival between three risk subgroups. The chi-square test results for these variables between the training and validation cohorts all had $P > 0.05$. All analyses were conducted using R version 4.1.3 in RStudio.

Results

Patient baseline characteristics

Our study identified 11,148 eligible patients diagnosed with CC from 2010 to 2016, with 7803 patients assigned to the training cohort and 3345 patients to the validation cohort. The demographic and clinicopathologic characteristics of patients in the training and validation cohorts are listed in Table 1. The median age of all patients was 47 years, with a range of 20–70 years. Most patients in both cohorts were older (≥40 years) and White. The most common pathological type of CC was SCC (squamous cell carcinoma) (69.62%). Regarding metastasis (5.10%), the most frequent site of metastasis was the lung (3.23%), followed by bone (1.96%), liver (1.52%), and brain (0.31%). In both cohorts, more than half of the patients were treated with radiotherapy or chemotherapy. In addition, initial examination of regional lymph nodes had been performed for only about 45% of patients.

Univariate and multivariate analyses

The results of the univariate and multivariate Cox regression analyses (16) for OS and CSS in the training cohort are shown in Table 2. In the univariate Cox regression, all variables were significant for both OS and CSS ($P < 0.05$). Therefore, all variables were included in the multivariate Cox regression analyses for OS and CSS to identify independent prognostic factors. For OS, the independent prognostic factors included age, race, insurance, grade, histology, chemotherapy, metastasis number, tumor size, regional nodes examined, FIGO stage, lymph vascular space invasion (LVSI), regional lymph node surgery (RLNS), and radiation. For CSS, the independent prognostic factors included marital status, insurance, grade, histology, chemotherapy, metastasis number, tumor size, regional nodes examined, FIGO stage, LVSI, and radiation. Compared with the independent for OS, these findings of CSS were not consistent in terms of independent prognostic variables including age, race, marital status, and RLNS.

Construction of prognostic nomograms

After selecting the minimum AIC value, the above-mentioned parameters were used to develop nomograms for predicting 1-, 3-, and 5-year OS and CSS (Figure 1). Each variable was given a score based on the corresponding point on the "point axis". Next, we added the scores of all variables to obtain a total score, and then drew a vertical line from the "total point axis" to the corresponding "survival axis" to estimate the predicted probability of 1-, 3-, and 5-year OS and CSS. According to the nomograms, we concluded that FIGO stage made the largest contribution to the predicted probability, followed by metastasis and grade respectively.

Validation of the nomograms

We performed internal training and external validation on the nomograms using different cohorts. In the internal cohort, we obtained C-index values of 0.831 (95% CI, 0.823–0.839) for prediction of OS, and 0.844 (95% CI, 0.836–0.852) for prediction of CSS. In the external validation cohort, we obtained C-index values of 0.824 (95% CI, 0.810–0.838) for OS and 0.841 (95% CI, 0.827–0.855) for CSS. The calibration plots for the nomograms showed that the predictions of OS (Figure 2) and CSS (Figure 3) made by the 1-, 3-, and 5-year survival probability models were almost consistent with actual observations, in both the internal and external cohorts.

10.3389/fonc.2022.961678

TABLE 1 Characteristics of patients with cervical cancer in the training cohort and validation cohort.

Characteristic	Training cohort	Validation cohort	All subjects	*P*
	7803 (70)	3345 (30)	11148 (100)	
Age, median [range]	47 [38, 56]	47 [38, 57]	47 [38, 56]	0.9977
Age, *n* (%)				0.7714
>=20 and <40	2198 (28.17)	952 (28.46)	3150 (28.26)	
>=40 and <70	5605 (71.83)	2393 (71.54)	7998 (71.74)	
Race, *n* (%)				0.2534
Black	1025 (13.14)	416 (12.44)	1441 (12.93)	
White	5953 (76.29)	2600 (77.73)	8553 (76.72)	
Other	825 (10.57)	329 (9.84)	1154 (10.35)	
Marital, *n* (%)				0.6559
Married	5177 (66.35)	2204 (65.89)	7381 (66.21)	
Single	2626 (33.65)	1141 (34.11)	3767 (33.79)	
Insurance, *n* (%)				0.2202
Insured	7301 (93.57)	3108 (92.91)	10409 (93.37)	
Uninsured	502 (6.43)	237 (7.09)	739 (6.63)	
Primary site, *n* (%)				0.5019
Cervix uteri	5971 (76.52)	2520 (75.34)	8491 (76.17)	
Endocervix	1556 (19.94)	708 (21.17)	2264 (20.31)	
Exocervix	141 (1.81)	57 (1.70)	198 (1.78)	
OLC	135 (1.73)	60 (1.79)	195 (1.75)	
Grade, *n* (%)				0.9313
Grade I	1238 (15.87)	531 (15.87)	1769 (15.87)	
Grade II	3385 (43.38)	1466 (43.83)	4851 (43.51)	
Grade III	2968 (38.04)	1253 (37.46)	4221 (37.86)	
Grade IV	212 (2.72)	95 (2.84)	307 (2.75)	
Histology, *n* (%)				0.7464
SCC	5443 (69.76)	2318 (69.30)	7761 (69.62)	
AC	1952 (25.02)	858 (25.65)	2810 (25.21)	
Other	408 (5.23)	169 (5.05)	577 (5.18)	
RSS, *n* (%)				0.4703
No	5569 (71.37)	2364 (70.67)	7933 (71.16)	
Yes	2234 (28.63)	981 (29.33)	3215 (28.84)	
Chemotherapy, *n* (%)				0.8528
Yes	4110 (52.67)	1769 (52.88)	5879 (52.74)	
No	3693 (47.33)	1576 (47.12)	5269 (47.26)	
Bone metastasis, *n* (%)				0.0979
No	7662 (98.19)	3268 (97.70)	10930 (98.04)	
Yes	141 (1.81)	77 (2.30)	218 (1.96)	
Brain metastasis, *n* (%)				0.7113
No	7777 (99.67)	3336 (99.73)	11113 (99.69)	
Yes	26 (0.33)	9 (0.27)	35 (0.31)	
Liver metastasis, *n* (%)				0.4488
No	7689 (98.54)	3289 (98.33)	10978 (98.48)	
Yes	114 (1.46)	56 (1.67)	170 (1.52)	
Lung metastasis, *n* (%)				0.3818
No	7559 (96.87)	3229 (96.53)	10788 (96.77)	
Yes	244 (3.13)	116 (3.47)	360 (3.23)	
Metastasis numbers, *n* (%)				0.3610

(Continued)

TABLE 1 Continued

Characteristic	Training cohort	Validation cohort	All subjects	*P*
0	7415 (95.03)	3164 (94.59)	10579 (94.90)	
1	271 (3.47)	120 (3.59)	391 (3.51)	
2	97 (1.24)	46 (1.38)	143 (1.28)	
>=3	20 (0.26)	15 (0.45)	35 (0.31)	
Tumor size, *n* (%)				0.4562
<4 cm	7158 (64.21)	2130 (63.68)	5028 (64.44)	
>=4 cm	3990 (35.79)	1215 (36.32)	2775 (35.56)	
Regional nodes examined, *n* (%)				0.0484
No	4160 (53.31)	1839 (54.98)	5999 (53.81)	
Yes	3614 (46.32)	1501 (44.87)	5115 (45.88)	
UNK	29 (0.37)	5 (0.15)	34 (0.30)	
Regional nodes positive, *n* (%)				0.0588
No	2773 (35.54)	1176 (35.16)	3949 (35.42)	
negative	4160 (53.31)	1839 (54.98)	5999 (53.81)	
positive	838 (10.74)	324 (9.69)	1162 (10.42)	
UNK	32 (0.41)	6 (0.18)	38 (0.34)	
FIGO, *n* (%)				0.4472
IA1	875 (11.21)	397 (11.87)	1272 (11.41)	
IA2	333 (4.27)	137 (4.10)	470 (4.22)	
IB1	2196 (28.14)	939 (28.07)	3135 (28.12)	
IB2	706 (9.05)	334 (9.99)	1040 (9.33)	
IIA	529 (6.78)	244 (7.29)	773 (6.93)	
IIB	1206 (15.46)	479 (14.32)	1685 (15.11)	
IIIA	229 (2.93)	99 (2.96)	328 (2.94)	
IIIB	865 (11.09)	356 (10.64)	1221 (10.95)	
IVA	296 (3.79)	135 (4.04)	431 (3.87)	
INOS	461 (5.91)	179 (5.35)	640 (5.74)	
IINOS	14 (0.18)	11 (0.33)	25 (0.22)	
IIINOS	93 (1.19)	35 (1.05)	128 (1.15)	
LVSI, *n* (%)				0.0931
No	5634 (72.20)	2457 (73.45)	8091 (72.58)	
Yes	2001 (25.64)	835 (24.96)	2836 (25.44)	
UNK	168 (2.15)	53 (1.58)	221 (1.98)	
Primary site surgery, *n* (%)				0.1676
No	4189 (53.68)	1844 (55.13)	6033 (54.12)	
Yes	3614 (46.32)	1501 (44.87)	5115 (45.88)	
RLNS, *n* (%)				0.2077
No	4191 (53.71)	1853 (55.40)	6044 (54.22)	
Yes	3549 (45.48)	1470 (43.95)	5019 (45.02)	
UNK	63 (0.81)	22 (0.66)	85 (0.76)	
Radiation, *n* (%)				0.9049
Beam radiation	2273 (29.13)	969 (28.97)	3242 (29.08)	
brachytherapy	10 (0.13)	4 (0.12)	14 (0.13)	
BRB	2235 (28.64)	981 (29.33)	3216 (28.85)	
No/UNK	3285 (42.10)	1391 (41.58)	4676 (41.94)	
months, median [range]	30 [16, 53]	30 [16, 53]	30 [16, 53]	0.8927

FIGO, International Federation of Gynecologists and Obstetricians; UNK, Unknown; OLC, overlap crossing; RSS, Radiation sequence with surgery; AC, adenocarcinoma; SCC, Squamous cell carcinoma; FIGO, the International Federation of Gynecology and Obstetrics; LVSI, lymph vascular space invasion; RLNS, Regional lymph node surgery; BRB, Combination of beam with brachytherapy.

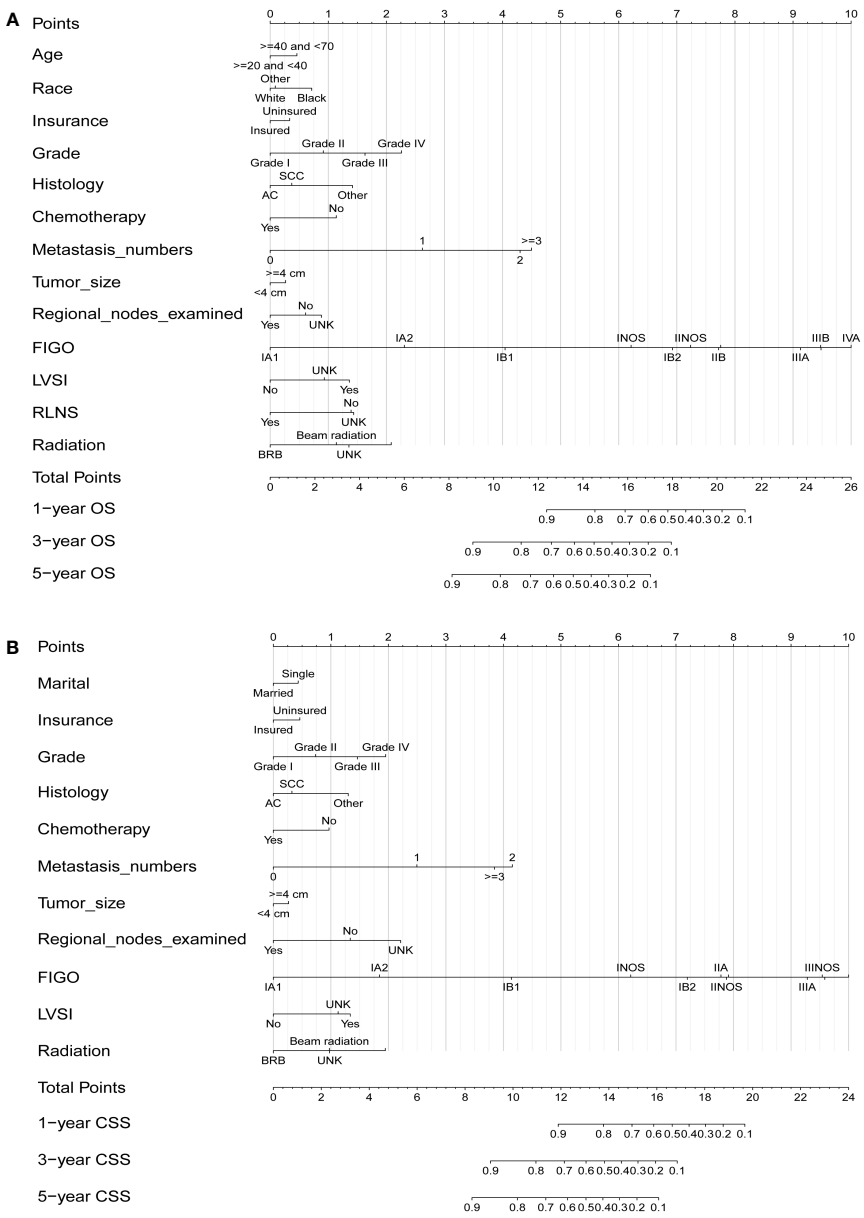

FIGURE 1
Nomograms for predicting 1-, 3-, and 5-year OS **(A)** and CSS **(B)** in patients with cervical cancer.

In the ROC curve analysis of the models, the area under the curve (AUC) values for prediction of 1-, 3-, and 5-year OS were 0.8888, 0.8618, and 0.8504 in the internal cohort, and 0.8758, 0.8560, and 0.8541 in the external cohort, respectively (Figures 4A, C). For prediction of 1-, 3-, and 5-year CSS, the AUC values were 0.8990, 0.8743, and 0.8652 in the training cohort, and 0.8934, 0.8701, and 0.8656 in the validation cohort, respectively (Figures 4B, D). The validation of these two nomograms demonstrated the excellent predictive accuracy for OS and CSS based on C-index and AUC.

Clinical applicability

DCA was used to evaluate the clinical applicability of the nomograms (17). Figure 5 shows decision curves for the nomograms and the FIGO stage for OS and CSS. These indicated that our model was superior to the FIGO stage, providing greater net clinical benefit with a threshold probability between 0 and 90%. CIC analysis (Figure 6) was performed to evaluate the clinical applicability of the risk prediction nomograms (18, 19) and FIGO stage. The DCA

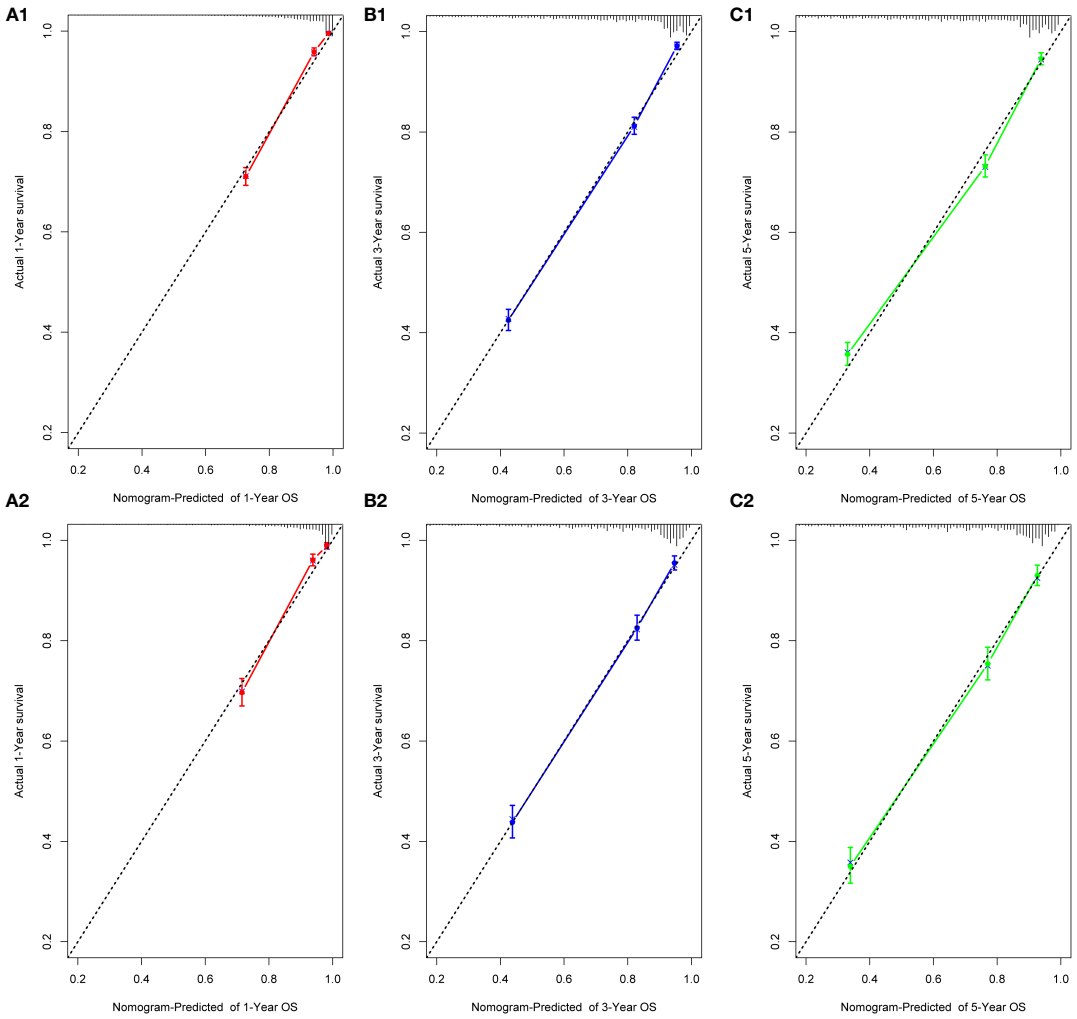

FIGURE 2
Calibration plots for 1-, 3-, and 5-year OS prediction for the training cohort (**A1, B1, C1**) and validation cohort (**A2, B2, C2**).

and CICs showed that the nomograms had greater net benefit within wide and practical ranges of threshold probabilities and impacted patient outcomes, indicating that our models have a significant predictive value.

Survival outcomes

During the follow-up period, the rates of OS- and CSS-related adverse events were 26% (2882/11148) and 21% (2332/11148), respectively. Analysis of survival outcomes (Table 3) showed that the 1-, 3-, and 5-year OS rates in the training cohort were 88.8, 73.5, and 67.7%, whereas those in the validation cohort were 88.1%, 73.9%, and 67.7%, respectively. The 1-, 3-, and 5-year CSS rates in the training cohort were 90.4%, 78.0%, and 73.6%, and those in the validation cohort were 90.1%, 77.7%, and 72.4%, respectively.

We used the nine prognostic factors to visually present OS and CSS in the training cohort (Figure 7). The CC patients with insurance had better survival outcomes (Figures 7A1, A2). OS and CSS decreased significantly with increasing grade (Figures 7B1, B2); that is, the higher the pathological grade, the worse the degree of differentiation and the higher the degree of malignancy. Patients with SCC had worse OS and CSS compared with patients with AC(adenocarcinoma) histopathology (Figures 7C1, C2). Patients who did not undergo chemotherapy treatment had obviously better survival outcomes in terms of both OS and CSS than those that received chemotherapy (Figures 7D1, D2). Patients diagnosed with metastasis (Figures 7E1, E2) or tumor size greater than 4 cm (Figures 7F1, F2) had worse survival. Regional lymph nodes with examination (Figures 7G1, G2) and those without positive lymph nodes (Figures 7H1, H2) were associated with better

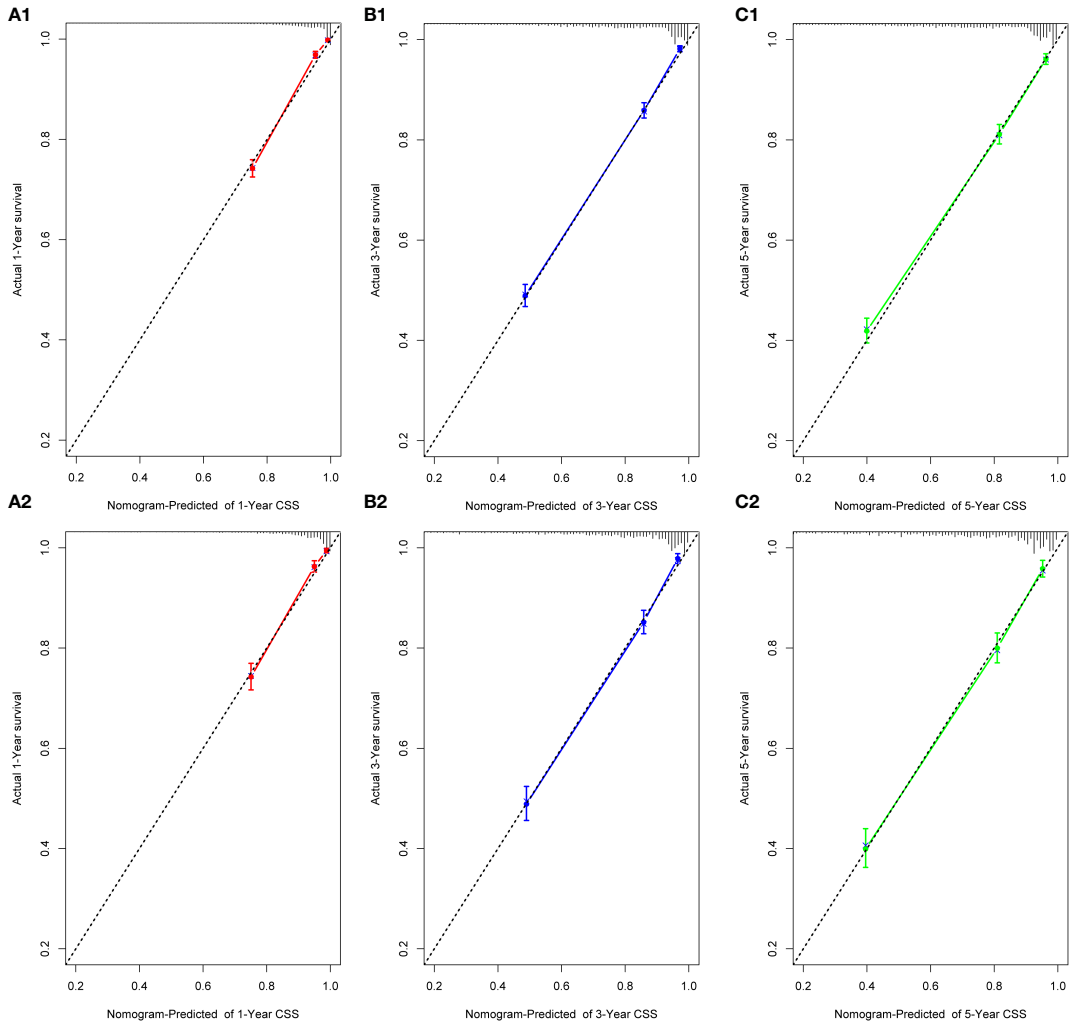

FIGURE 3
Calibration plots for 1-, 3-, and 5-year CSS prediction for the training cohort **(A1, B1, C1)** and validation cohort **(A2, B2, C2)**.

prognosis. Compared with beam radiation, BRB treatment had better survival outcomings (Figures 7I1, I2).

Discussion

Among female malignant tumors, CC ranks fifth in incidence and seventh in mortality worldwide (2022 Cancer Report). Owing to improvements in health awareness, early diagnosis, and early treatment, the incidence and mortality of CC have improved in developed countries; however, the early clinical symptoms of cervical cancer are not obvious, and the disease is usually locally advanced at first diagnosis. Comprehensive treatment of CC in the early stage is mainly based on surgery, and radiotherapy has a pivotal role in the treatment of patients with locally advanced stage disease. Global large-scale prospective randomized controlled clinical trials of concurrent chemoradiotherapy and radiotherapy alone in the treatment of CC have clarified the normative status of concurrent chemoradiotherapy (20–22).

Although technologies for CC treatment have become increasingly advanced, and the use of surgery and concurrent chemoradiotherapy have enabled curative effects in more patients, 20–40% of patients with CC still experience recurrence or metastasis within 2 years (23), with a recurrence rate within 3 years after radiotherapy that exceeds 70% (24). Therefore, there is an urgent need for a more accurate and effective method to evaluate OS and CSS in patients with CC. According to studies of CC at different FIGO stages, failure rates of local treatment in patients with stage IB, IIA, IIB, III, and IV CC were 10%, 17%, 23%, 42%, and 74%, respectively.

TABLE 2 Univariate and multivariate Cox regression analysis of OS and CSS in cervical cancer (training cohort).

Variables	Reference	Characteristic	OS Univariate Cox HR	*P*	Multivariate Cox HR	*P*	CSS Univariate Cox HR	*P*	Multivariate Cox HR	*P*
Age	>=20 and <40	>=40 and <70	1.93 (1.72 - 2.16)	**<0.001**	1.21 (1.08 - 1.36)	**0.0015**	1.66 (1.47 - 1.87)	**<0.001**	1.02 (0.9 - 1.16)	0.7322
Race	Black	White	0.63 (0.56 - 0.7)	**<0.001**	0.82 (0.73 - 0.93)	**0.0013**	0.67 (0.59 - 0.76)	**<0.001**	0.9 (0.79 - 1.03)	0.1201
	Black	Other	0.62 (0.52 - 0.74)	**<0.001**	0.81 (0.68 - 0.97)	**0.0199**	0.7 (0.57 - 0.84)	**<0.001**	0.93 (0.77 - 1.14)	0.4912
Marital	Married	Single	1.2 (1.09 - 1.31)	**<0.001**	1.06 (0.96 - 1.16)	0.2557	1.28 (1.16 - 1.41)	**<0.001**	1.12 (1.01 - 1.25)	**0.031**
Insurance	Insured	Uninsured	1.59 (1.36 - 1.86)	**<0.001**	1.24 (1.06 - 1.45)	**0.0086**	1.7 (1.44 - 2.01)	**<0.001**	1.35 (1.13 - 1.6)	**<0.001**
Primary site	Cervix uteri	Endocervix	0.6 (0.53 - 0.68)	**<0.001**	0.99 (0.86 - 1.14)	0.8986	0.6 (0.52 - 0.69)	**<0.001**	1.02 (0.87 - 1.19)	0.8149
	Cervix uteri	Exocervix	0.62 (0.41 - 0.93)	**0.02**	0.83 (0.55 - 1.24)	0.3641	0.71 (0.47 - 1.08)	0.11	0.99 (0.65 - 1.51)	0.9557
	Cervix uteri	OLC	0.97 (0.7 - 1.34)	0.835	1.23 (0.89 - 1.72)	0.2111	1.08 (0.76 - 1.53)	0.661	1.37 (0.97 - 1.95)	0.0776
Grade	Grade I	Grade II	2.61 (2.14 - 3.18)	**<0.001**	1.32 (1.07 - 1.62)	**0.0091**	2.88 (2.28 - 3.64)	**<0.001**	1.35 (1.06 - 1.72)	**0.017**
	Grade I	Grade III	4.66 (3.84 - 5.66)	**<0.001**	1.72 (1.4 - 2.11)	**<0.001**	5.49 (4.36 - 6.92)	**<0.001**	1.84 (1.45 - 2.35)	**<0.001**
	Grade I	Grade IV	6.82 (5.2 - 8.94)	**<0.001**	2.48 (1.86 - 3.3)	**<0.001**	7.97 (5.85 - 10.87)	**<0.001**	2.64 (1.91 - 3.66)	**<0.001**
Histology	AC	SCC	1.77 (1.58 - 2)	**<0.001**	1.09 (0.95 - 1.25)	0.222	1.78 (1.56 - 2.04)	**<0.001**	1.09 (0.93 - 1.27)	0.2706
	AC	Other	3.33 (2.78 - 4)	**<0.001**	1.55 (1.28 - 1.89)	**<0.001**	3.57 (2.93 - 4.37)	**<0.001**	1.6 (1.3 - 1.99)	**<0.001**
RSS	No	Yes	0.72 (0.65 - 0.8)	**<0.001**	1.05 (0.92 - 1.2)	0.4688	0.74 (0.67 - 0.83)	**<0.001**	1.04 (0.9 - 1.21)	0.582
Chemotherapy	No	Yes	2.81 (2.54 - 3.1)	**<0.001**	0.61 (0.54 - 0.69)	**<0.001**	3.06 (2.73 - 3.43)	**<0.001**	0.59 (0.52 - 0.68)	**<0.001**
bone metastasis	No	Yes	11.46 (9.54 - 13.76)	**<0.001**	0.89 (0.52 - 1.5)	0.6565	12.03 (9.88 - 14.64)	**<0.001**	0.71 (0.4 - 1.27)	0.2497
brain metastasis	No	Yes	17.97 (12.16 - 26.6)	**<0.001**	1.46 (0.76 - 2.79)	0.2555	17.84 (11.67 - 27.27)	**<0.001**	1.13 (0.56 - 2.31)	0.7291
liver metastasis	No	Yes	11.02 (9.01 - 13.47)	**<0.001**	0.85 (0.5 - 1.44)	0.5441	12.31 (9.98 - 15.19)	**<0.001**	0.74 (0.41 - 1.31)	0.3012
lung metastasis	No	Yes	9.01 (7.8 - 10.42)	**<0.001**	0.69 (0.4 - 1.18)	0.1708	9.72 (8.32 - 11.35)	**<0.001**	0.57 (0.31 - 1.03)	0.0626
Metastasis numbers	>=3	0	0.05 (0.03 - 0.08)	**<0.001**	0.12 (0.04 - 0.37)	**<0.001**	0.06 (0.03 - 0.09)	**<0.001**	0.08 (0.02 - 0.26)	**<0.001**
	>=3	1	0.46 (0.29 - 0.73)	**0.001**	0.43 (0.23 - 0.81)	**0.0094**	0.51 (0.3 - 0.86)	**0.012**	0.34 (0.17 - 0.67)	**0.002**
	>=3	2	0.91 (0.55 - 1.49)	0.698	NA	NA	1.09 (0.63 - 1.89)	0.758	NA	NA
Tumor size	<4 cm	>=4 cm	2.68 (2.45 - 2.93)	**<0.001**	1.14 (1.03 - 1.26)	**0.0121**	2.92 (2.65 - 3.22)	**<0.001**	1.14 (1.02 - 1.28)	**0.02**
Regional nodes examined	No	Yes	0.29 (0.26 - 0.32)	**<0.001**	0.57 (0.41 - 0.79)	**<0.001**	0.29 (0.26 - 0.33)	**<0.001**	0.55 (0.38 - 0.79)	**0.001**
	No	UNK	1.85 (1.15 - 2.98)	**0.012**	50639.75 (0 - Inf)	0.9816	2.33 (1.44 - 3.75)	**0.001**	44977 (0 - Inf)	0.9841
Regional nodes positive	negative	No	5.83 (5.07 - 6.71)	**<0.001**	NA	NA	6.15 (5.24 - 7.23)	**<0.001**	NA	NA
	negative	positive		**<0.001**	1.96 (1.57 - 2.44)	**<0.001**		**<0.001**	1.83 (1.43 - 2.33)	**<0.001**

(Continued)

TABLE 2 Continued

Variables	Reference	Characteristic	OS Univariate Cox		Multivariate Cox		CSS Univariate Cox		Multivariate Cox	
			HR	*P*	HR	*P*	HR	*P*	HR	*P*
			4.16 (3.47 - 4.98)				4.71 (3.84 - 5.76)			
	negative	UNK	8.87 (5.42 - 14.52)	**<0.001**	0 (0 - Inf)	0.9817	11.84 (7.19 - 19.5)	**<0.001**	0 (0 - Inf)	0.9844
FIGO	IA1	IA2	1.85 (0.93 - 3.69)	0.08	2.54 (1.27 - 5.08)	**0.0085**	1.76 (0.67 - 4.63)	0.25	2.23 (0.85 - 5.89)	0.1041
	IA1	IB1	3.62 (2.25 - 5.81)	**<0.001**	5.51 (3.39 - 8.97)	**<0.001**	4.37 (2.29 - 8.35)	**<0.001**	6 (3.1 - 11.61)	**<0.001**
	IA1	IB2	13.73 (8.57 - 22.01)	**<0.001**	15.13 (9.2 - 24.88)	**<0.001**	21.95 (11.59 - 41.59)	**<0.001**	22.03 (11.35 - 42.8)	**<0.001**
	IA1	IIA	19.38 (12.08 - 31.1)	**<0.001**	18.5 (11.3 - 30.28)	**<0.001**	28.5 (15.01 - 54.1)	**<0.001**	25.22 (13.03 - 48.8)	**<0.001**
	IA1	IIB	17.98 (11.34 - 28.5)	**<0.001**	18.42 (11.36 - 30)	**<0.001**	27.62 (14.72 - 51.83)	**<0.001**	26.82 (13.98 - 51.5)	**<0.001**
	IA1	IIIA	44.08 (27.29 - 71.2)	**<0.001**	31.6 (19.1 - 52.29)	**<0.001**	69.83 (36.62 - 133.2)	**<0.001**	47.69 (24.44 - 93.1)	**<0.001**
	IA1	IIIB	43.59 (27.57 - 68.9)	**<0.001**	34.48 (21.3 - 55.9)	**<0.001**	69.5 (37.13 - 130.1)	**<0.001**	51.91 (27.07 - 99.6)	**<0.001**
	IA1	IVA	64.41 (40.28 - 103)	**<0.001**	37.4 (22.83 - 61.3)	**<0.001**	101.13 (53.48 - 191)	**<0.001**	55.23 (28.54 - 107)	**<0.001**
	IA1	INOS	11.23 (6.89 - 18.3)	**<0.001**	9.96 (6.07 - 16.36)	**<0.001**	13.67 (7.04 - 26.55)	**<0.001**	11.51 (5.88 - 22.52)	**<0.001**
	IA1	IINOS	25.41 (10.15 - 63.6)	**<0.001**	20.74 (8.17 – 52.6)	**<0.001**	39.84 (13.62 - 117)	**<0.001**	33.17 (11.17 - 98.5)	**<0.001**
	IA1	IIINOS	45.83 (27.29 - 77)	**<0.001**	31.38 (18.28 - 54)	**<0.001**	73.62 (37.33 - 145)	**<0.001**	46.93 (23.28 - 94.6)	**<0.001**
LVSI	No	Yes	3.19 (2.92 - 3.49)	**<0.001**	1.43 (1.28 - 1.6)	**<0.001**	3.68 (3.33 - 4.07)	**<0.001**	1.55 (1.37 - 1.76)	**<0.001**
	No	UNK	4.36 (3.51 - 5.41)	**<0.001**	1.4 (1.12 - 1.76)	**0.0037**	5.18 (4.11 - 6.53)	**<0.001**	1.62 (1.26 - 2.07)	**<0.001**
Primary site surgery	No	Yes	0.28 (0.26 - 0.32)	**<0.001**	NA (NA - NA)	NA	0.29 (0.26 - 0.32)	**<0.001**	NA	NA
RLNS	No	Yes	0.27 (0.24 - 0.3)	**<0.001**	0.6 (0.44 - 0.82)	**0.0013**	0.28 (0.25 - 0.31)	**<0.001**	0.73 (0.52 - 1.03)	0.0768
	No	UNK	0.78 (0.5 - 1.21)	0.263	1.19 (0.72 - 1.97)	0.5	0.89 (0.56 - 1.42)	0.619	1.39 (0.81 - 2.4)	0.2335
Radiation	Beam radiation	brachytherapy	0.73 (0.23 - 2.25)	0.579	0.9 (0.29 - 2.8)	0.8495	0.59 (0.15 - 2.37)	0.458	0.78 (0.19 - 3.15)	0.7293
	Beam radiation	BRB	0.65 (0.59 - 0.72)	**<0.001**	0.68 (0.61 - 0.76)	**<0.001**	0.65 (0.58 - 0.72)	**<0.001**	0.7 (0.62 - 0.79)	**<0.001**
	Beam radiation	No/UNK	0.32 (0.28 - 0.35)	**<0.001**	1.09 (0.94 - 1.26)	0.24	0.29 (0.26 - 0.33)	**<0.001**	1.04 (0.88 - 1.22)	0.6586

HR, hazard Ratio; CI, confidence interval; P<0.05 is marked with bold black. NA, not applicable.

In recent years, increasing numbers of studies have focused on the use of predictive models to improve survival, although bottlenecks and deficiencies exist. As a novel, simple, and direct prediction model, the nomogram can directly visualize predicted OS and CSS and provide a reference for further examination and clinical decision-making. In our study, factors including age, race, marital status, insurance status, grade, histology, chemotherapy, metastasis number, tumor size, regional node examination, FIGO stage, LVSI, RLNS, and radiation showed associations with prognosis in patients with CC, and we built nomograms for both OS and CSS based on these factors. Finally, nomograms were developed to calculate the probabilities of 1-, 3-, and 5-year OS (based on 13 independent prognostic factors) and CSS (based on 11 independent prognostic factors) in patients with CC. Our nomograms indicated that FIGO stage made the largest contribution to the predicted probability

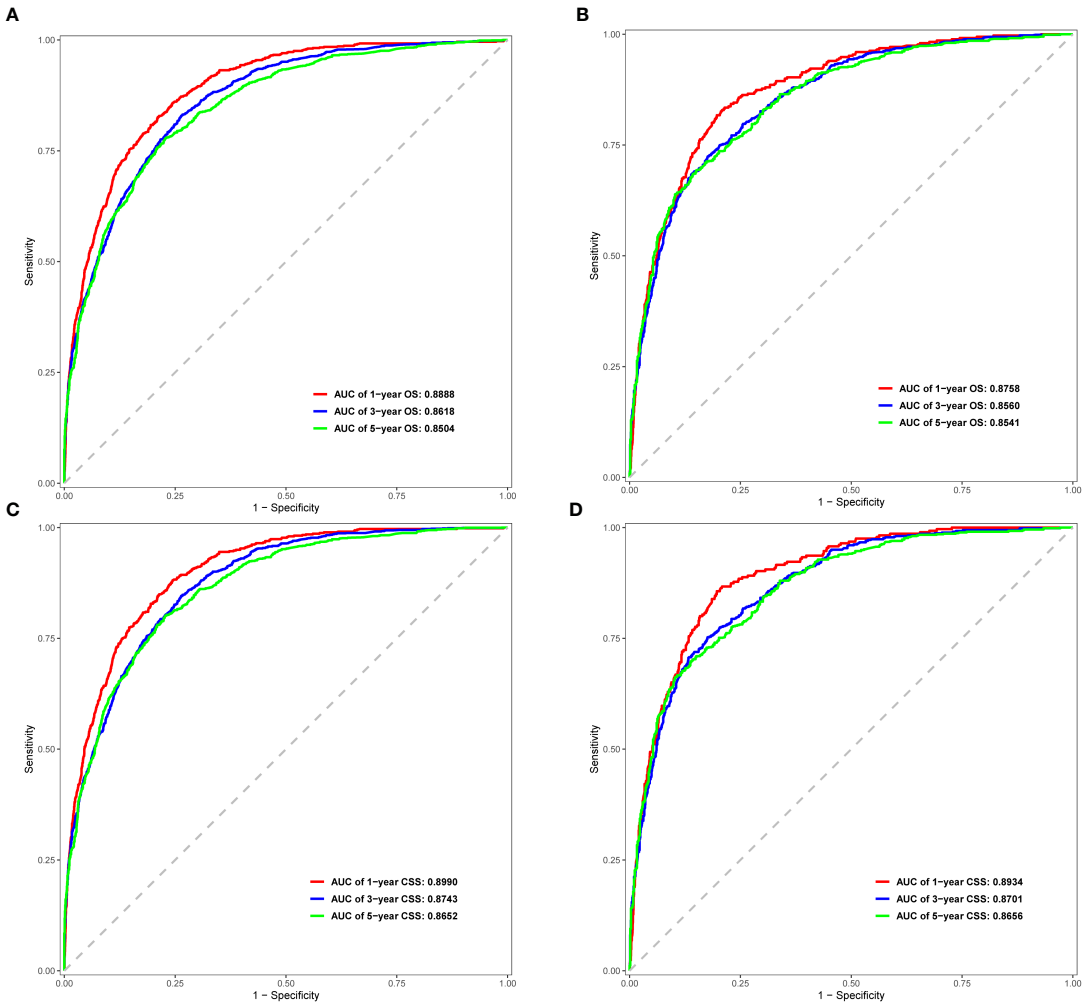

FIGURE 4
ROC curves for 1-, 3-, and 5-year OS and CSS in the training cohort **(A, C)** and validation cohort **(B, D)**.

between 1-, 3-, and 5-year OS and CSS, which was consistent with a large body of previous research (6, 9, 25).

We analyzed the survival outcomes (OS and CSS) of patients stratified by the following factors: insurance status, grade, histology, chemotherapy, metastasis number, tumor size, regional node examination, LVSI, and radiation. Patients with insurance had better survival outcomes, and this has not been reported by previous studies (6–9). CC patients with AC histopathology had slightly better prognoses than those with SCC; similarly, this result has rarely been reported in previous studies (8, 9, 26, 27). Only about 45% of the patients with CC benefited from initial regional lymph node examination. It had been reported that LVSI was an important poor prognostic factor for patients with early cervical cancer. Diffuse lymphatic involvement (diffuse LVSI) has predictive significance for the survival prognosis of patients compared with focal or non-focal lesions (28). In our study, patients with LVSI had worse OS and CSS ($P<0.001$). In clinical practice, radiation and chemotherapy are the most commonly used effective treatments for patients with CC and lead to significant improvements in survival time (7). Our results indicated that CC patients without chemotherapy treatment had better prognoses than those that received chemotherapy. Compared with beam radiation, patients who chose BRB had a more favorable survival outcome (13).

Surgery is still the main treatment method for early cervical cancer, particularly laparoscopic minimally invasive surgery is currently a popular surgical method. However, combined with the prospective large-scale clinical study LACC trial (Laparoscopic Approach to Cervical Cancer) and meta-analysis (29, 30), it was concluded that this surgical method did not benefit the survival of these patients. In our study, we mainly focus on RSS, primary site surgery and RLNS. In the univariate Cox regression, the three variables were significant for

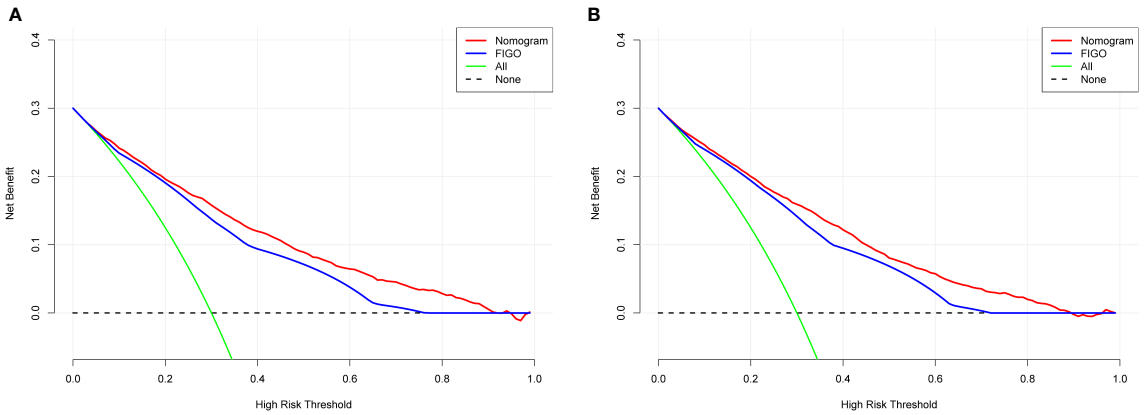

FIGURE 5
Decision curve analysis of the nomogram and FIGO stage prediction model for predicting OS **(A)** and CSS **(B)** in the training cohort. The x-axis represents the percentage of threshold probability, whereas the y-axis represents the net benefit, calculated by adding the true positives and subtracting the false positives.

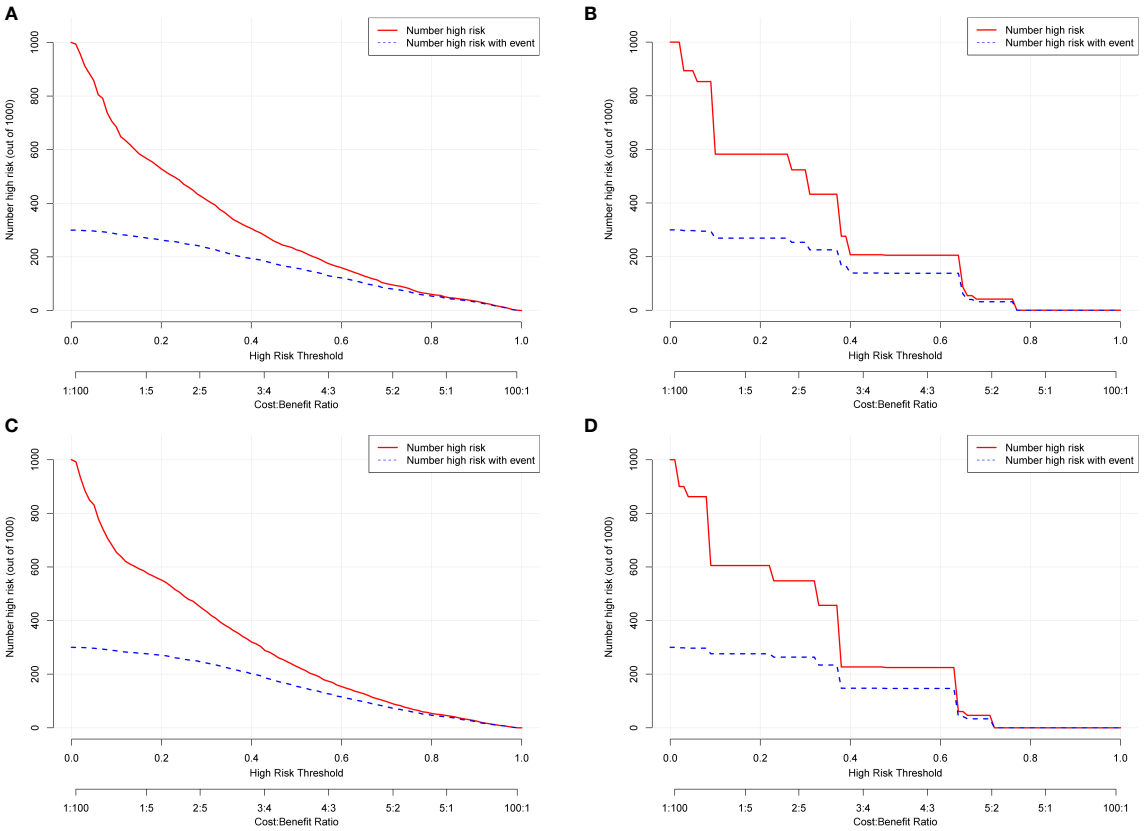

FIGURE 6
Clinical impact curves (CICs) for OS and CSS of the nomogram **(A, C)** and FIGO stage **(B, D).** The red curve (number of high-risk individuals) indicates the number of people who were classified as positive (high risk) by the model at each threshold probability; the blue curve (number of high-risk individuals with outcome) is the number of true positives at each threshold probability. The CICs provided visual confirmation of the high net clinical benefit of the nomograms and confirmed the clinical value of the model.

10.3389/fonc.2022.961678

TABLE 3 Survival analysis of OS and CSS in the training cohort and validation cohort.

Endpoints	Months	n.risk	n.event	Survival	std.err	95% CI
OS of training cohort	12	6619	851	0.888	0.0036	0.881 - 0.895
	36	3375	937	0.735	0.0055	0.725 - 0.746
	60	1453	197	0.677	0.0065	0.665 - 0.690
OS of validation cohort	12	2819	384	0.881	0.0057	0.870 - 0.893
	36	1445	375	0.739	0.0084	0.722 - 0.755
	60	629	89	0.677	0.0100	0.657 - 0.696
CSS of training cohort	12	6619	724	0.904	0.0034	0.897 - 0.910
	36	3375	735	0.780	0.0052	0.770 - 0.791
	60	1453	142	0.736	0.0062	0.724 - 0.748
CSS of validation cohort	12	2819	317	0.901	0.0053	0.891 - 0.911
	36	1445	314	0.777	0.0080	0.761 - 0.793
	60	629	72	0.724	0.0097	0.705 - 0.743

both OS and CSS (P<0.001), in the multivariate Cox regression, they had no significant for both OS and CSS (P>0.05). Since there is no detailed record of specific surgical approaches, more prospective studies may be needed to further determine the safety and efficacy of minimally invasive surgery.

Survival and prognosis studies on patients with locally advanced cervical cancer showed that (31), multivariate analysis of tumors ≥6 cm had worse loco-regional-recurrence-free survival (LRFS) and OS; AC and positive lymph nodes were associated with distant-metastasis-free survival (DMFS); adjuvant chemotherapy has longer DMFS and OS. In our study, tumor size ≥4 cm were poor prognostic factors for OS and CSS; patients with AC had better OS and CSS; those with positive lymph nodes and a history of chemotherapy had worse OS and CSS, because the data source did not clearly classify neoadjuvant chemotherapy or adjuvant chemotherapy, so more follow-up studies are needed to confirm the contribution of chemotherapy timing.

Previously, many studies developed nomograms for diagnosis and prognostic prediction in patients with CC; however, these studies had many limitations, including insufficient sample size (7), the model having a low C-index and prediction accuracy (6, 32), insufficient inclusion and exclusion criteria (6, 33), and a single study endpoint (8, 9). To our knowledge, compared with other studies evaluating CC survival using nomograms (6–9), the present study considered more real-time sample data and a more complete set of patient prognostic factors (13) than previous studies, showed excellent predictive accuracy for OS and CSS (6–9, 33), and demonstrated greater clinical net benefit. The calibration plots were almost consistent with actual observations, and we obtained excellent C-index (approximately 0.84) and AUC (approaching 0.89) values, indicating that our nomograms showed outstanding performance in predicting 1-, 3-, and 5-year OS and CSS. In addition, we compared FIGO staging and the nomograms with respect to their net benefit. FIGO stage is widely used clinically, and the use of a nomogram could reduce the diversity due to different treatments and sociodemographic statuses when predicting the prognosis of patients with CC (25, 32). We found that the nomograms had greater net benefit than the FIGO stage according to DCA and CIC. Therefore, our nomograms could represent a reliable alternative or supplementary tool to predict survival outcomes.

Our study included the latest and sufficient data sets through the SEER database, which contained enough clinical and non-clinical factors to have better practical significance in line with the real world. We constructed more 10 independent prognostic factors nomograms to calculate the probabilities of 1-, 3-, and 5-year OS (13 factors) and CSS (11 factors) in patients with CC. To provide strong evidence, we evaluated our model internally and externally using five approaches: the C-index, ROC, calibration plots, DCA, and CICs, which made our study more complete and reliable compared with previous studies. From the 1-, 3-, and 5-year OS and CSS nomograms, it was found that the scores of FIGO stage, metastasis number, and grade were the three highest in all indicators, which can provide direct and effective actual clinical implications for survival prognostic assessment. However, this study had some limitations. First, this was a retrospective population analysis without multicenter validation data. Second, there was a lack of information about other important factors, including HPV infection status and blood type parameters; future studies could refine the nomograms by incorporating these predictors. Third, our data were from the US population only, and the demographic data was relatively homogeneous. Future analyses of multicenter data with larger sample sizes, more variables including clinical and non-clinical factors, and patients of different ethnicities are required to validate our conclusions.

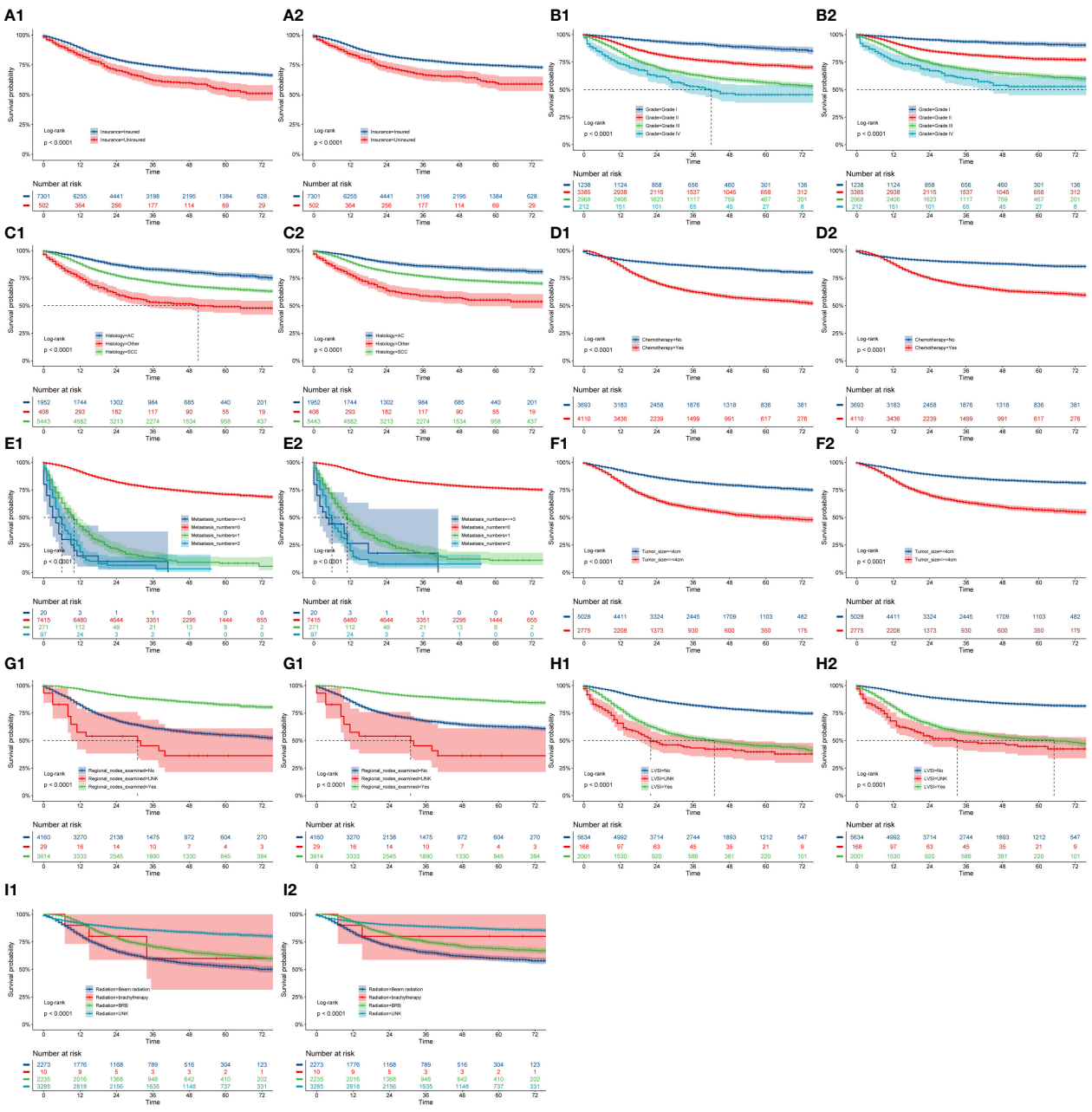

FIGURE 7
OS and CSS stratified by patient characteristics in the training cohort: **(A1, A2)** insurance; **(B1, B2)** grade; **(C1, C2)** history; **(D1, D1)** chemotherapy; **(E1, E2)** metastasis numbers; **(F1, F2)** tumor size; **(G1, G2)** regional nodes examined; **(H1, H2)** LVSI; **(I1, I2)** radiation.

Conclusions

We used the SEER database to analyze prognostic data for CC patients, identified independent prognostic factors, and constructed nomograms for estimating 1-, 3-, and 5-year OS and CSS. Internal and external validation showed that these models had excellent predictive performance. They could thus be considered as reliable tools to predict prognosis, which is essential for maximizing the patient's chance of survival.

Data availability statement

Publicly available datasets were analyzed in this study. The data can be found at SEER National Cancer Institute (via accession number: 19279-Nov2020).

Author contributions

KJ , YL and YA conceived and designed the study. The YL and LJ provided administrative and funding support. KJ and YL collected and assembled the data. KJ and YL contributed to data processing, interpretation of results, and drafting of the manuscript. All authors read and approved the manuscript.

Funding

This study was supported by the Scientific Research Fund project of Yunnan Education Department (2022J0265). This research was funded by the National Natural Science Foundation of China under Grant No. 62262035.

Acknowledgments

We thank the Third Affiliated Hospital of Kunming Medical University for supporting the writing of this manuscript.

Conflict of interest

The authors declare that the research was conducted in the absence of any commercial or financial relationships that could be construed as a potential conflict of interest.

Publisher's note

References

1. Siegel RL, Miller KD, Fuchs HE, Jemal A. Cancer statistics, 2021. *CA Cancer J Clin* (2021) 71(1):7–33. doi: 10.3322/caac.21654

2. Islami F, Fedewa SA, Jemal A. Trends in cervical cancer incidence rates by age, race/ethnicity, histological subtype, and stage at diagnosis in the united states. *Prev Med* (2019) 123:316–23. doi: 10.1016/j.ypmed.2019.04.010

3. Saslow D, Andrews KS, Manassaram–Baptiste D, Smith RA, Fontham ETH. Human papillomavirus vaccination 2020 guideline update: American cancer society guideline adaptation. *CA Cancer J Clin* (2020) 70(4):274–80. doi: 10.3322/caac.21616

4. Fontham ETH, Wolf AMD, Church TR, Etzioni R, Flowers CR, Herzig A, et al. Cervical cancer screening for individuals at average risk: 2020 guideline update from the American cancer society. *CA Cancer J Clin* (2020) 70(5):321–46. doi: 10.3322/caac.21628

5. Waggoner SE. Cervical cancer. *Lancet* (2003) 361(9376):2217–25. doi: 10.1016/s0140–6736(03)13778–6

6. Li Z, Lin Y, Cheng B, Zhang Q, Cai Y. Prognostic model for predicting overall and cancer–specific survival among patients with cervical squamous cell carcinoma: a SEER based study. *Front Oncol* (2021) 11:651975. doi: 10.3389/fonc.2021.651975

7. Zhang S, Wang X, Li Z, Wang W, Wang L. Score for the overall survival probability of patients with first–diagnosed distantly metastatic cervical cancer: a novel nomogram–based risk assessment system. *Front Oncol* (2019) 9:1106. doi: 10.3389/fonc.2019.01106

8. Wang C, Yang C, Wang W, Xia B, Li K, Fet S, et al. A prognostic nomogram for cervical cancer after surgery from SEER database. *J Cancer* (2018) 9(21):3923–8. doi: 10.7150/jca.26220

9. Xie G, Wang R, Shang L, Qi C, Yang L, Huang L, et al. Calculating the overall survival probability in patients with cervical cancer: a nomogram and decision curve analysis–based study. *BMC Cancer* (2020) 20(1):833. doi: 10.1186/s12885–020–07349–4

10. Balachandran VP, Gonen M, Smith JJ, DeMatteo RP. Nomograms in oncology: more than meets the eye. *Lancet Oncol* (2015) 16:173–80. doi: 10.1016/S1470–2045(14)71116–7

11. Song Z, Wang Y, Zhou Y, Zhang D. A Novel Predictive Tool for Determining the Risk of Early Death From Stage IV Endometrial Carcinoma: A Large Cohort Study. *Front Oncol* (2020) 10:620240. doi: 10.3389/fonc.2020.620240

12. Iasonos A, Schrag D, Raj GV, Panageas KS. How to build and interpret a nomogram for cancer prognosis. *J Clin Oncol* (2008) 26(8):1364–70. doi: 10.1200/jco.2007.12.9791

13. Tian T, Gong X, Gao X, Li Y, Ju W, Ai Y. Comparison of survival outcomes of locally advanced cervical cancer by histopathological types in the surveillance, epidemiology, and end results (SEER) database: a propensity score matching study. *Infect Agent Cancer* (2020) 15:33. doi: 10.1186/s13027–020–00299–3

14. Liang W, Yang P, Huang R, Xu L, Wang J, Liu W, et al. A combined nomogram model to preoperatively predict histologic grade in pancreatic neuroendocrine tumors. *Clin Cancer Res* (2019) 25(2):584–94. doi: 10.1158/1078–0432.Ccr–18–1305

15. Vickers AJ, Elkin EB. Decision curve analysis: a novel method for evaluating prediction models. *Med Decis Making* (2006) 26:565–74. doi: 10.1177/0272989X06295361

16. Tolles J, Meurer WJ. Logistic regression: relating patient characteristics to outcome. *JAMA* (2016) 316(5):533–4. doi: 10.1001/jama.2016.7653

17. Van Calster B, Wynants L, Verbeek JFM, Verbakel JY, Christodoulou E, Vickers AJ, et al. Reporting and interpreting decision curve analysis: a guide for investigators. *Eur Urol* (2018) 74(6):796–804. doi: 10.1016/j.eururo.2018.08.038

18. Qi Y, Wu S, Tao L, Xu G, Chen J, Feng Z, et al. A population–based study: how to identify high–risk T1–2 esophageal cancer patients? *Front Oncol* (2021) 11:766181. doi: 10.3389/fonc.2021.766181

19. Zhu YJ, Chen Y, Hu HY, Zhou YW, Zhu YT, Liu JY. Predictive risk factors and online nomograms for synchronous colon cancer with liver metastasis. *Front Oncol* (2020) 10:. doi: 10.3389/fonc

20. Morris M, Eifel PJ, Lu J, Grigsby PW, Levenback C, Stevens RE, et al. Pelvic radiation with concurrent chemotherapy compared with pelvic and para–aortic radiation for high–risk cervical cancer. *N Engl J Med* (1999) 340(15):1137–43. doi: 10.1056/NEJM199904153401501

21. Peters WA, Liu PY, Barrett RJ, Stock RJ, Monk BJ, Berek JS, et al. Concurrent chemotherapy and pelvic radiation therapy compared with pelvic radiation therapy alone as adjuvant therapy after radical surgery in high–risk early–stage cancer of the cervix. *J Clin Oncol* (2000) 18(8):1606–13. doi: 10.1200/JCO.2000.18.8.1606

22. Thomas GM. Improved treatment for cervical cancer–concurrent chemotherapy and radiotherapy. *N Engl J Med* (1999) 340(15):1198–200. doi: 10.1056/NEJM199904153401509

23. Peiretti M, Zapardiel I, Zanagnolo V, Landoni F, Morrow CP, Maggioni A. Management of recurrent cervical cancer: a review of the literature. *Surg Oncol* (2012) 21(2):e59–66. doi: 10.1016/j.suronc.2011.12.008

24. Goncalves A, Fabbro M, Lhommé C, Gladieff L, Extra JM, Floquet A, et al. A phase II trial to evaluate gefitinib as second– or third–line treatment in patients with recurring locoregionally advanced or metastatic cervical cancer. *Gynecol Oncol* (2008) 108(1):42–6. doi: 10.1016/j.ygyno.2007.07.057

25. Tang X, Guo C, Liu S, Guo J, Hua K, Qiu J. A novel prognostic nomogram utilizing the 2018 FIGO staging system for cervical cancer: a large multicenter study. *Int J Gynaecol Obstet* (2021) 155(1):86–94. doi: 10.1002/ijgo.13644

26. Yang J, Tian G, Pan Z, Zhao F, Feng X, Liu Q, et al. Nomograms for predicting the survival rate for cervical cancer patients who undergo radiation therapy: a SEER analysis. *Future Oncol* (2019) 15(26):3033–45. doi: 10.2217/fon–2019–0029

27. Liu Q, Li W, Xie M, Yang M, Xu M, Yang L, et al. Development and validation of a SEER–based prognostic nomogram for cervical cancer patients below the age of 45 years. *Bosn J Basic Med Sci* (2021) 21(5):620–31. doi: 10.17305/bjbms.2020.5271

28. Ronsini C, Anchora LP, Restaino S, Fedele C, Arciuolo D, Teodorico E, et al. The role of semiquantitative evaluation of lympho–vascular space invasion in early stage cervical cancer patients. *Gynecol Oncol* (2021) 162(2):299–307. doi: 10.1016/j.ygyno.2021.06.002

29. Ramirez PT, Frumovitz M, Pareja R, Lopez A, Vieira M, Ribeiro R, et al. Minimally invasive versus abdominal radical hysterectomy for cervical cancer. *N Engl J Med* (2018) 379(20):1895–904. doi: 10.1056/NEJMoa1806395

30. Ronsini C, Köhler C, De Franciscis P, La Verde M, Mosca L, Solazzo MC, et al. Laparo–assisted vaginal radical hysterectomy as a safe option for minimal invasive surgery in early stage cervical cancer: A systematic review and meta–analysis. *Gynecol Oncol* (2022) 166(1):188–95. doi: 10.1016/j.ygyno.2022.04.010

31. Queiroz ACM, Fabri V, Mantoan H, Sanches SM, Guimarães APG, Ribeiro ARG, et al. Risk factors for pelvic and distant recurrence in locally advanced cervical cancer. *Eur J Obstet Gynecol Reprod Biol* (2019) 235:6–12. doi: 10.1016/j.ejogrb.2019.01.028

32. Zang L, Chen Q, Zhang X, Zhang X, Chen J, Fang Y, et al. Nomogram predicting overall survival in patients with FIGO II to III squamous cell cervical carcinoma under radical radiotherapy: A retrospective analysis based on 2018 FIGO staging. *Cancer Manag Res* (2021) 13:9391–400. doi: 10.2147/CMAR.S336892

33. Jiang AG, Cai X. Construction and validation of the prognostic model for patients with neuroendocrine cervical carcinoma: a competing risk nomogram analysis. *BMC Cancer* (2022) 22(1):4. doi: 10.1186/s12885–021–09104–9

frontiers | Frontiers in Oncology

TYPE Case Report
PUBLISHED 27 October 2022
DOI 10.3389/fonc.2022.1024173

OPEN ACCESS

EDITED BY
Federico Ferrari,
University of Brescia, Italy

REVIEWED BY
Brannan B. Griffin,
Vanderbilt University Medical Center, United States
Wenxin Zheng,
University of Texas Southwestern Medical Center, United States

*CORRESPONDENCE
Jiao Wang
wangjiao881130@163.com

SPECIALTY SECTION
This article was submitted to Gynecological Oncology, a section of the journal Frontiers in Oncology

RECEIVED 21 August 2022
ACCEPTED 17 October 2022
PUBLISHED 27 October 2022

CITATION
Wang Y, Sun M and Wang J (2022) Superficial vaginal myofibroblastoma with mushroom-like appearance: A case report with colposcopic findings and literature review.
Front. Oncol. 12:1024173.
doi: 10.3389/fonc.2022.1024173

Superficial vaginal myofibroblastoma with mushroom-like appearance: A case report with colposcopic findings and literature review

Yibei Wang[1], Meige Sun[2] and Jiao Wang[2]*

[1]Department of Thoracic Surgery, Shengjing Hospital of China Medical University, Shenyang, Liaoning, China, [2]Department of Obstetrics and Gynecology, Shengjing Hospital of China Medical University, Shenyang, Liaoning, China

Superficial myofibroblastoma (SMF) of the lower female genital tract is a relatively rare benign mesenchymal tumor. The diagnosis is usually challenging as it shares several similar clinicopathological features with other tumors. Herein, we present a case of a 71-year-old Chinese female patient with postmenopausal vaginal bleeding. Colposcopy imaging revealed a well-circumscribed mass in the vagina with a wide pedicle, resembling a mushroom. The patient underwent surgery, and the tumor was histologically diagnosed as SMF. To the best of our knowledge, this is the first report of colposcopic imaging of a superficial vaginal myofibroblastoma. In this case study, we review the clinicopathological features of SMF of the lower female genital tract reported in the literature to improve the understanding of the disease.

KEYWORDS

superficial myofibroblastoma, vagina, mesenchymal tumor, colposcope, diagnosis

Introduction

In 2001, Laskin et al. described a distinctive tumor of the cervix and vagina, which they named "superficial cervicovaginal myofibroblastoma (SCVM)" (1). In 2005, Ganesan et al. proposed that the term "superficial myofibroblastoma (SMF) of the lower female genital tract" be used instead of SCVM as some neoplasms have a vulvar location (2, 3). SMFs of the lower female genital tract are an unusual type of benign mesenchymal tumor (4). Only 57 cases have been reported in the literature, among which 43 cases arose in the vagina; the clinical manifestations were not specific, and the lesions were not typical, which makes pre-pathological diagnoses of patients challenging. Here,

we present the diagnosis and treatment of a patient with superficial vaginal myofibroblastoma presenting with postmenopausal vaginal bleeding. To further clarify the location, scope, and nature of the lesion, we performed colposcopy on the patient prior to surgery. In addition, we review the literature on the clinicopathological features of this distinctive tumor.

Case report

The patient was a 71-year-old postmenopausal woman (gravida 2, para 2). On December 17, 2020, the patient visited our hospital for "a small amount of vaginal bleeding for 1 day." Upon gynecological examination, a 2.0 cm × 2.0 cm mass was found in the upper part of the right wall of the vagina, protruding from the vaginal wall with a smooth surface. On December 22, 2020, a pelvic ultrasound showed endometrial thickening (0.7 cm) and an uneven echo. A 1.2 cm × 0.6 cm × 0.5 cm mass was observed on the anterior wall of the vagina, with a fuzzy boundary, and a hypoechoic inside with multiple strong echoes. Color Doppler flow imaging (CDFI) could detect a few blood flow signals. On December 23, 2020, pelvic enhancement magnetic resonance (MR) was performed, which indicated endometrial thickening and uneven internal signal and enhancement. An oval equal T1 mixed T2 signal shadow was observed on the anterior wall of the upper segment of the vagina, approximately 1.7 cm × 1.4 cm × 1.9 cm, with obvious ring reinforcement (Figures 1A-C). We suggested that the patient be hospitalized for surgery, but the patient was not hospitalized in time owing to atrial fibrillation. Therefore, the patient was regularly reviewed using pelvic ultrasound while treating her atrial fibrillation. Ultrasound showed that the vaginal mass gradually increased in size, and there was effusion with a medium echo mass in the uterine cavity. On December 11, 2021, a pelvic ultrasound showed that the thickness of the single-layer endometrium was approximately 0.3 cm, and the echo was uneven. A liquid area with a depth of approximately 0.7 cm was observed in the uterine cavity. The mass on the anterior wall of the vagina grew to be 2.1 cm × 1.5 cm × 1.4 cm in size. CDFI could detect blood flow signals (Figures 1D-F).

The patient did not visit our department for hospitalization until June 22, 2022. She was not on any current medications and had no history of tamoxifen or hormonal therapy. On June 23, 2022, the pelvic ultrasound showed that the mass on the anterior wall of the vagina increased to 2.9 cm × 1.7 cm × 1.5 cm in size. Before surgery, we performed a colposcopy to further clarify the location, scope, and nature of the mass. Under the colposcope, a mass was observed on the right anterior wall of the upper part of the vagina, approximately 3.0 cm × 3.0 cm × 1.0 cm in size, pink, tough in texture, smooth on the surface, small vesicles visible inside the mass, a wide pedicle connected to the vaginal wall, and the shape similar to a mushroom (Figures 2A-C). There was no significant change in the tumor epithelium after staining with 5% acetic acid (Figures 2D, E), and the tumor epithelium appeared brownish-black after staining with 5% Lugol's solution (an iodine-

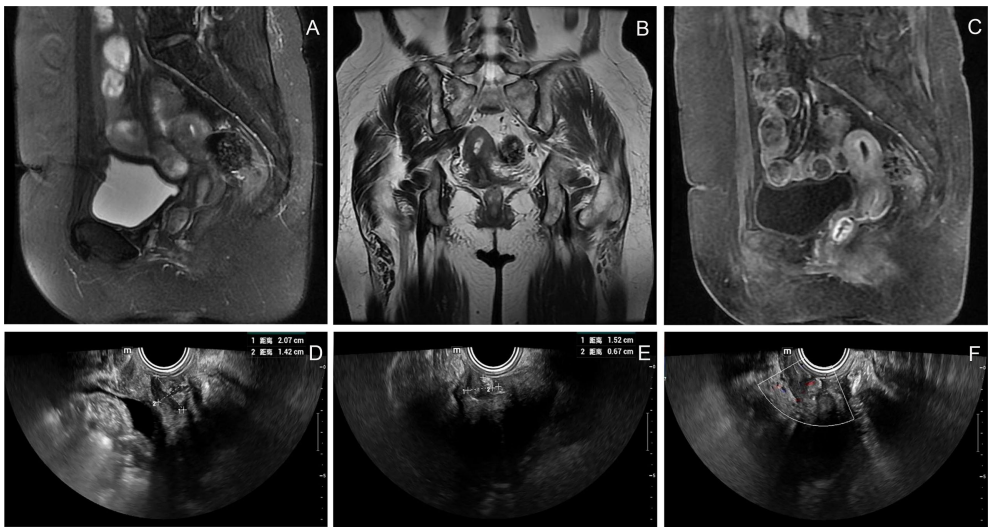

FIGURE 1
Imaging and ultrasound findings of the patient. **(A–C)** Pelvic enhancement MR: an oval equal T1 mixed T2 signal shadow was observed on the anterior wall of the upper segment of the vagina, approximately 1.7 cm × 1.4 cm × 1.9 cm, with obvious ring reinforcement; **(D–F)** Pelvic ultrasound: a 2.1 cm × 1.5 cm × 1.4 cm mass was observed on the anterior wall of the vagina, with a fuzzy boundary and a hypoechoic inside with multiple strong echoes. CDFI could detect blood flow signals.

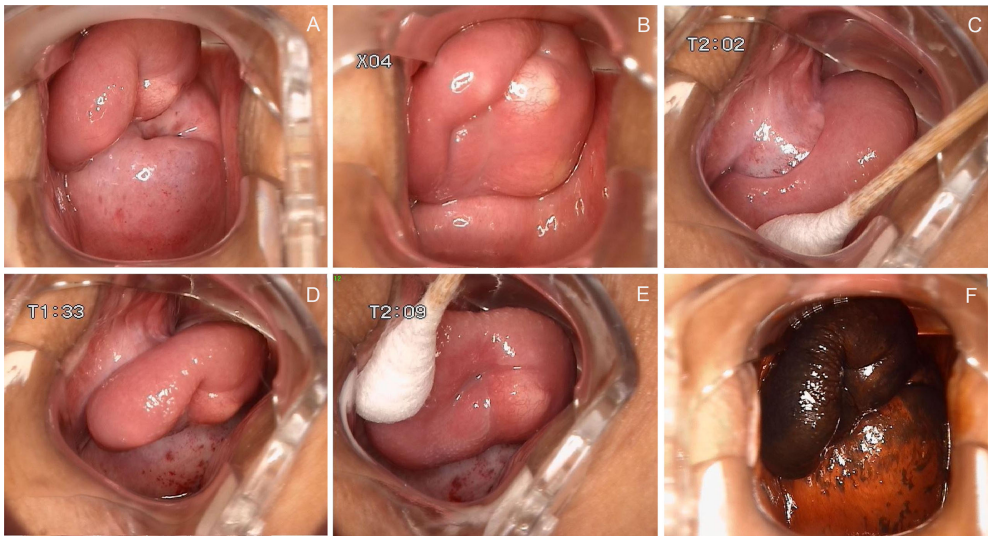

FIGURE 2
Colposcopy findings of the patient. **(A–C)** A mass was observed on the right anterior wall of the upper part of the vagina, approximately 3.0 cm × 3.0 cm × 1.0 cm in size, pink, tough in texture, smooth on the surface, small vesicles visible inside the mass, a wide pedicle connected to the vaginal wall, and the shape similar to a mushroom; **(D, E)** There was no significant change in the tumor epithelium after staining with 5% acetic acid; **(F)** The tumor epithelium appeared brownish-black after staining with 5% Lugol's solution.

containing solution) (Figure 2F). Therefore, we speculated that this mass was a benign tumor with normal squamous epithelium on its surface. On June 28, 2022, the patient underwent vaginal mass resection and hysteroscopic endometrial polypectomy under general anesthesia. The vaginal mass was completely removed during the surgery, and the frozen section was pathologically determined to be benign. The patient recovered well and was discharged on the third postoperative day. The pathological results of the vaginal wall tumor indicated that it was a superficial vaginal myofibroblastoma. The gross pathological examination showed that the size of the tumor was approximately 3.2 cm × 2.8 cm × 0.8 cm, the texture was tough and slightly soft, and the color was pink white (Figure 3A). Microscopic examination revealed that the tumor tissue was located under the squamous epithelium (Figure 3B) and was composed of spindle and stellate-shaped cells and contained abundant thin-walled blood vessels, with some mast cells scattered in the tissue (Figures 3C, D). Immunohistochemical analysis showed that the tumor was positive for caldesmon, desmin, CD34, estrogen receptor (ER), and progesterone receptor (PR) (Figures 3E-I); was focally positive for α-smooth muscle actin (SMA) (Figure 3J); and was approximately 3% positive for Ki-67 (Figure 3K) and negative for cytokeratin (CK), epithelial membrane antigen (EMA), and S-100 (Figures 3L-N). The scattered mast cells were positive for CD117 (Figure 3O). No abnormalities were found in the outpatient follow-up 1 month postoperatively.

Discussion

SMF has been recognized as a mesenchymal neoplasm arising from the superficial portion of the lower genital tract in women (5). The exact etiology and pathogenic mechanisms underlying tumor development remain unclear (5, 6). Liu et al. suggested no association between an SMF tumor and infection with human papilloma virus, Epstein-Barr virus, or human herpesvirus 8 (6). Many gynecologists and pathologists may not be familiar with the disease owing to its rarity. We performed a PubMed-indexed, English-language literature search that yielded 57 reported cases of SMF of the lower female genital tract (Table 1). Among them, 75.4% (43/57) occurred in the vagina, 12.3% (7/57) in the cervix, and 12.3% (7/57) in the vulva. The five non-classical myofibroblastoma cases reported by Magro et al. (9) were excluded because it was not clear if the tumors were histologic variants or other types of myofibroblastoma. In the reported cases, 19.5% (8/41) of patients had been taking tamoxifen for whom a history of drug use was available, raising the possibility of a hormone-responsive neoplasm.

The symptoms in patients with SMF were non-specific. The main clinical manifestations were asymptomatic polypoid or nodular masses of varying sizes (0.2–12 cm). Occasionally, the mass may prolapse out of the vagina or manifest as abnormal vaginal bleeding. Only five of the 57 patients had two lesions, and the rest had single lesions. The patients ranged in age from 23–80 years, with a mean age

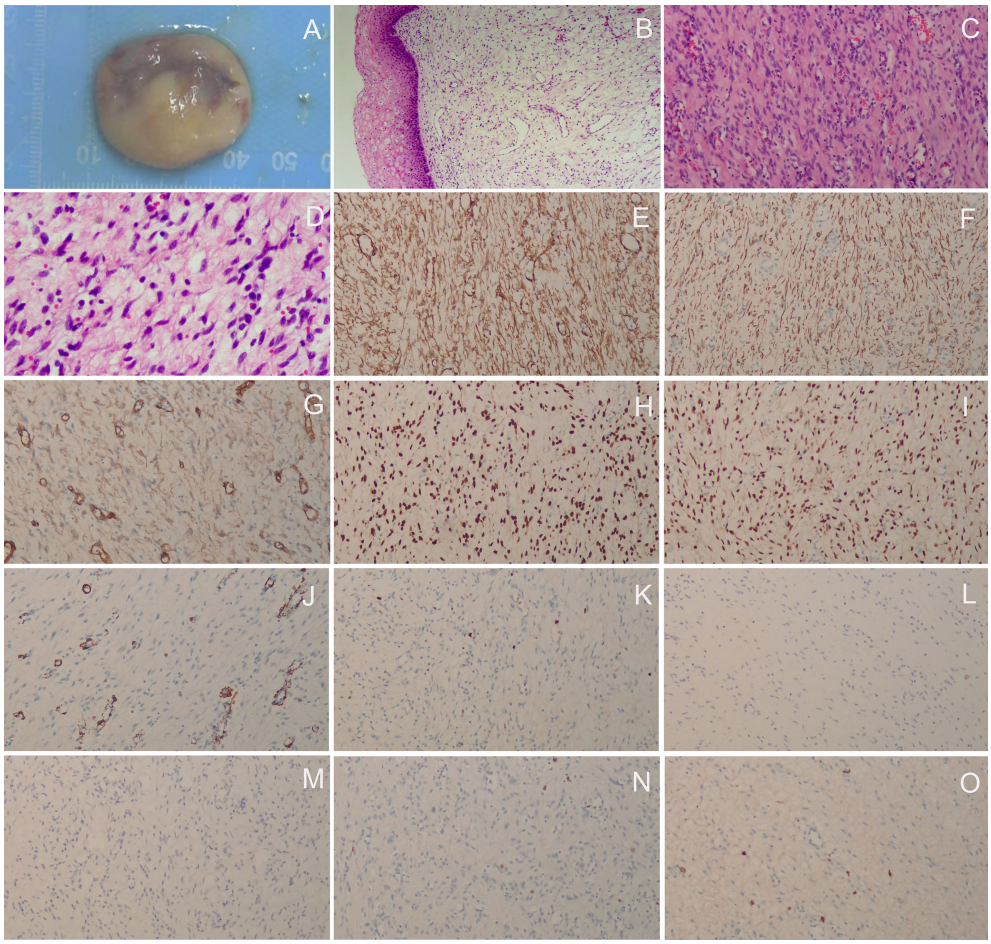

FIGURE 3
Histopathological and immunohistochemical staining findings. **(A)** The gross pathological examination showed that the size of the tumor was approximately 3.2 cm × 2.8 cm × 0.8 cm, the texture was tough and slightly soft, and the color was pink white; **(B)** The tumor tissue was located under the squamous epithelium (H&E staining, ×40); **(C, D)** The tumor tissue was composed of spindle and stellate-shaped cells and contained abundant thin-walled blood vessels, with some mast cells scattered in the tissue (H&E staining, C, ×100; D, × 200); **(E)** caldesmon (+), **(F)** desmin (+), **(G)** CD34 (+), **(H)** ER (+), **(I)** PR (+), **(J)** αSMA (focally +), **(K)** Ki-67 (approximately 3% +), **(L)** CK (–), **(M)** EMA (–), **(N)** S-100 (–); **(O)** The scattered mast cells were positive for CD117 (**E-O**, ×100).

of 54.7 and a median age of 55.5 years. Only six patients were younger than 40 years of age, and only one of them was pregnant. In our case, a vaginal mass was found during gynecological examination due to postmenopausal vaginal bleeding, which may have been caused by endometrial polyps.

The diagnosis of SMF of the lower female genital tract is usually challenging because it is rare and shares many clinicopathological features with other mesenchymal tumors, such as fibroepithelial stromal polyps, angiomyofibroblastoma, mammary-type myofibroblastoma, cellular angiofibroma, and aggressive angiomyxoma (12, 18). The diagnosis should be combined with gynecological examination, ultrasound, and MRI, and the final diagnosis still depends on histopathology. Histological examination shows a well-circumscribed, yet unencapsulated lesion, covered by unremarkable or hyperplastic squamous epithelium (19). Tumors usually present with spindle and stellate-shaped cells within a collagenous stroma, showing an expansive growth pattern with a grenz zone of uninvolved tissue (12). Multiple patterns, including lace-like, sieve-like, and fascicular, are characteristic features, as are myxoid or edematous foci, and few mitotic figures (19). Cells are positive for vimentin and usually for desmin. CD34 and αSMA are positive in some cases, and most neoplasms are positive for ER and PR. Tumors are negative for S100, EMA, and CK (19). The case described in this report is consistent with the above histopathological features, and the histopathological features of other mesenchymal lesions have been described in detail previously (12, 18, 19).

As described in the literature, SMF often presents as a well-circumscribed polypoid or nodular mass. Our case also presented as a nodular mass, and we used colposcopy to magnify the lesion to visualize a more intuitive manifestation

TABLE 1 Cases of superficial myofibroblastoma of the lower female genital tract in the English language literature.

Case	Age (yr)	Symptoms	Location	Gross Lesion	Size (cm)	Hormones	Outcome	Follow-up (mon)
1 (1)	40	Asymptomatic	Vagina	Mass	4.5	BCP	NED	120
2 (1)	44	Asymptomatic	Vagina	Polyp	NG	No	NED	240
3 (1)	50	Asymptomatic	Vagina	Polyp	1.3	Tam	NED	48
4 (1)	51	NG	Vagina	Mass	2.0	NG	NG	
5 (1)	54	Asymptomatic	Vagina	Polyp	2.0	No	LTF	
6 (1)	58	Asymptomatic	Vagina	Polyp	1.5	HRT	NED	72
7 (1)	61	Asymptomatic	Vagina	Mass	2.0	HRT+Tam	NED	12
8 (1)	63	Asymptomatic	Vagina	Polyp	1.5	HRT	NED	60
9 (1)	63	NG	Vagina	Mass	1.5	HRT	NED	18
10 (1)	66	NG	Vagina	Polyp	2.0	NG	LTF	
11 (1)	71	Asymptomatic	Vagina	Polyp	1.0	No	NED	12
12 (1)	74	Vaginal bleeding	Vagina	Polyp	6.5	No	NED	60
13 (3)	57	Asymptomatic	Vagina	Nodule	0.2	Tam	NED	14
14 (3)	54	Vaginal bleeding	Vagina	Nodule	0.8 and 0.4	Tam	NED	24 and 12
15 (3)	49	Asymptomatic	Vagina	Nodule	0.4	Tam	NED	24
16 (3)	63	Asymptomatic	Vagina	Polyp	1.4	No	NED	12
17 (3)	80	Asymptomatic	Vagina	Polyp	3.5	No	NED	8
18 (3)	23	Asymptomatic	Vagina	Polyp	4.0	No	NED	8
19 (3)	63	Asymptomatic	Vagina	Polyp	2.7	NG	NED	8
20 (3)	60	Asymptomatic	Vagina	Polyp	1.5	NG	NED	10
21 (3)	62	Asymptomatic	Vagina	Nodule	0.4	NG	NED	11
22 (7)	40	Asymptomatic	Vagina	Polyp or nodule	1.9	No	Recurrence	108
23 (7)	71	Asymptomatic	Vagina	Polyp or nodule	1.9	Tam	NED	6-18
24 (7)	61	Asymptomatic	Vagina	Polyp or nodule	1.6 and 2.2	No	NED	6-18
25 (8)	63	Prolapsed out of vagina	Vagina	Polyp	2.6 and 1.5	Tam	NED	64
26 (8)	47	Asymptomatic	Vagina	Mass	1.5	No	NED	6
27 (8)	54	Prolapsed out of vagina	Vagina	Polyp	3.7	No	NED	4
28 (8)	56	Prolapsed out of vagina	Vagina	Polyp	3.0	No	NED	2
29 (9)	73	NG	Vagina	Polyp or nodule	2.5	No	NG	
30 (9)	69	NG	Vagina	Polyp or nodule	2.0	No	NED	96
31 (9)	44	NG	Vagina	Polyp or nodule	1.5	BCP	NED	11
32 (9)	77	NG	Vagina	Polyp or nodule	0.4	No	NED	6
33 (10)	63	Asymptomatic	Vagina	Polyp	4.0	No	NG	
34 (4)	73	Prolapsed out of vagina	Vagina	Mass	4.7	Tam	NG	
35 (6)	59	Postcoital bleeding	Vagina	Polyp	2.0	No	NED	12
36 (11)	50	Vaginal bleeding	Vagina	Nodule	1.6	No	NED	96
37 (12)	42	Vaginal bleeding	Vagina	Mass	3.2	No	NG	
38*	71	Vaginal bleeding	Vagina	Mass	2.9	No	NED	1
39 (5)	40	NG	Vagina	Nodule	5.0	NG	NG	
40 (5)	55	NG	Vagina	Nodule	1.0	NG	NG	
41 (5)	45	NG	Vagina	Nodule	1.1	NG	NG	

(Continued)

TABLE 1 Continued

Case	Age (yr)	Symptoms	Location	Gross Lesion	Size (cm)	Hormones	Outcome	Follow-up (mon)
42 (5)	60	NG	Vagina	Nodule	1.0	NG	NG	
43 (5)	55	NG	Vagina	Nodule	5.0	NG	NG	
44 (1)	40	Asymptomatic	Cervix	Polyp	4.0	No	NED	36
45 (1)	58	Vaginal discharge and prolapsed out of vagina	Cervix	Polyp	5.0	HRT	NED	48
46 (7)	49	Asymptomatic	Cervix	Fibroid	4.5	No	NED	6-18
47 (13)	27	Prolapsed out of vagina	Cervix	Mass	5.0	No	NG	
48 (14)	45	Menometrorrhagia	Cervix	Mass	3.8	No	NG	
49 (15)	45	Pelvic pain and menometorrhagia	Cervix	Mass	6.5	No	NED	96
50 (5)	74	NG	Cervix	Nodule	3.0	NG	NG	
51 (3)	27	Asymptomatic	Vulva	Mass	2.7	NG	NED	60
52 (3)	38	Asymptomatic	Vulva	Mass	4.5	NG	NG	
53 (9)	NG	NG	Vulva	Mass	1.2	No	NG	
54 (16)	37	Asymptomatic	Vulva	Mass	7.0	NG	NED	12
55 (17)	77	Bulky swelling	Vulva	Mass	12.0	No	NG	
56 (5)	46	NG	Vulva	Nodule	10.0	NG	NG	
57 (5)	26	NG	Vulva	Nodule	6.5	NG	NG	

NG, not given; BCP, birth control pills; Tam, Tamoxifen; HRT, hormone replacement therapy; NED, no evidence of disease; LTF, lost to follow-up. *current case.

of this mass. Simultaneously, we observed a wide pedicle that connected the mass to the vaginal wall, similar to that reported by Tomita et al. (12) and Adams et al. (13). Owing to the small number of cases, it is unclear whether this phenomenon is unique to SMF. To the best of our knowledge, this is the first report of colposcopy as an aid in the diagnosis and evaluation of SMF. Colposcopy is a procedure in which a lighted, magnifying instrument called a colposcope is used to examine the cervix, vagina, and vulva (20). Colposcopy is important in the diagnosis of cervical lesions. It also plays a significant role in the diagnosis of vaginal lesions, because the shape, location, and scope of the lesions can be clearly observed, and the reaction of the lesion epithelium to 5% acetic acid and Lugo's solution can be applied in this small space. In the present case, no abnormal changes were observed after the use of acetic acid or Lugol's solution. Dysplastic cells dehydrate and turn densely white with the application of acetic acid (20). Lugol's solution may also be used to highlight the dysplastic area, where the dysplastic cells remain yellow owing to a lack of absorption of the solution (20). Although definitive diagnosis should be based on histopathological assessment, colposcopic features such as well-defined morphology and coverage with normal squamous epithelium may contribute to differentiating from more aggressive entities such as malignant tumors.

Surgical resection is the main clinical treatment for SMF; among 37 patients with available follow-up information (1 month to 20 years), only one case had local recurrence 9 years after initial incomplete excision (7), indicating a good prognosis and low recurrence rate, although long-term follow-up is still recommended (7, 11). The patient in this case study completed the treatment and remained in good condition without recurrence.

Conclusions

SMF of the lower female genital tract is a relatively rare benign mesenchymal tumor most likely to occur in the vagina. The age range of SMF patients is wide; however, it mainly occurs in perimenopausal and postmenopausal women. Here, we report the diagnosis and treatment of superficial vaginal myofibroblastoma in a postmenopausal woman. For the first time, colposcopy was used for auxiliary diagnosis and evaluation before surgery. The lesion was covered with normal squamous epithelium with a wide pedicle and a mushroom-like appearance. The patient had a good prognosis and experienced no recurrence after surgical treatment.

Data availability statement

The original contributions presented in the study are included in the article/supplementary material. Further inquiries can be directed to the corresponding author.

Ethics statement

The studies involving human participants were reviewed and approved by Institutional Review Board of Shengjing Hospital of China Medical University. The patients/participants provided their written informed consent to participate in this study. Written informed consent was obtained from the individual(s) for the publication of any potentially identifiable images or data included in this article.

Author contributions

YW was responsible for drafting of the manuscript. MS analyzed the literature. JW was responsible for the data collection and critical revision of the manuscript. All authors contributed to the article and approved the submitted version.

Funding

This work was supported by the Shengjing Hospital of China Medical University 345 Talent Project (No. 30B).

Acknowledgments

We would like to thank the patient for her permission to present this case report to sensitize practitioners. We also thank all the medical staff who participated in the diagnosis and treatment of this patient.

Conflict of interest

The authors declare that the research was conducted in the absence of any commercial or financial relationships that could be construed as a potential conflict of interest.

Publisher's note

All claims expressed in this article are solely those of the authors and do not necessarily represent those of their affiliated organizations, or those of the publisher, the editors and the reviewers. Any product that may be evaluated in this article, or claim that may be made by its manufacturer, is not guaranteed or endorsed by the publisher.

References

1. Laskin WB, Fetsch JF, Tavassoli FA. Superficial cervicovaginal myofibroblastoma: fourteen cases of a distinctive mesenchymal tumor arising from the specialized subepithelial stroma of the lower female genital tract. *Hum Pathol* (2001) 32(7):715–25. doi: 10.1053/hupa.2001.25588

2. McCluggage WG. A review and update of morphologically bland vulvovaginal mesenchymal lesions. *Int J Gynecol Pathol* (2005) 24(1):26–38. doi: 10.1097/01.pgp.0000148336.77264.6e

3. Ganesan R, McCluggage WG, Hirschowitz L, Rollason TP. Superficial myofibroblastoma of the lower female genital tract: Report of a series including tumours with a vulval location. *Histopathology* (2005) 46(2):137–43. doi: 10.1111/j.1365-2559.2005.02063.x

4. Smith SA, Doyle V, Rutherford E, Elliot V, Blaquiere RM. Superficial myofibroblastoma of the lower female genital tract with description of the MRI features. *BJR Case Rep* (2017) 3(1):20160052. doi: 10.1259/bjrcr.20160052

5. Tajiri R, Shiba E, Iwamura R, Kubo C, Nawata A, Harada H, et al. Potential pathogenetic link between angiomyofibroblastoma and superficial myofibroblastoma in the female lower genital tract based on a novel MTG1-CYP2E1 fusion. *Mod Pathol* (2021) 34(12):2222–8. doi: 10.1038/s41379-021-00886-8

6. Liu JL, Su TC, Shen KH, Lin SH, Wang HK, Hsu JC, et al. Vaginal superficial myofibroblastoma: a rare mesenchymal tumor of the lower female genital tract and a study of its association with viral infection. *Med Mol Morphol* (2012) 45(2):110–4. doi: 10.1007/s00795-011-0566-z

7. Stewart CJ, Amanuel B, Brennan BA, Jain S, Rajakaruna R, Wallace S. Superficial cervico-vaginal myofibroblastoma: a report of five cases. *Pathology* (2005) 37(2):144–8. doi: 10.1080/00313020500058284

8. Wang QF, Wu YY, Wang J. Superficial cervicovaginal myofibroblastoma: report of four cases and literature review. *Chin Med J (Engl)* (2010) 123(8):1093–6. doi: 10.3760/cma.j.issn.0366-6999.2010.08.022

9. Magro G, Caltabiano R, Kacerovská D, Vecchio GM, Kazakov D, Michal M. Vulvovaginal myofibroblastoma: expanding the morphological and immunohistochemical spectrum. a clinicopathologic study of 10 cases. *Hum Pathol* (2012) 43(2):243–53. doi: 10.1016/j.humpath.2011.04.027

10. Olinici CD, Crişan D, Zolog A, Puşcaş M. Vaginal superficial myofibroblastoma. case report and review of the literature. *Rom J Morphol Embryol* (2007) 48(2):165–70.

11. Atinga A, El-Bahrawy M, Stewart V, Bharwani N. Superficial myofibroblastoma of the genital tract: a case report of the imaging findings. *BJR Case Rep* (2019) 5(1):20180057. doi: 10.1259/bjrcr.20180057

12. Tomita Y, Takabayashi E, Yuzawa S, Okizaki A. Superficial myofibroblastoma of the vagina with a stalk: Case report of a rare vaginal tumor with notable radiological findings. *Radiol Case Rep* (2021) 16(12):3690–4. doi: 10.1016/j.radcr.2021.08.064

13. Adams B, Fogarty P, McKenna M, McManus D. Superficial myofibroblastoma of the lower female genital tract: First case report of a pregnant patient. *J Obstet Gynaecol* (2008) 28(6):657–8. doi: 10.1080/01443610802421668

14. Abdelaziz M, Eziba N, Sharma S, Kleven D, Al-Hendy A. Cervical superficial myofibroblastoma: Case report and review of the literature. *SAGE Open Med Case Rep* (2017) 5:2050313x17726936. doi: 10.1177/2050313x17726936

15. Cinel L, O'Hara B, Prestipino A. Superficial myofibroblastoma of the lower female genital tract in the uterine cervix showing focal pseudosarcomatous morphology. *Pathology* (2009) 41(7):691–3. doi: 10.3109/00313020903305837

16. Peng WX, Wada R, Kure S, Fukunaga M, Naito Z. Superficial myofibroblastoma in the vulva mimicking aggressive angiomyxoma: A case report and review of the literature. *Case Rep Pathol* (2019) 2019:1582714. doi: 10.1155/2019/1582714

17. Patrizi L, Borelli B, Di Prete M, Bruno V, Mauriello A, Piccione E, et al. A rare case of vulvar superficial myofibroblastoma associated with ambigous and unusual differential diagnosis. *Gynecol Oncol Rep* (2020) 34:100637. doi: 10.1016/j.gore.2020.100637

18. Schoolmeester JK, Fritchie KJ. Genital soft tissue tumors. *J Cutan Pathol* (2015) 42(7):441–51. doi: 10.1111/cup.12507

19. McCluggage WG. Recent developments in vulvovaginal pathology. *Histopathology* (2009) 54(2):156–73. doi: 10.1111/j.1365-2559.2008.03098.x

20. Cooper DB, Dunton CJ. Colposcopy. In: *StatPearls [Internet]*. Treasure Island (FL: StatPearls Publishing (2022).

frontiers | Frontiers in Oncology

TYPE Original Research
PUBLISHED 31 October 2022
DOI 10.3389/fonc.2022.956380

OPEN ACCESS

EDITED BY
Federico Ferrari,
University of Brescia, Italy

REVIEWED BY
Carlo Ronsini,
Università degli Studi della Campania "Luigi Vanvitelli", Italy
Federica Perelli,
Santa Maria Annunziata Hospital, Italy

*CORRESPONDENCE
Dongyan Cao
caodongyan@pumch.cn

SPECIALTY SECTION
This article was submitted to Gynecological Oncology, a section of the journal Frontiers in Oncology

RECEIVED 30 May 2022
ACCEPTED 20 September 2022
PUBLISHED 31 October 2022

CITATION
Li J and Cao D (2022) Prognostic nomogram that predicts progression-free survival and overall survival of patients with ovarian clear cell carcinoma.
Front. Oncol. 12:956380.
doi: 10.3389/fonc.2022.956380

Prognostic nomogram that predicts progression-free survival and overall survival of patients with ovarian clear cell carcinoma

Jiayi Li[1,2,3] and Dongyan Cao[2,3]*

[1]Department of Nuclear Medicine, Peking Union Medical College Hospital, Chinese Academy of Medical Sciences & Peking Union Medical College, Beijing, China, [2]Department of Obstetrics and Gynecology, Peking Union Medical College Hospital, Chinese Academy of Medical Sciences & Peking Union Medical College, Beijing, China, [3]National Clinical Research Center for Obstetric & Gynecologic Diseases Department of Obstetrics and Gynecology, Peking Union Medical College Hospital, Chinese Academy of Medical Sciences & Peking Union Medical College, Beijing, China

Objectives: We aims to develop nomograms to predict progression-free survival (PFS) and overall survival (OS) in patients with ovarian clear cell carcinoma (OCCC) after primary treatment and compare the predictive accuracy with the currently used International Federation of Gynecology and Obstetrics (FIGO) system.

Methods: We collected data from 358 Chinese patients diagnosed with OCCC and who underwent standard treatment at our hospital. Patients diagnosed from 1982-9 to 2011-12 were classified as the training group and patients diagnosed from 2012-1 to 2016-11 were classified as the validation group. Nomograms were developed based on the training group and was validated in the validation group. The predictive performance was determined by concordance index and calibration curve.

Results: The most predictive nomogram for PFS was constructed using variables: thrombosis, the FIGO staging, residual of the tumor and distant metastasis, with a concordance index of 0.738. While the nomogram for OS consisted of thrombosis, lymph node metastasis, residual of the tumor, malignant ascites/washing, and platinum resistance, with a concordance index of 0.835. The nomograms were internally validated by concordance indexes of 0.775 and 0.807 for predicting PFS and OS, respectively. In comparison, the concordance statistics for OS based on the FIGO staging was significantly lower ($P<0.05$).

Conclusion: We have established two prognostic nomograms for recurrence and long-term survival in patients with OCCC after primary treatment in a large

Chinese center and validated them in patients from the same center. This tool used variables specifically related to OCCC and was more accurate than the FIGO system. It is relatively easy to use in clinic for patient counseling, postoperative management, and follow-up for individual patients.

KEYWORDS

nomogram, ovarian clear cell carcinoma, progression-free survival, overall survival, predictive model

Introduction

Ovarian clear cell carcinoma (OCCC) is a rare subtype of epithelial ovarian cancer in the United States, while it represents 11.1% of epithelial ovarian cancer in Asians (1–3). In general, OCCC is thought to have different biological characteristics from other types of epithelial ovarian cancer. OCCC is found to arise from endometriosis or clear cell adenofibroma, and is likely to be diagnosed at early-stage, with a relatively good prognosis (2, 4–6). However, advanced-stage OCCC is found to have poor prognosis due to its resistance to chemotherapy (1, 7).

Nomograms have been developed to be an alternative standard for cancer prognosis in recent years (8, 9). Several nomograms have been established on epithelial ovarian cancer (10, 11). However, most nomograms on epithelial ovarian cancer are based on mixed histology of epithelial ovarian cancer, with high-grade serous ovarian cancer being the most common type. Predictors of different types of epithelial ovarian cancer are different and there is rare attempt to establish a nomogram especially on OCCC.

Considering the relative high incidence of OCCC in Asians, the present study enrolled OCCC patients treated at Department of Obstetrics and Gynecology in Peking Union Medical College Hospital, a large ovarian carcinoma center in China and the aims of the present study were to identify significant indicators and develop nomograms for progression-free survival (PFS) and overall survival (OS) for patients with OCCC in China. In addition, the present study compared the predictive accuracy with the currently used International Federation of Gynecology and Obstetrics (FIGO) staging system.

Methods

Participants

Patients diagnosed with pure OCCC and treated in Peking Union Medical College Hospital, Beijing, China from 1982-9 to 2016-11 were enrolled in our study. Patients with early stage (stage I and II) OCCC have undergone radical surgical staging (RSS) including total abdominal hysterectomy, bilateral salpingo-oophorectomy, systematic pelvic and para-aortic lymphadenectomy, and radical omentectomy. Patients with advanced OCCC (stage III and IV) have received either primary debulking surgery (PDS), followed by platinum and taxane chemotherapy, or neoadjuvant chemotherapy (NACT), followed by interval debulking surgery (IDS) and subsequent chemotherapy. Although optimal debulking (less than 1 cm in maximum diameter of residual tumor) or complete resection (no residual tumor) is desirable, those with unresectable tumors received suboptimal debulking surgery. In terms of surgical approaches, both laparotomy and laparoscopy were performed by our center.

They all received adjuvant platinum-based chemotherapy after primary surgery. Women who did not received surgery, women who did not received platinum-based chemotherapy after primary surgery, women with mixed type of ovarian carcinoma and women with concurrent cancer other than ovarian cancer were excluded. All participants provided written informed consent. The study was approved by the Ethics Committee of Peking Union Medical College Hospital (S-K903).

For the assessment of survival, PFS was defined as the time from diagnosis to the date of disease progression or end of the study. OS was defined as the time from the date of initial diagnosis to the date of cancer-related death or loss of follow-up.

Variables

Preoperative demographics and clinical information such as: diagnosed age, body mass index, carbohydrate antigen 125 before operation, endometriosis, thrombosis, past medical history, operative procedure, postoperative chemotherapy (taxane and platinum based chemotherapy), the FIGO staging (according to the 2014 the FIGO staging for ovarian, fallopian tube and peritoneal cancer), macroscopical information

(maximal tumor diameter, bilateral or unilateral of tumor, and the residual of the tumor), microscopical information (histologic type, the presence of lymph node metastasis, peritoneal cytology, and malignant ascites or washing), and mode of recurrence and death were collected from medical records and clinical follow-up visit. We also analyzed platinum resistance: Patients who showed recurrence in less than 6 months after completion of primary treatment were classified into platinum resistant group, while patients who relapsed 6 months or more or those who completed taxane and platinum-based chemotherapy and did not experience disease recurrence for at least 6 months of the follow-up period were classified into platinum sensitive group. Patients with insufficient observable time to determine platinum sensitivity were also excluded.

Statistical analyses

Categorical variables were compared using the $\chi 2$ test or Fisher's exact test. Continuous variables were compared using the t test or Mann-Whitney U test for variables with an abnormal distribution. In the univariate analysis, crude analyses were performed to identify potential risk factors. Then, multivariate analyses with backward procedures were used to select the best-fit model. A statistical significance level of 0.20 was used to select variables into the model.

Stage I and II were combined and Stage III and IV were combined in the FIGO staging due to the small sample size of Stage II and Stage IV patients. Platinum resistance was considered a variable in the analyses of OS prognosis.

Patients diagnosed from 1982-9 to 2011-12 were classified as the training group and patients diagnosed from 2012-1 to 2016-11 were classified as the validation group. Nomograms were constructed based on the results of multivariate analysis to predict PFS, and OS from the training group. The performance of the nomogram was measured by concordance index and calibration curve using a bootstrapped sample. Model validation was performed using bootstrap resampling to quantify the overfitting of our modeling strategy and predict future performance of the model. Then, internal validation was performed on the validation group. Statistical analyses were performed using the package in R version 2.14.1 (http://www.r-project.org/).

Results

A total of 358 patients were included in the study, with 247 (69.0%) enrolled in the training group and 111 (31.0%) recruited in the validation group. The mean diagnosed age was 49.5 ± 10.5 years. Of these patients, 13.69% had thrombosis and 37.63% had endometriosis before operation. The training group and validation group had no significant difference in age, body mass index, thrombosis, endometriosis, surgical approaches and surgical procedures. The validation group underwent less advanced-stage patients and less residual tumor than the training group (Table 1).

At the end of this study, recurrence occurred in 130 (36.3%) patients, while 55 (15.4%) patients were lost to follow-up, and 173 (48.3%) patients remained progression-free. 61 (17.0%) patients had died of OCCC, 34 (9.5%) patients were lost to follow-up, and 263 (73.5%) patients remained alive.

Backward stepwise selection in Cox proportional hazards regression model identified several variables that were the most associated with PFS and OS, respectively (Tables 2, 3). Then, nomograms were developed using the selected variables (Figures 1, 2). The nomogram for the prediction of PFS included thrombosis, the FIGO staging, residual of the tumor, distant metastasis. Each factor was assigned a weighted point and patients with a higher total score had a higher risk for recurrence. Discrimination of the model measured by the Harrell concordance index was 0.738 (Figure 1). By the same algorithm, the nomogram for predicting OS was developed. The nomogram consisted of thrombosis, lymph node metastasis, residual of the tumor, malignant ascites/washing, and platinum resistance, with a Harrell concordance index of 0.835 (Figure 2).

Bootstrap validation of the model with 500 iterations revealed minimal evidence of model overfit. The calibration plot of the models showed good predictive accuracy (Figures 3, 4). In the validation cohort, the concordance index of were 0.775 and 0.807 for predicting PFS and OS, respectively.

In comparison, the concordance statistics for PFS and OS of OCCC based on the FIGO staging were 0.715 and 0.727, respectively. The concordance indice of the FIGO staging for OS was significantly lower than that of the nomogram ($P < 0.05$) while the concordance indice for PFS showed no significance.

Discussion

In the present study, we successfully established nomograms for predicting PFS and OS of patients with OCCC in a large ovarian cancer center in China. The Harrell concordance indexes of these models were 0.873, 0.738 and 0.835, respectively.

OCCC is thought to have different biological characteristics from other types of epithelial ovarian cancer while there are rare attempts to establish a nomogram especially on OCCC. Therefore, we successfully established nomograms using special prognostic factors in this type of ovarian cancer. In addition, it was firstly demonstrated that our nomogram was more accurate than the FIGO system. It is relatively easy to use in clinic for patient counseling, postoperative management, and follow-up for individual patients.

Such predictive nomograms are of great clinical value with the era of precision medicine. In clinic, these indicators were

TABLE 1 Patients' characteristics.

Variables	All patients (n = 358)	Training group (n = 247)	Validation group (n = 111)	P value
Age of diagnosis/y (mean ± standard deviation)	49.5 ± 10.5	50.0 ± 10.5	48.4 ± 10.4	0.197
Body mass index of diagnosis/kg/m2 (mean ± standard deviation)	22.6 ± 3.1	25.5 ± 7.2	22.5 ± 2.7	0.704
Thrombosis n(%)				0.119
No n (%)	309 (86.31%)	208 (84.21%)	101 (90.99%)	
Yes n (%)	49 (13.69%)	39 (15.79%)	10 (9.01%)	
Endometriosis n(%)				0.726
No n (%)	179 (62.37%)	111 (61.33%)	68 (64.15%)	
Yes n (%)	108 (37.63%)	70 (38.67%)	38 (35.85%)	
Elevated Carbohydrate antigen 125 n(%)				0.010
No n (%)	159 (44.41%)	107 (43.32%)	52 (46.85%)	
Yes n (%)	199 (55.59%)	140 (56.68%)	59 (53.15%)	
Surgical approaches				0.405
Laparotomy n(%)	326 (91.06%)	227 (91.90%)	99 (89.19%)	
Laparoscopy n(%)	32 (8.94%)	20 (8.10%)	12 (10.81%)	
Surgical procedures for patients with advanced stages				0.006
Primary debulking surgery n(%)	72 (52.17%)	59 (54.63%)	13 (43.33%)	0.273
Interval debulking surgery n(%)	66 (47.83%)	49 (45.37%)	17 (56.67%)	
Tumor side				0.006
Unilateral n(%)	265 (74.86%)	171 (70.37%)	94 (84.68%)	
Bilateral n(%)	89 (25.14%)	72 (29.63%)	17 (15.32%)	
The International Federation of Gynecology and Obstetrics staging				0.004
I n(%)	196 (54.75%)	122 (49.39%)	74 (66.67%)	
II n(%)	24 (6.7%)	17 (6.88%)	7 (6.31%)	
III n(%)	120 (33.52%)	97 (39.27%)	23 (20.72%)	
IV n(%)	18 (5.03%)	11 (4.45%)	7 (6.31%)	
Maximal diameter/cm (mean ± standard deviation)	11.1 ± 6.7	11.3 ± 5.6	10.8 ± 8.5	0.529
Lymph node metastasis				0.082
Negative n (%)	287 (82%)	193 (79.42%)	94 (87.85%)	
Positive n (%)	63 (18%)	50 (20.58%)	13 (12.15%)	
Residual of the tumor n(%)				0.002
Negative n (%)	274 (76.54%)	177 (71.66%)	97 (87.39%)	
Positive n (%)	84 (23.46%)	70 (28.34%)	14 (12.61%)	
Ascites/malignant washing n(%)				0.261
Negative n (%)	296 (82.68%)	200 (80.97%)	96 (86.49%)	
Positive n (%)	62 (17.32%)	47 (19.03%)	15 (13.51%)	
Peritoneal cytology n(%)				0.002
Negative n (%)	228 (63.69%)	144 (58.3%)	84 (75.68%)	
Positive n (%)	130 (36.31%)	103 (41.7%)	27 (24.32%)	
Distant metastasis n(%)				0.631
Negative n (%)	340 (94.97%)	236 (95.55%)	104 (93.69%)	
Positive n (%)	18 (5.03%)	11 (4.45%)	7 (6.31%)	

found to be of great significance for prediction. For example, if an OCCC patient comes to the clinic after primary treatment, the doctor can directly tell him/her the probability of recurrence and prediction of OS using our nomograms. In addition, this model will have a great effect on guiding the next treatment plan in clinical work. If a patient has a high risk of recurrence, more aggressive treatments such as intraperitoneal chemotherapy and more frequent follow-up might be recommended. Therefore, our

TABLE 2 Progression-free survival of patients with ovarian clear cell carcinoma.

Variables	Univariate analysis			Multivariate analysis		
	Harzard ratio	95% Confidence interval	P value	Harzard ratio	95% Confidence interval	P value
Age of diagnosis/y	1.01	0.99-1.03	0.332			
Body mass index of diagnosis/kg/m2	1.04	0.89-1.21	0.655			
Thrombosis	2.20	1.41-3.44	<0.001	1.64	1.02-2.66	0.042
Endometriosis	1.27	0.73-2.2	0.395			
Elevated Carbohydrate antigen 125	4.03	2.06-7.88	<0.001			
Surgical approaches			0.765			
Laparotomy	Reference	Reference	Reference			
Laparoscopy	1.01	0.65-1.33	0.765			
Surgical procedures for patients with advanced stages			0.685			
Primary debulking surgery	Reference	Reference	Reference			
Interval debulking surgery	1.05	0.78-1.21	0.685			
Bilateral tumor side	2.20	1.46-3.32	<0.001			
The International Federation of Gynecology and Obstetrics staging			<0.001			<0.001
I/II	Reference	Reference	Reference	Reference	Reference	Reference
III/IV	4.41	2.94-6.6	<0.001	3.41	2.03-5.73	<0.001
Maximal diameter/cm	1.00	0.96-1.05	0.838			
Lymph node metastasis	2.92	1.86-4.57	<0.001			
Residual of the tumor	3.73	2.47-5.62	<0.001	1.7	0.99-2.91	0.053
Positive ascites/malignant washing	2.27	1.46-3.52	<0.001			
Positive peritoneal cytology	4.19	2.81-6.25	<0.001			
Distant metastasis	6.03	2.83-12.87	0.000	3.18	1.44-7.02	0.004

nomogram makes our evaluation system applicable to patients who have undergone surgery, and can also calculate the prognosis of patients at follow-up.

Several nomograms for predicting survival prognosis of epithelial ovarian cancer have been developed. Obermair et al. (12) introduced a nomogram to predict the recurrence probability in patients with borderline ovarian tumors, while Meurs et al. (13) developed models to predict the risk of recurrence free survival for various types of ovarian tumor. Several studies also (14–16) published nomograms predicting survival for epithelial ovarian cancer. Thus, nomograms for epithelial ovarian cancer have been developed in multiple populations. However, nomograms for OCCC are sparse. One reason might be due to the low incidence in Western women (1). In addition, OCCC has some special characteristics such as the large amount of endometriosis complications, the high rate of thromboembolic complications, and the poor response to chemotherapy, which are different from other subtypes of epithelial ovarian cancer and might influence the prognosis of OCCC (4, 5). Some studies evaluated OCCC (14, 15) with small sample size, while Chen et al. established a nomogram for patients with OCCC based on the Surveillance, Epidemiology, and End Results database (17). However, these studies rarely considered factors specially related with OCCC. Our nomograms for PFS and OS of OCCC combined a series of prognostic factors, such as thrombosis and platinum resistance, which were not incorporated in the FIGO system and previous Chen's research (17). Widely used prognostic systems like the FIGO classification include a limited number of tumor-related variables and it is unknown that whether additional risk factors are of important prognostic values.

In our study, thrombosis was found to be a prognostic factor for OCCC for both PFS and OS, and remained an independent prognostic factor for PFS and OS. The risk of thromboembolic events is demonstrated to higher in OCCC than other histologic subtypes of epithelial ovarian cancer (18). Elena et al. in 2013 demonstrated that thromboembolic events during OCCC primary treatment were associated with a significantly higher risk of cancer recurrence and death (19), which was consistent with our results. Tissue factor is a transmembrane glycoprotein that serves as a physiologic initiator of coagulation and implicates in tumor growth, metastasis, and angiogenesis (20, 21). It was found to be a modulator in thromboembolic events in epithelial ovarian cancer (22). The hypothesis that a paracrine circuit involving thrombosis could lead to more aggressive tumor biology might also contribute to this increased risk (19).

TABLE 3 Overall survival of patients with ovarian clear cell carcinoma.

Variables	Univariate analysis			Multivariate analysis		
	Harzard ratio	95% Confidence interval	P value	Harzard ratio	95% Confidence interval	P value
Age of diagnosis/y	1.02	1-1.05	0.084			
Body mass index of diagnosis/kg/m2	0.69	0.4-1.18	0.173			
Thrombosis	2.65	1.53-4.6	<0.001	2.98	1.4-6.34	0.005
Endometriosis	1.11	0.58-2.13	0.752			
Elevated Carbohydrate antigen 125	5.23	2.23-12.25	<0.001			
Surgical approaches			0.694			
Laparotomy	Reference	Reference	Reference			
Laparoscopy	1.04	0.78-1.37	0.694			
Surgical procedures for patients with advanced stages			0.324			
Primary debulking surgery	Reference	Reference	Reference			
Interval debulking surgery	1.02	0.89-1.13	0.324			
Bilateral tumor side	4.00	2.4-6.65	<0.001			
The International Federation of Gynecology and Obstetrics staging			<0.001			
I/II	Reference	Reference	Reference			
III/IV	<0.001	<0.001	<0.001			
Maximal diameter/cm	1.00	0.95-1.05	0.949			
Lymph node metastasis	4.69	2.75-8.01	<0.001	2.47	1.12-5.42	0.025
Residual of the tumor	8.30	4.92-14	<0.001	1.73	0.8-3.74	0.162
Positive ascites/malignant washing	4.32	2.57-7.25	<0.001	1.95	0.93-4.08	0.076
Positive peritoneal cytology	5.32	3.12-9.06	<0.001			
Distant metastasis	3.40	1.44-8.02	0.005			
Neoadjuvant chemotherapy	2.73	1.56-4.76	<0.001			
Platinum resistance	1.84	0.99-3.4	0.053	10.27	4.5-23.45	<0.001

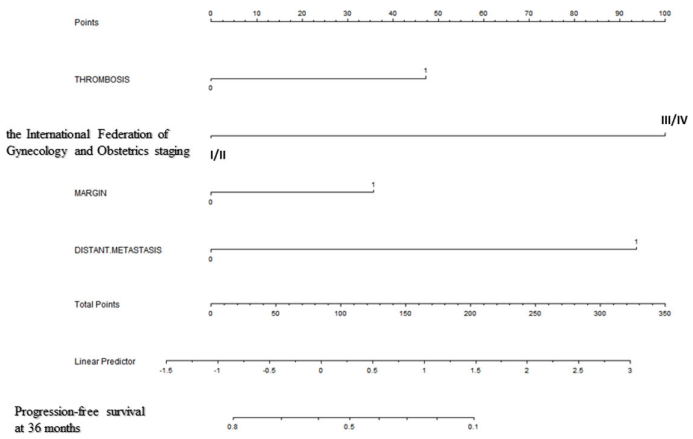

FIGURE 1
A Nomogram for Predicting Progression-free Survival of Patients With Resectable Ovarian Clear Cell Carcinoma After Primary Treatment. To calculate predicted progression-free survival, an individual patient's value is located on each variable axis, and a straight line is drawn upward to the "Points" row to determine the points associated with each factor. After summing the total points, one locates the appropriate total point number and draws a straight line from this to the bottom rows to determine the patient's predicted survival probability. (For each variable: Thrombosis: 0=no thrombosis, 1=exist; The International Federation of Gynecology and Obstetrics staging: I/II=stage I/II, III/IV=stage III/IV; Residual of the tumor: 0=negative, 1=positive; Distant metastasis: 0=no distant metastasis, 1=positive distant metastasis).

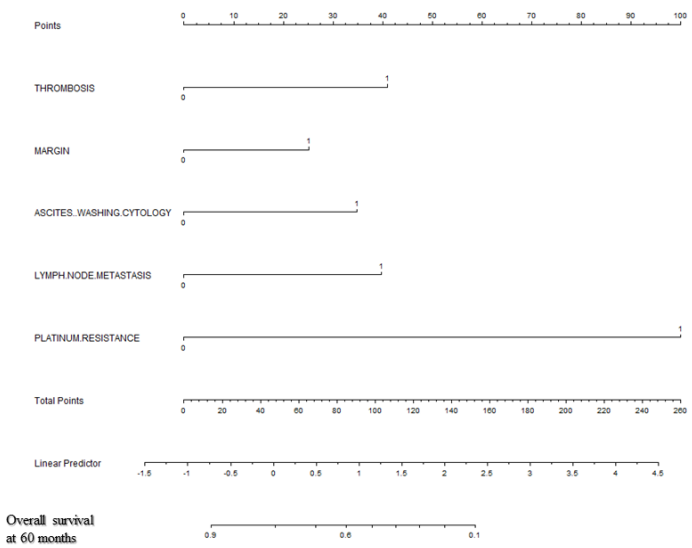

FIGURE 2
A Nomogram for Predicting Overall Survival of Patients With Resectable Ovarian Clear Cell Carcinoma After Primary Treatment. To calculate predicted overall survival, an individual patient's value is located on each variable axis, and a straight line is drawn upward to the "Points" row to determine the points associated with each factor. After summing the total points, one locates the appropriate total point number and draws a straight line from this to the bottom rows to determine the patient's predicted survival probability. (For each variable: Thrombosis: 0=no thrombosis, 1=exist; Residual of the tumor: 0=negative, 1=positive; Malignant ascites/washing: 0=no malignant ascites/washing, 1= malignant ascites/washing; Lymph node metastasis: 0=negative lymph node metastasis, 1=positive lymph node metastasis; Platinum resistance: 0=platinum sensitive, 1=platinum resistant).

Thus, we included thrombosis in both PFS and OS nomogram establishment.

Platinum resistance was another factor which was independently associated with OS for our OCCC patients. A lot of retrospective studies showed that the response rate of OCCC to traditional platinum-based chemotherapy was significantly lower than serous adenocarcinoma (23–25). A Korea group (15) in 2019 also considered platinum resistance

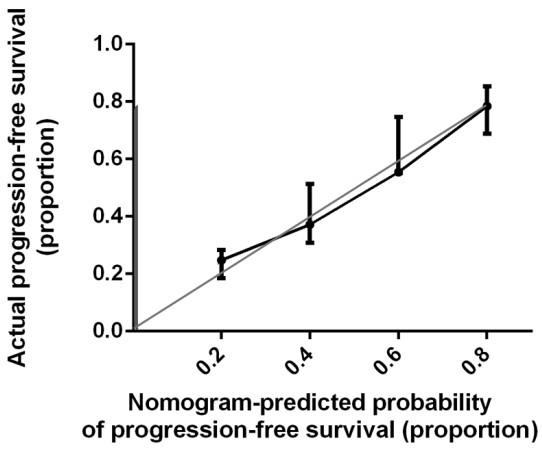

FIGURE 3
Calibration Plot Comparing Predicted and Actual Progression-free Survival Probabilities. The calibration curve for predicting patient progression-free survival is stated in Figure 3. Nomogram-predicted probability of progression-free survival is plotted on the x-axis; actual progression-free survival is plotted on the y-axis. Thin gray line represents the reference line.

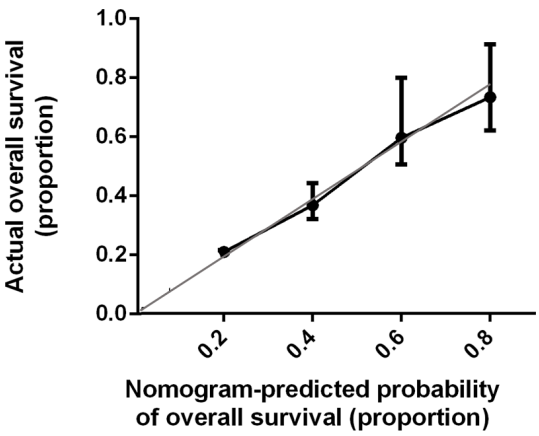

FIGURE 4
Calibration Plot Comparing Predicted and Actual Overall Survival Probabilities. The calibration curve for predicting patient overall survival is stated in Figure 4. Nomogram-predicted probability of overall survival is plotted on the x-axis; actual overall survival is plotted on the y-axis. Thin gray line represents the reference line.

as a prognostic factor in developing nomogram for OS in epithelial ovarian cancer. Therefore, considering the high rate of platinum resistance in OCCC and its prognostic value, we also included it in the development of OS nomogram.

In addition, we have explored the influence of surgery approaches and surgery approaches on PFS and OS. No significant difference was found in OS and PFS between patients undergoing laparotomy and minimally invasive surgery, which was consistent with previous research (26, 27). This indicated that both laparotomy and laparotomy would be applicable in the surgery of ovarian cancer and would not influence the survival of patients. We also explored the influence of PDS vs. IDS in the sub group of patients with advanced OCCC and found that none of the two investigated procedures has proven to be superior in terms of OS and PFS, which was also consistent with the previous research (28, 29).

Furthermore, our nomograms were comparable with the FIGO staging. The concordance statistics of the nomogram was even significantly higher than that of the FIGO staging for OS assessment. Thus, our nomograms had great prognostic value. In this study, we established two prognostic nomograms for recurrence and long-term survival after primary treatment in a large center in China and validated them in patients from the same center. The nomogram is relatively easy to use in clinic for predicting the survival rate for individual patients.

The study has some limitations. First, this study was conducted in a single institution. Further studies in multicenter should be constructed. Second, it was a retrospective data analysis. Although we performed internal validation with a good result, future externally validation is needed. In future research, we would combine a multicenter data analysis to verify the accuracy and usefulness of our model and to increase the validity of the data. Last but not least, it was not well-known by obstetrician and gynecologist. An app which embedded this nomogram might be designed in the future to make it easier and faster to provide prognostic information.

Data availability statement

The raw data supporting the conclusions of this article will be made available by the authors, without undue reservation.

Ethics statement

The study was approved by the Ethics Committee of Peking Union Medical College Hospital (S-K903). The patients/participants provided their written informed consent to participate in this study.

Author contributions

JL: Conceptualization; Data curation; Formal analysis; Investigation; Methodology; Software; Visualization; Writing–original draft. DC: Conceptualization; Funding acquisition; Methodology; Project administration; Resources; Software; Supervision; Validation; Visualization; Writing–review & editing. All authors read and approved the final manuscript.

Acknowledgments

The authors would like to thank Dr. Yan You in pathology department of Peking Union Medical College Hospital, for helping the confirmation the diagnosis of the patients. And the authors would like to thank Dr Xiaoshuang Zhou, Shuang Ye, Dr Xiao Huo and Dr Hengzi Sun for helps.

Conflict of interest

The authors declare that the research was conducted in the absence of any commercial or financial relationships that could be construed as a potential conflict of interest.

Publisher's note

References

1. Sugiyama T, Kamura T, Kigawa J, Terakawa N, Kikuchi Y, Kita T, et al. Clinical characteristics of clear cell carcinoma of the ovary: A distinct histologic type with poor prognosis and resistance to platinum-based chemotherapy. *Cancer* (2000) 88(11):2584–9. doi: 10.1002/1097-0142(20000601)88:11<2584::AID-CNCR22>3.0.CO;2-5

2. Kennedy AW, Biscotti CV, Hart WR, Webster KD. Ovarian clear cell adenocarcinoma. *Gynecol Oncol* (1989) 32(3):342–9. doi: 10.1016/0090-8258(89)90637-9

3. Chan JK, Teoh D, Hu JM, Shin JY, Osann K, Kapp DS. Do clear cell ovarian carcinomas have poorer prognosis compared to other epithelial cell types? A study of 1411 clear cell ovarian cancers. *Gynecol Oncol* (2008) 109(3):370–6. doi: 10.1016/j.ygyno.2008.02.006

4. Czernobilsky B, Silverman BB, Enterline HT. Clear-cell carcinoma of the ovary. A clinicopathologic analysis of pure and mixed forms and comparison with endometrioid carcinoma. *Cancer* (1970) 25(4):762–72. doi: 10.1002/1097-0142(197004)25:4<762::aid-cncr2820250404>3.0.co;2-3

5. Matsuura Y, Robertson G, Marsden DE, Kim SN, Gebski V, Hacker NF. Thromboembolic complications in patients with clear cell carcinoma of the ovary. *Gynecol Oncol* (2007) 104(2):406–10. doi: 10.1016/j.ygyno.2006.08.026

6. Jenison EL, Montag AG, Griffiths CT, Welch WR, Lavin PT, Greer J, et al. Clear cell adenocarcinoma of the ovary: A clinical analysis and comparison with serous carcinoma. *Gynecol Oncol* (1989) 32(1):65–71. doi: 10.1016/0090-8258(89)90852-4

7. Goff BA, Sainz de la Cuesta R, Muntz HG, Fleischhacker D, Ek M, Rice LW, et al. Clear cell carcinoma of the ovary: A distinct histologic type with poor prognosis and resistance to platinum-based chemotherapy in stage III disease. *Gynecol Oncol* (1996) 60(3):412–7. doi: 10.1006/gyno.1996.0065

8. Bochner BH, Kattan MW, Vora KC. Postoperative nomogram predicting risk of recurrence after radical cystectomy for bladder cancer. *J Clin Oncol* (2006) 24 (24):3967–72. doi: 10.1200/JCO.2005.05.3884

9. Wang L, Hricak H, Kattan MW, Chen HN, Scardino PT, Kuroiwa K. Prediction of organ-confined prostate cancer: incremental value of MR imaging and MR spectroscopic imaging to staging nomograms. *Radiology* (2006) 238 (2):597–603. doi: 10.1148/radiol.2382041905

10. Chi DS, Palayekar MJ, Sonoda Y, Abu-Rustum NR, Awtrey CS, Huh J, et al. Nomogram for survival after primary surgery for bulky stage IIIC ovarian carcinoma. *Gynecol Oncol* (2008) 108(1):191–4. doi: 10.1016/j.ygyno.2007.09.020

11. Gerestein CG, Eijkemans MJ, de Jong D, van der Burg ME, Dykgraaf RH, Kooi GS, et al. The prediction of progression-free and overall survival in women with an advanced stage of epithelial ovarian carcinoma. *Bjog* (2009) 116(3):372–80. doi: 10.1111/j.1471-0528.2008.02033.x

12. Obermair A, Tang A, Kondalsamy-Chennakesavan S, Ngan H, Zusterzeel P, Quinn M, et al. Nomogram to predict the probability of relapse in patients diagnosed with borderline ovarian tumors. *Int J Gynecol Cancer* (2013) 23 (2):264–7. doi: 10.1097/IGC.0b013e31827b8844

13. van Meurs HS, Schuit E, Horlings HM, van der Velden J, van Driel WJ, Mol BW, et al. Development and internal validation of a prognostic model to predict recurrence free survival in patients with adult granulosa cell tumors of the ovary. *Gynecol Oncol* (2014) 134(3):498–504. doi: 10.1016/j.ygyno.2014.06.021

14. Barlin JN, Yu C, Hill EK, Zivanovic O, Kolev V, Levine DA, et al. Nomogram for predicting 5-year disease-specific mortality after primary surgery for epithelial ovarian cancer. *Gynecol Oncol* (2012) 125(1):25–30. doi: 10.1016/j.ygyno.2011.12.423

15. Kim SI, Song M, Hwangbo S, Lee S, Cho U, Kim JH, et al. Development of web-based nomograms to predict treatment response and prognosis of epithelial ovarian cancer. *Cancer Res Treat* (2019) 51(3):1144–55. doi: 10.4143/crt.2018.508

16. Lee CK, Simes RJ, Brown C, Gebski V, Pfisterer J, Swart AM, et al. A prognostic nomogram to predict overall survival in patients with platinum-sensitive recurrent ovarian cancer. *Ann Oncol* (2013) 24(4):937–43. doi: 10.1093/annonc/mds538

17. Chen Q, Wang S, Lang JH. Development and validation of nomograms for predicting overall survival and cancer-specific survival in patients with ovarian clear cell carcinoma. *J Ovarian Res* (2020) 13(1):123. doi: 10.1186/s13048-020-00727-3

18. Duska LR, Garrett L, Henretta M, Ferriss JS, Lee L, Horowitz N. When 'never-events' occur despite adherence to clinical guidelines: the case of venous thromboembolism in clear cell cancer of the ovary compared with other epithelial histologic subtypes. *Gynecol Oncol* (2010) 116(3):374–7. doi: 10.1016/j.ygyno.2009.10.069

19. Diaz ES, Walts AE, Karlan BY, Walsh CS. Venous thromboembolism during primary treatment of ovarian clear cell carcinoma is associated with decreased survival. *Gynecol Oncol* (2013) 131(3):541–5. doi: 10.1016/j.ygyno.2013.09.005

20. Kasthuri RS, Taubman MB, Mackman N. Role of tissue factor in cancer. *J Clin Oncol* (2009) 27(29):4834–8. doi: 10.1200/JCO.2009.22.6324

21. Young A, Chapman O, Connor C, Poole C, Rose P, Kakkar AK. Thrombosis and cancer. *Nat Rev Clin Oncol* (2012) 9(8):437–49. doi: 10.1038/nrclinonc.2012.106

22. Ma Z, Zhang T, Wang R, Cheng Z, Xu H, Li W, et al. Tissue factor-factor VIIa complex induces epithelial ovarian cancer cell invasion and metastasis through a monocytes-dependent mechanism. *Int J Gynecol Cancer* (2011) 21 (4):616–24. doi: 10.1097/IGC.0b013e3182150e98

23. Mackay HJ, Brady MF, Oza AM, Reuss A, Pujade-Lauraine E, Swart AM, et al. Prognostic relevance of uncommon ovarian histology in women with stage III/IV epithelial ovarian cancer. *Int J Gynecol Cancer* (2010) 20(6):945–52. doi: 10.1111/IGC.0b013e3181dd0110

24. Ku FC, Wu RC, Yang LY, Tang YH, Chang WY, Yang JE, et al. Clear cell carcinomas of the ovary have poorer outcomes compared with serous carcinomas: Results from a single-center Taiwanese study. *J Formos Med Assoc* (2018) 117 (2):117–25. doi: 10.1016/j.jfma.2017.03.007

25. Miyamoto M, Takano M, Goto T, Kato M, Sasaki N, Tsuda H, et al. Clear cell histology as a poor prognostic factor for advanced epithelial ovarian cancer: A single institutional case series through central pathologic review. *J gynecol Oncol* (2013) 24(1):37–43. doi: 10.3802/jgo.2013.24.1.37

26. Cianci S, Capozzi VA, Rosati A, Rumolo V, Corrado G, Uccella S, et al. Different surgical approaches for early-stage ovarian cancer staging. A Large monocentric experience. *Front Med* (2022) 9:880681. doi: 10.3389/fmed.2022.880681

27. Gueli Alletti S, Capozzi VA, Rosati A, De Blasis I, Cianci S, Vizzielli G, et al. Laparoscopy vs. laparotomy for advanced ovarian cancer: A systematic review of the literature. *Minerva medica* (2019) 110(4):341–57. doi: 10.23736/S0026-4806.19.06132-9

28. Chiofalo B, Bruni S, Certelli C, Sperduti I, Baiocco E, Vizza E. Primary debulking surgery vs. interval debulking surgery for advanced ovarian cancer: Review of the literature and meta-analysis. *Minerva medica* (2019) 110(4):330–40. doi: 10.23736/S0026-4806.19.06078-6

29. Onda T, Satoh T, Ogawa G, Saito T, Kasamatsu T, Nakanishi T, et al. Comparison of survival between primary debulking surgery and neoadjuvant chemotherapy for stage III/IV ovarian, tubal and peritoneal cancers in phase III randomised trial. *Eur J Cancer (Oxford Engl 1990)* (2020) 130:114–25. doi: 10.1016/j.ejca.2020.02.020

frontiers | Frontiers in Oncology

TYPE Original Research
PUBLISHED 15 November 2022
DOI 10.3389/fonc.2022.970985

OPEN ACCESS

EDITED BY
Federica Perelli,
Santa Maria Annunziata Hospital, Italy

REVIEWED BY
Eugenia De Crescenzo,
Sant'Orsola-Malpighi Polyclinic, Italy
Andrea Giannini,
University of Pisa, Italy

*CORRESPONDENCE
Xiaohan Chang
13019360812@163.com

SPECIALTY SECTION
This article was submitted to Gynecological Oncology, a section of the journal Frontiers in Oncology

RECEIVED 16 June 2022
ACCEPTED 27 October 2022
PUBLISHED 15 November 2022

CITATION
Pang L, Chen J and Chang X (2022) Large-cell neuroendocrine carcinoma of the gynecologic tract: Prevalence, survival outcomes, and associated factors. *Front. Oncol.* 12:970985. doi: 10.3389/fonc.2022.970985

Large-cell neuroendocrine carcinoma of the gynecologic tract: Prevalence, survival outcomes, and associated factors

Li Pang[1], Jie Chen[2] and Xiaohan Chang[1]*

[1]Department of Obstetrics and Gynecology, Shengjing Hospital of China Medical University, Shenyang, Liaoning, China, [2]Centre of Journals, China Medical University, Shenyang, Liaoning, China

Background: We aimed to assess the clinical behavior of gynecologic large-cell neuroendocrine carcinoma (LCNEC) *via* a retrospective analysis of data from 469 patients.

Methods: Patients diagnosed with gynecologic LCNEC from 1988 to 2015 were identified using the Surveillance, Epidemiology, and End Results database. Univariate and multivariate Cox hazard regression analyses were performed to assess independent predictors of overall survival (OS) and cancer-specific survival (CSS). OS and CSS were also evaluated using the Kaplan–Meier method, and the effects of different treatment regimens on prognosis were compared according to disease stage.

Results: Cervical, ovarian, and endometrial LCNEC were observed in 169, 219, and 79 patients, respectively. The 5-year OS rates for patients with cervical, ovarian, and endometrial LCNEC were 35.98%, 17.84%, and 23.21%, respectively, and the median duration of overall survival was 26, 11, and 11 months in each group. The 5-year CSS rates for the three groups were 45.23%, 19.23%, and 31.39%, respectively, and the median duration of CSS was 41, 12, and 11 months in each group. Multivariate analysis revealed that American Joint Committee on Cancer stage, lymph node metastasis, and chemotherapy were independent prognostic factors for OS and CSS in patients with cervical LCNEC. Lymph node metastasis, surgery, and chemotherapy were independent prognostic factors for OS and CSS in the ovarian group and for OS in the endometrial group. Lymph node metastasis and surgery were also independent prognostic factors for CSS in the endometrial group.

Conclusion: Surgery alone may help to improve overall survival and CSS in patients with early-stage cervical LCNEC. In contrast, surgery+chemotherapy and surgery+radiotherapy may help to improve survival in those with early-stage ovarian and endometrial LCNEC, respectively. Regardless of subtype, comprehensive treatment involving surgery, CTX, and RT should be considered to improve prognosis in patients with advanced-stage gynecologic LCNEC.

KEYWORDS

Large-cell neuroendocrine carcinoma, SEER, ovarian, endometrial, cervical, prognostic factors

Introduction

Neuroendocrine tumors (NETs) are neuroendocrine cell-derived malignancies that can occur in various parts of the body, most commonly in the lungs. Among them, neuroendocrine carcinoma is a rare subtype that can be further classified into four types according to the College of American Pathologists and the National Cancer Institute: carcinoid, atypical carcinoid, large-cell carcinoma, and small-cell carcinoma. This classification is comparable to that used for NETs of the lung (1). In 2014, the World Health Organization (WHO) updated the classification of NETs occurring in different areas of the female genital tract, classifying them as either low-grade or high-grade NETs. Low-grade NETs include carcinoid and atypical carcinoid tumors, while high-grade NETs include small-cell carcinoma and large-cell carcinoma (LCC) (2–6).

The occurrence of gynecologic LCNEC is extremely rare, with most tumors arising in the cervix and following an aggressive clinical course (7, 8), followed by the ovary and endometrium. Previous studies have reported that cervical LCNEC accounts for only 0.087–0.6% of all cervical cancers (9, 10). At present, there are no survey-based data regarding the relative incidence of ovarian or endometrial LCNEC. However, data extracted from the Surveillance, Epidemiology, and End Results (SEER) database indicate that incidence rates for LCNEC of the ovary and endometrium are approximately 0.15% and 0.029%, respectively.

Given the low incidence of gynecologic LCNEC, most published articles are case reports or small case series. Such reports have highlighted the aggressive biological behavior and poor prognosis of gynecologic LCNEC, for which rates of recurrence and distant metastasis are high even in the early stages of disease. Gynecologic LCNEC has also been described as highly invasive and malignant, resulting in low survival rates (11–13). However, these previous studies examined single disease entities only, and cross-sectional analyses and comparisons remain lacking. Furthermore, treatments for gynecologic LCNEC are considered experimental. In principle, surgical treatments for cervical, ovarian, and endometrial LCNEC are the same as those for cervical squamous cell carcinoma, epithelial ovarian cancer, and endometrial adenocarcinoma, respectively. Furthermore, although the adjuvant chemotherapy scheme for gynecological LCNEC is similar to that for primary lung LCNEC, there is no consensus regarding the optimal treatment plan or prognostic factors for each site. In the present study, we aimed to address these issues by summarizing and comparing clinical characteristics, treatment methods, prognosis, and prognostic factors among cervical, ovarian, and endometrial LCNEC.

Materials and methods

Data source and patient selection

The SEER database of the National Cancer Institute, which covers 30 percent of the U.S. population across 14 states, provides cancer statistics including incidence and survival data for the targeted geographic areas. Using this database, we identified patients who had been histologically diagnosed with NETs from 1988 to 2015, selecting those with primary malignancies of the cervix, ovary, and uterine body (ICD-O-3/WHO 2008 website code; described as 8012/3: large-cell carcinoma and 8046/3: non-small-cell carcinoma). The exclusion criteria were as follows: previous benign or borderline tumor confirmed *via* autopsy or based on information from the patient's death certificate, diagnosis of carcinoma in situ, not the first tumor, etc. SEER*Stat 8.3.9 software (https://seer.cancer.gov/data/) was used to generate the case list. Staging was determined in accordance with the American Joint Committee on Cancer (AJCC) staging system. As the SEER database is public and includes de-identified data only, approval from the local ethics committee was not required for the current analysis.

Clinical and demographic characteristics

We analyzed demographic data including race (black, white, other, unknown), age at diagnosis (≥85 years, 65–84 years, 45–64 years, <45 years), marital status (widowed, divorced/separated, single/unmarried, married, unknown), insurance status (uninsured, requiring any medical assistance, insured, unknown), year of diagnosis (<2004, 2004–2009, 2010–2015), AJCC stage (I, II, III, IV, or unknown), grade (well/moderately/poorly differentiated, undifferentiated, unknown), lymph node status (not examined, positive, negative, unknown), and site of metastasis (bone, brain, liver, and lung [yes/no for each]). Data were also analyzed in terms of the following treatment patterns: surgery alone, surgery plus chemotherapy (surgery+CTX), surgery plus concurrent chemoradiotherapy (surgery+CCRT), surgery plus radiotherapy (surgery+RT), CTX alone, CCRT, RT alone, and no treatment.

Statistical analysis

Clinical and demographic characteristics were compared among sites of gynecologic LCNEC using chi-square tests. Categorical data are presented as numbers and percentages, while quantitative data are presented as the means ± standard deviations. Univariate and multivariate Cox risk regression analyses were performed to identify independent predictors of overall survival (OS) and cancer-specific survival. OS durations were calculated using Kaplan–Meier plots and compared using the log-rank test. All data were analyzed using SPSS 25.0 software (SPSS, Chicago, IL, USA). Kaplan–Meier survival curves were drawn using GraphPad Prism (9.2.0 GraphPad Software, San Diego, CA, USA), and P values < 0.05 were considered statistically significant.

Results

Patients

A total of 467 women with gynecologic LCNEC registered in the SEER database fulfilled the criteria and were included in our study (Table 1), including 169 (36.2%), 219 (46.9%), and 79 (16.9%) with cervical, ovarian, and endometrial LCNEC, respectively. The median ages in the cervical, ovarian, and endometrial groups were 48.48 ± 15.24, 69.79 ± 13.54, and 55.37 ± 13.39 years, respectively. Patient characteristics, including AJCC stage, sampled pelvic nodes, grade, age, lymph node status, year of diagnosis, rates of distant metastasis, and treatment strategies, are summarized in Table 1.

Age at onset was the highest in the ovarian group (69.79 years) and lowest in the cervical group (48.48 years), and significant differences in the prevalence of gynecologic LCNEC were observed among different age groups (P < 0.001). Most cases of cervical LCNEC occurred in patients <45 years old, while most cases of ovarian and endometrial LCNEC occurred in those who were 65–84 years old (54.8% and 44.4%, respectively). Most patients in each group were white (75.8% vs. 82.6% vs. 75.9%) (P = 0.028), and roughly 40% in each group were married (43.8% vs. 42.0% vs. 39.2%) (P < 0.001). Advanced-stage (stages III-IV) gynecologic LCNEC was more common in the endometrial group (60.9%) than in the cervical and ovarian groups (26.1% and 51.7%, respectively). Cervical LCNEC was primarily diagnosed before 2004 (60.9%), while ovarian and endometrial LCNEC were commonly diagnosed from 2004–2009 (44.3%) and from 2010–2015 (43.0%), respectively. The rate of lymph node dissection was higher in the endometrial group (25.3%) than in the cervical (23.7%) and ovarian (17.5%) groups. In terms of treatment strategies, CTX was more common in the ovarian group (54.8%) than in the cervical and endometrial groups (42.0% and 45.5%, respectively), while RT was more common in the cervical group (23.0%) than in the other two groups (ovarian: 3.1%; endometrial: 13.9%). Distant metastasis was common in patients with endometrial LCNEC (endometrial 30.4% vs cervical: 17.8%; ovarian: 7.8%).

Survival curves

The 5-year OS rates for patients with cervical, ovarian, and endometrial LCNEC were 35.98%, 17.84%, and 23.21%, respectively, and the median duration of OS was 26, 11, and 11 months in each group. The 5-year CSS rates for the three groups were 45.23%, 19.23%, and 31.39%, respectively, and the median duration of CSS was 41, 12, and 11 months in each group (Figure 1).

We also evaluated OS and CSS curves for various stages of gynecologic LCNEC (Figure 2). For cervical LCNEC, the 5-year OS rates for patients with stage I, II, III, and IV disease were 51.14%, 29.17%, 25.71%, and 6.81%, respectively; for ovarian LCNEC, they were 60.00%, 37.5%, 11.10%, and 6.36%, respectively; for endometrial LCNEC, they were 57.14%, 40.00%, 20.00%, and 15.41%, respectively. The 5-year CSS rates for patients with stage I, II, III, and IV cervical LCNEC were 51.14%, 29.17%, 25.71%, and 7.65%, respectively; for ovarian LCNEC they were 37.50%, 37.50%, 12.08%, and 9.72%, respectively; for endometrial LCNEC they were 66.67%, 40.00%, 26.67%, and 16.05%, respectively.

Figures 3 and 4 summarize differences in prognosis based on treatment modality for patients with early- and advanced-stage LCNEC. Among patients with early-stage cervical LCNEC, the 5-year OS and CSS rates for cases treated with surgery alone were 95.65% and 95.65%, while those for patients with advanced cervical LCNEC treated with surgery+CCRT were highest at 66.67% and

10.3389/fonc.2022.970985

TABLE 1 Demographic and clinical characteristics of patients with gynecologic large-cell neuroendocrine carcinoma (LCNEC).

Patient characteristics	Cervical LCNEC N(%)	Ovarian LCNEC N (%)	Endometrial LCNEC N (%)	*P-value*
Mean age (years,SD)	48.48 (±15.24)	69.79 (±13.54)	65.37 (±13.39)	
ALL (467)	169 (36.2)	219 (46.9)	79 (16.9)	
Age at diagnosis (years)				**<0.001**
<45	81 (47.9)	8 (3.7)	5 (6.3)	
45-64	54 (32.0)	61 (27.9)	33 (41.8)	
65-84	32 (18.9)	120 (54.8)	35 (44.4)	
≥85	2 (1.2)	30 (13.6)	6 (7.5)	
Race				0.028
White	128 (75.8)	181 (82.6)	60 (75.9)	
Black	28 (16.5)	15 (6.9)	9 (11.3)	
Other	12 (7.2)	23 (10.5)	10 (12.8)	
Unknown	1 (0.5)	0 (0)	0 (0)	
Marital status				**<0.001**
Single/unmarried	36 (21.3)	22 (10.02)	15 (19.0)	
Married	74 (43.8)	92 (42.0)	31 (39.2)	
Divorced/separated	27 (16.0)	23 (10.5)	11 (14.0)	
Widowed	21 (12.4)	77 (35.1)	18 (22.8)	
Unknown	11 (6.5)	5 (2.2)	4 (5.0)	
Insurance status				
Insured	30 (17.7)	59 (26.9)	35 (44.3)	0.021
Any Medicaid	15 (8.8)	7 (3.2)	10 (12.6)	
Uninsured	4 (2.5)	1 (0.5)	3 (3.8)	
Unknown	120 (71.0)	152 (69.4)	31 (39.3)	
AJCC Stage				0.001
I	14 (8.3)	5 (2.3)	8 (10.1)	
II	8 (4.7)	5 (2.3)	5 (6.3)	
III	10 (5.9)	36 (16.4)	10 (12.7)	
IV	34 (20.2)	77 (35.2)	38 (48.2)	
Unknown	103 (60.9)	96 (43.8)	18 (22.7)	
Year of diagnosis				
<2004	103 (60.9)	83 (37.9)	18 (22.8)	**<0.001**
2004-2009	26 (15.4)	97 (44.3)	27 (34.2)	
2010-2015	40 (23.7)	39 (17.8)	34 (43.0)	
Grade				
Well differentiated	0 (0)	0 (0)	0 (0)	0.11
Moderately differentiated	1 (0.6)	0 (0)	0 (0)	
Poorly differentiated	18 (10.7)	54 (24.7)	34 (43.0)	
Undifferentiated	4 (2.7)	39 (17.8)	18 (22.8)	
Unknown	146 (86.4)	126 (57.5)	27 (34.2)	
Lymph nodes status				
Negative	24 (14.2)	17 (7.8)	15 (19.0)	0.002
Positive	16 (9.5)	21 (9.7)	5 (6.3)	
No examined	67 (39.6)	161 (73.5)	55 (69.7)	
Unknown	62 (36.7)	20 (9.0)	4 (5.0)	
Sampled pelvic nodes				0.02
1–9	13 (7.7)	18 (8.4)	7 (8.8)	
10–19	10 (5.9)	9 (4.1)	6 (7.6)	
≥20	16 (9.5)	11 (5.0)	7 (8.8)	

(Continued)

TABLE 1 Continued

Patient characteristics	Cervical LCNEC N(%)	Ovarian LCNEC N (%)	Endometrial LCNEC N (%)	*P-value*
Not examined	63 (37.3)	161 (73.5)	55 (69.7)	
Unknown	67 (39.6)	20 (9.0)	4 (5.1)	
Surgery performed				0.01
Surgery	83 (49.1)	77 (35.2)	38 (48.1)	
No surgery	84 (49.7)	141 (64.3)	41 (51.9)	
Unknown	2 (1.2)	1 (0.5)	0 (0)	
Chemotherapy				
Yes	71 (42)	120 (57.5)	36 (45.5)	0.037
No	98 (58)	99 (45.2)	43 (54.4)	
Radiotherapy				
Yes	39 (23)	7 (3.1)	11 (13.9)	**<0.001**
No	130 (77)	212 (96.9)	68 (86.1)	
Distant metastasis				
bone	9 (5.3)	3 (1.4)	5 (6.3)	0.034
brain	3 (1.8)	0 (0)	2 (2.5)	
liver	6 (3.6)	10 (4.6)	7 (8.9)	
lung	12 (7.1)	4 (1.8)	10 (12.7)	
No	10 (5.9)	21 (9.6)	9 (11.4)	
Unknown	129 (76.3)	181 (82.6)	46 (58.2)	
Treatment				**<0.001**
Surgery alone	32 (18.9)	19 (8.7)	14 (17.8)	
Surgery + CTX	15 (8.9)	52 (23.8)	13 (16.5)	
Surgery + CCRT	17 (10.1)	6 (2.7)	6 (7.6)	
Surgery + RT	19 (11.2)	0 (0)	5 (6.3)	
CTX alone	36 (21.3)	62 (28.3)	17 (21.5)	
CCRT	3 (1.8)	0 (0)	0 (0)	
RT alone	0 (0)	1 (0.5)	0 (0)	
No treatment	47 (27.8)	79 (36.0)	24 (30.4)	

LCNEC, large-cell neuroendocrine carcinoma; RT, radiotherapy; CTX, chemotherapy; CCRT, concurrent chemoradiotherapy; AJCC, American Joint Commission on Cancer; black bold means p<0.05.

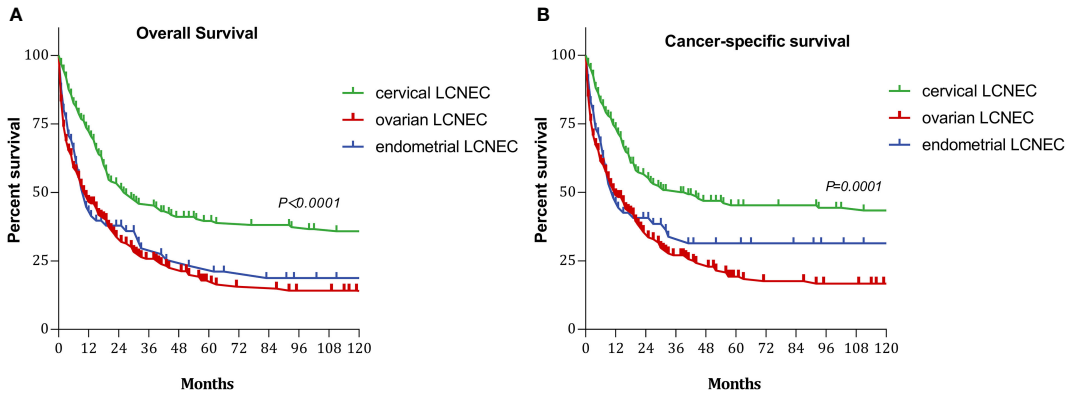

FIGURE 1
Survival curves with cervical, ovarian and endometrial LCNEC: **(A)** overall survival (OS); **(B)** cancer-specifi;c survival (CSS).

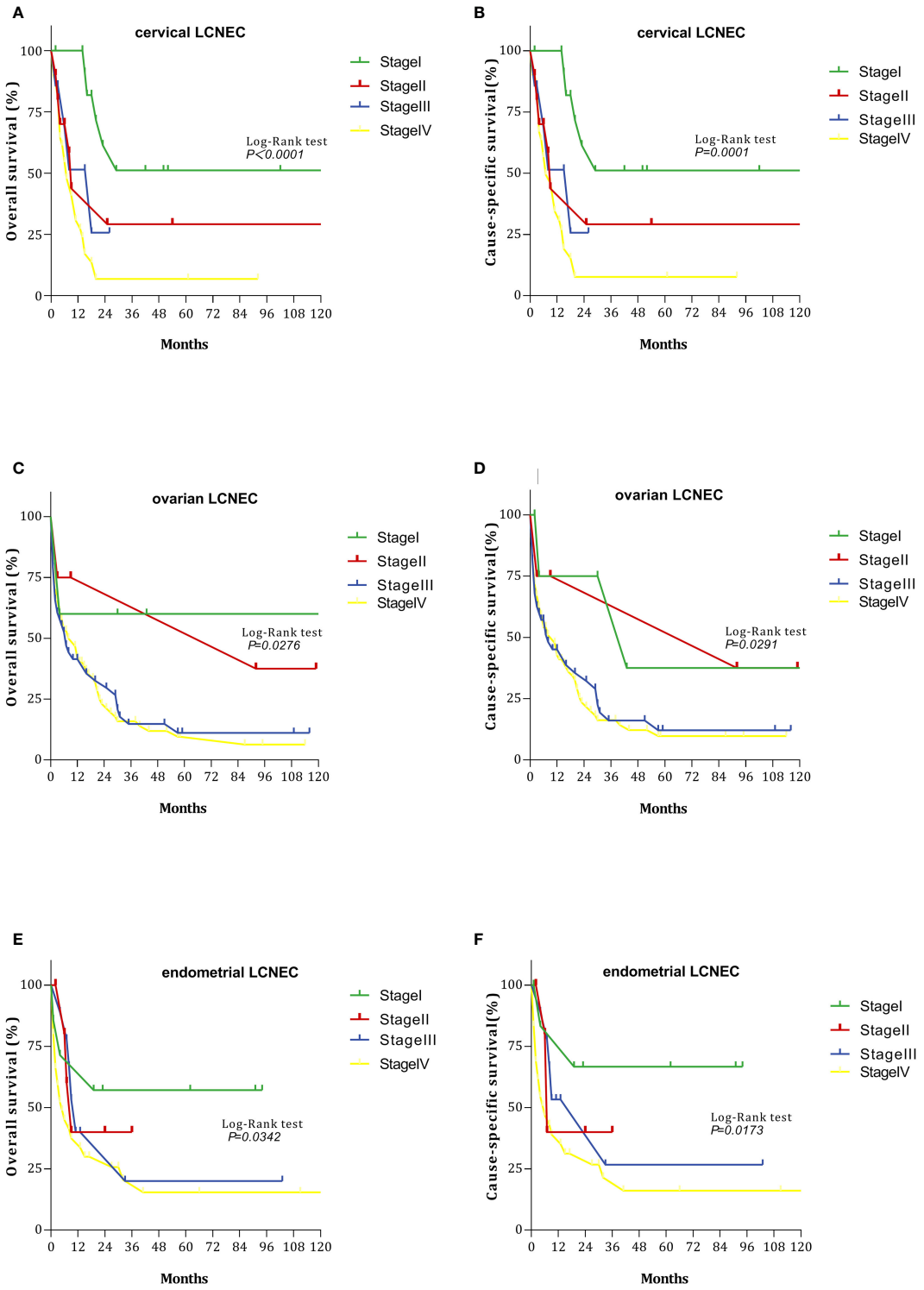

FIGURE 2
Survival curves with cervical, ovarian, and endometrial LCNEC at each stage: **(A)** overall survival (OS)with cervical LCNEC; **(B)** cancer-specific survival (CSS)with cervical LCNEC. **(C)** overall survival (OS)with ovarian LCNEC; **(D)** cancer-specific survival (CSS)with ovarian LCNEC; **(E)** overall survival (OS)with endometrial LCNEC; **(F)** cancer-specific survival (CSS)with endometrial LCNEC.

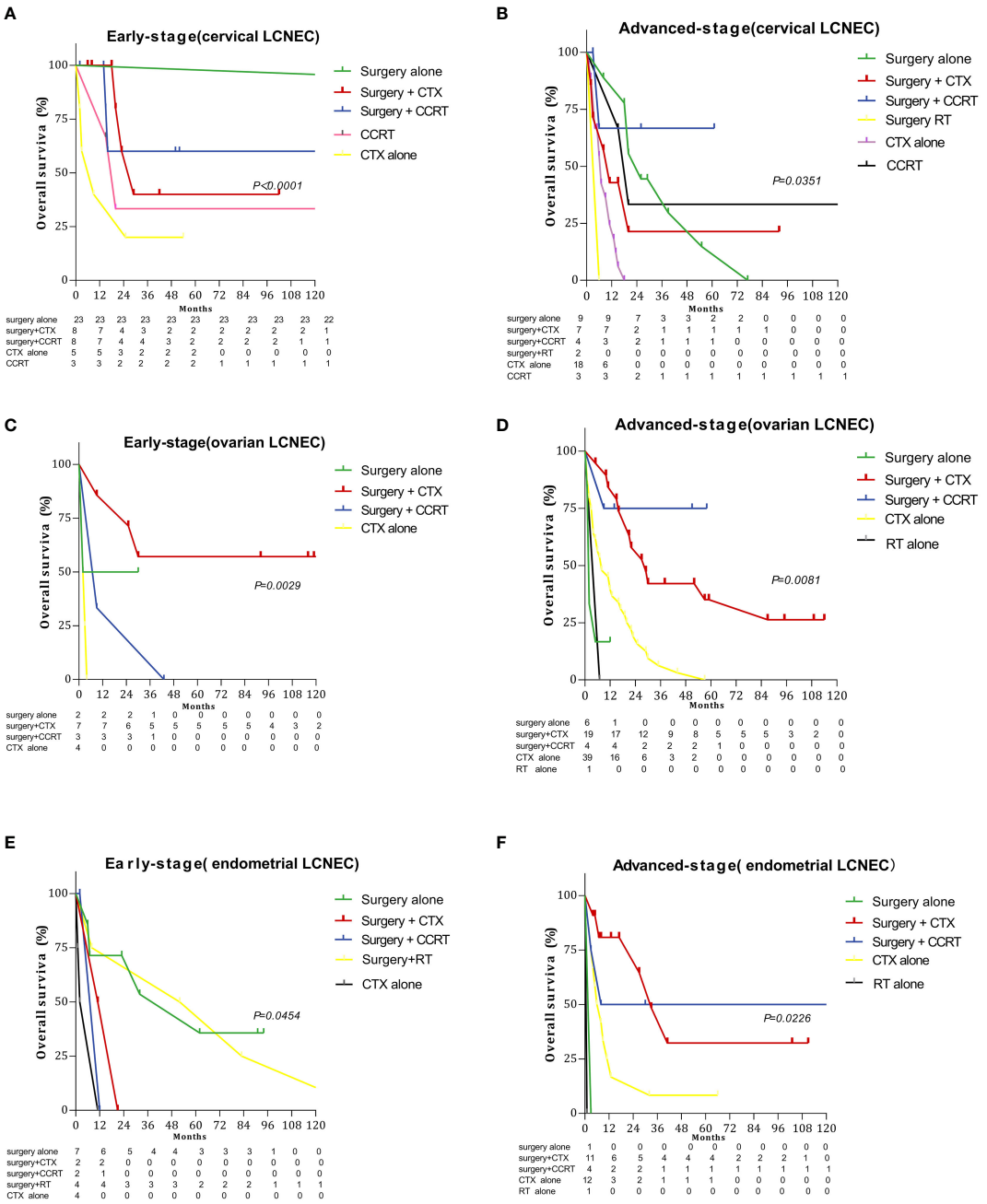

FIGURE 3
Survival curves for gynecologic LCNEC patients with early- and advanced-stage disease for different treatment regimens: **(A)** overall survival (OS) in the early stage with cervical LCNEC; **(B)** overall survival (OS) in the advanced stage with cervical LCNEC; **(C)** overall survival (OS) in the early stage with ovarian LCNEC; **(D)** overall survival (OS) in the advanced stage with ovarian LCNEC; **(E)** overall survival (OS) in the early stage with endometrial LCNEC; **(F)** overall survival (OS) in the advanced stage with endometrial LCNEC.

50.00%, respectively. Among patients with early-stage ovarian LCNEC, the 5-year OS and CSS rates for cases treated with surgery+CTX were highest at 57.14% and 66.67%, while those for patients with advanced ovarian LCNEC treated with surgery +CCRT were highest at 75.00% and 75.00%, respectively. Among patients with early-stage endometrial LCNEC, the 5-year OS and CSS rates for cases treated with surgery+RT were 48.14% and 71.43%, respectively, while those for advanced cases treated with

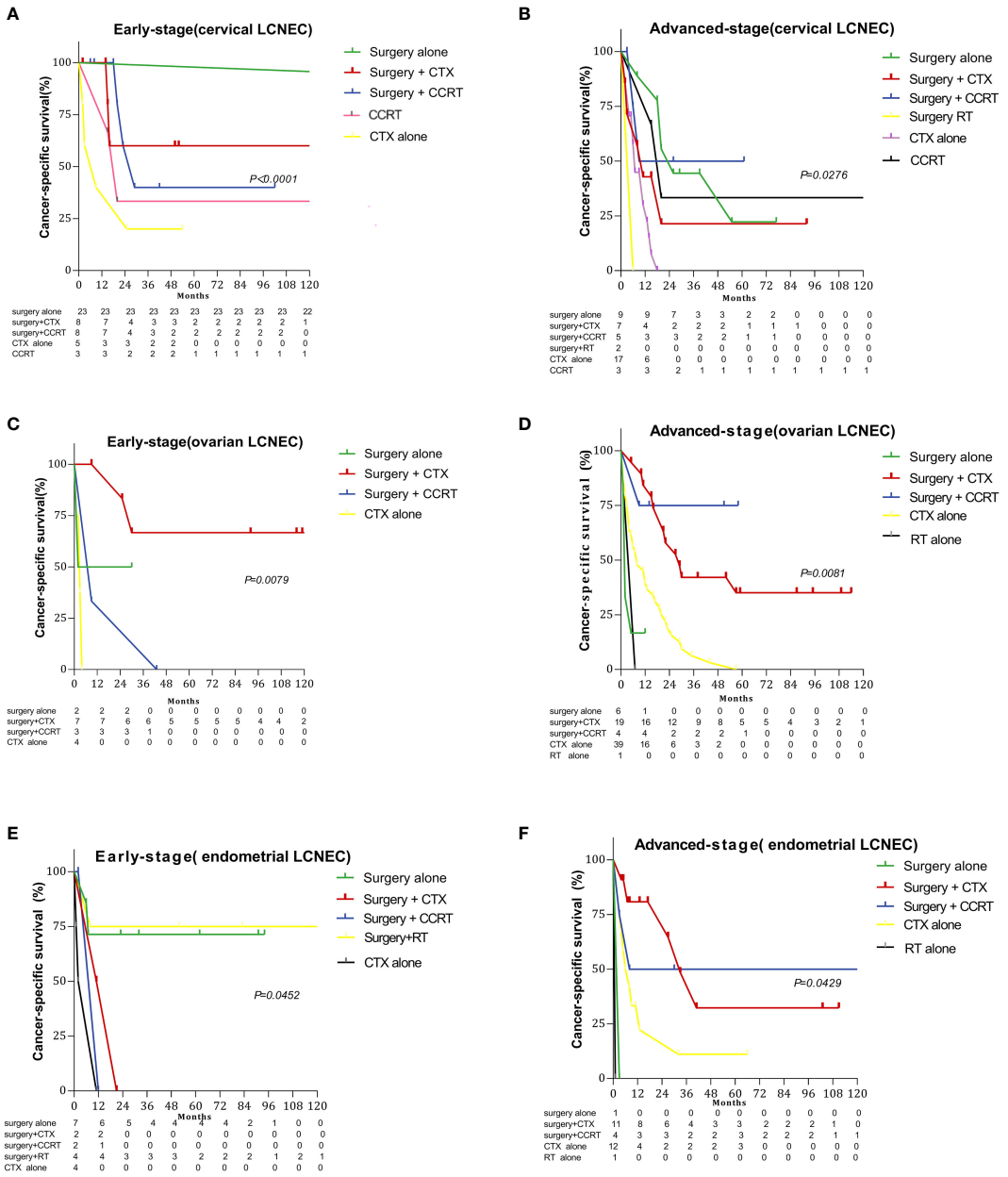

FIGURE 4
Survival curves for gynecologic LCNEC patients with early- and advanced-stage disease for different treatment regimens: **(A)** cancer-specific survival (CSS) in the early stage with cervical LCNEC; **(B)** cancer-specific survival (CSS) in the advanced stage with cervical LCNEC; **(C)** cancer-specific survival (CSS) in the early stage with ovarian LCNEC; **(D)** cancer-specific survival (CSS) in the advanced stage with ovarian LCNEC; **(E)** cancer-specific survival (CSS) in the early stage with endometrial LCNEC; **(F)** cancer-specific survival (CSS) in the advanced stage with endometrial LCNEC.

surgery+CCRT were 50.00% and 50.00%. These rates were also higher than those for other treatment options (Table 2).

We also examined the effect of different treatments on prognosis in the cervical, ovarian, and endometrial groups. Among patients treated with surgery alone, the 5-year OS rates were 77.89%, 18.18%, and 60.61%, while the 5-year CSS rates were 81.00%, 18.18%, and 72.73%, respectively. Among patients treated with surgery+CTX, the 5-year OS rates were 65.44%, 47.64%, and 26.11%, while the 5-year CSS rates were 66.77%, 50.42%, and 26.11%, respectively. Among patients treated with surgery+CCRT, the 5-year OS rates 43.14%, 44.44%, and 40.00%, while the 5-year CSS rates were 48.23%,

TABLE 2 Univariate-Prognostic factors for gynecologic large-cell neuroendocrine carcinoma (LCNEC).

Subject	Overall survival						Cancer-specific survival					
Characteristics	Cervical LCNEC		Ovarian LCNEC		Endometrial LCNEC		Cervical LCNEC		Ovarian LCNEC		Endometrial LCNEC	
	HR (95% CI)	*P*-value	HR (95% CI)	*P*-value	HR (95% CI)	*P*-value	HR (95% CI)	*P*-value	HR (95% CI)	*P*-value	HR (95% CI)	*P*-value
Age												
<45	1	**<0.001**	1	**<0.001**	1	**0.01**	1	**0.001**	1	**<0.001**	1	**0.01**
45-64	3.068 (1.993-4.721)	<0.001	1.002 (0.453-2.215)	0.996	0.551 (0.189-1.606)	0.005	2.515 (1.573-4.020)	<0.001	0.95 (0.429-2.104)	0.899	0.511 (0.174-1,506)	0.003
65-84	3.019 (1.846-4.937)	<0.001	1.298 (0.604-2.791)	0.504	0.685 (0.238-1.969)	0.012	2.068 (1.177-3.633)	0.012	1.126 (0.552-2.428)	0.762	0.568 (0.194-1.664)	0.013
≥85	3.929 (0.942-16.393)	0.06	3.061 (1.326-7.063)	0.009	0.631 (0.164-2.419)	0.006	1.864 (0.254-13.663)	0.54	2.819 (1.219-6.518)	0.015	0.826 (0.22-3.099)	0.007
AJCC stsge												
I	1	**0.001**	1	0.532	1	0.188	1	**0.002**	1	0.331	1	0.078
II	1.976 (0.529-7.382)	0.311	0.557 (0.161-1.932)	0.357	1.848 (0.490-6.976)	0.365	1.98 (0.530-7.400)	0.310	0.44 (0.099-1.954)	0.280	2.208 (0.441-11.05)	0.335
III	4.252 (1.281-14.121)	0.018	1.217 (0.655-2.259)	0.534	1.220 (0.369-4.026)	0.745	4.349 (1.309-14.450)	0.016	1.266 (0.654-2.449)	0.484	1.617 (0.384-6.804)	0.512
IV	6.158 (2.351-16.130)	<0.001	1.230 (0.701-2.157)	0.470	2.403 (0.925-6.246)	0.072	5.723 (2.168-15.105)	<0.001	1.381 (0.760-2.510)	0.289	3.672 (1.11-12.152)	**0.03**
Unknown	NA		NA		NA		NA		NA		NA	
Lymph nodes status												
Negative	1	**0.002**	1	**<0.001**	1	**0**	1	**0.003**	1	**<0.001**	1	**0.01**
Positive	2.319 (0.932-5.773)	0.071	3.474 (1.418-8.512)	0.006	4.942 (1.209-20.209)	0.026	2.387 (0.908-6.277)	0.078	5.259 (1.738-15.911)	0.003	5.172 (1.149-23.289)	0.032
No examined	3.667 (1.743-7.715)	0.001	6.347 (2.935-13.727)	<0.001	7.058 (2.504-19.897)	<0.001	3.848 (1.741-8.505)	0.001	9.607 (3.523-26.198)	<0.001	6.666 (2.046-21.719)	0.002
Unknown	NA		NA		NA		NA		NA		NA	
Surgery performed												
Surgery	1		1		1		1		1		1	
No surgery	2.857 (1.954-4.178)	**<0.001**	3.565 (2.588-4.910)	**<0.001**	3.839 (2.178-6.675)	**<0.001**	2.807 (1.823-4.322)	**<0.001**	3.555 (2.554-4.948)	**<0.001**	3.611 (1.974-6.605)	**<0.001**
Unknown	NA		NA		NA		NA		NA		NA	
Chemotherapy												
Yes	1		1		1		1		1		1	
No	1.623 (1.107-2.379)	**0.013**	3.575 (2.625-4.869)	**<0.001**	1.402 (0.832-2.354)	**0.02**	1.513 (1.101-2.332)	**0.003**	3.419 (2.490-4.694)	**<0.001**	1.179 (0.674-2.062)	**0.03**
Radiotherapy												
Yes	1		1		**1**		1		1		1	
No	1.362 (0.87-2.133)	0.177	2.197 (0.815-5.921)	0.1199	1.647 (0.777-3.491)	0.193	1.297 (0.790-2.129)	0.305	2.082 (0.772-5.615)	0.148	1.998 (0.792-5.046)	0.143
Distant metastasis												
Yes	1		1.000		1.000		1		1.000		1	
No	0.187 (0.075-0.466)	**<0.001**	0.885 (0.399-1.961)	0.763	0.681 (0.282-1.644)	0.393	0.239 (0.103-0.555)	**0.001**	0.421 (0.454-2.298	0.960	0.58 (0.224-1.502)	0.262
Unknown	NA		NA		NA		NA		NA		NA	

AJCC, American Joint Commission on Cancer; LCNEC, large-cell neuroendocrine carcinoma; HR, hazard ratio; CI, confidence interval; NA, Not available;black bold means p<0.05.

44.44%, and 40.00%, respectively. The 5-year OS rates for patients treated with CTX only were 11.93%, 2.09%, and 6.25%, respectively, while the 5-year CSS rates were 14.91%, 2.13%, and 8.33%, respectively (Figure 5). Among patients treated with surgery alone, 5-year OS and CSS rates were highest in the cervical group and lowest in the ovarian group (OS: P=0.0023, CSS: P < 0.0001). Among patients treated with surgery+CTX, these rates were also best in the cervical group, although they were worst in the endometrial group (OS: P = 0.0058, CSS: P = 0075). There were no significant differences in OS or CSS rates among the three LCNEC sites for patients treated CTX only or surgery+CCRT (CTX only: OS: P = 0.195, CSS: P = 0.182; surgery+CCRT: OS: P = 0.415, CSS: P = 0.306).

Prognostic factors

Univariate and multivariate analyses of age, AJCC stage, lymph node status, surgery, CTX, RT, and distant metastasis were used to identify prognostic factors for gynecologic LCNEC (Tables 2, 3). Multivariate analysis revealed that lymph node metastasis, chemotherapy, and AJCC stage were independent prognostic factors for OS and CSS in patients with cervical LCNEC. Lymph node metastasis, chemotherapy, and surgery were independent prognostic factors for OS and CSS in the ovarian group and for OS in the endometrial group. Lymph node metastasis and surgery were also independent prognostic factors for CSS in the endometrial group (Table 3).

Discussion

Given our limited understanding regarding the occurrence, development, and pathogenesis of gynecologic LCNEC, we examined the clinical behavior of the disease *via* a retrospective analysis of data from 469 patients, representing the largest cohort of patients with gynecologic LCNEC in the literature to date. No previous studies have performed such comparisons among different subtypes of gynecologic LCNEC, highlighting the practical significance of the current results for guiding clinical work.

Our data suggest that gynecologic LCNEC exhibits a unique natural history and aggressive clinical course, with the highest and lowest survival rates occurring in patients with cervical and ovarian disease, respectively. The results of our analysis suggest that surgery alone can improve OS and CSS in patients with early-stage LCNEC (I/II). In contrast, surgery+CTX and surgery +RT may help improve survival for early-stage ovarian and endometrial LCNEC, respectively. Moreover, regardless of subtype, our data suggest that comprehensive treatment with surgery, CTX, and RT should be considered to improve prognosis in patients with advanced-stage gynecologic LCNEC.

Embry et al. (11) reported 62 cases of cervical LCNEC, representing the largest series thus far, in which the median patient age was 37 years, and the median duration of OS was 16.5 months (0.5–151 months). In their multivariate analysis, early-stage disease and CTX treatment were associated with improved survival. The use of platinum agents and platinum plus

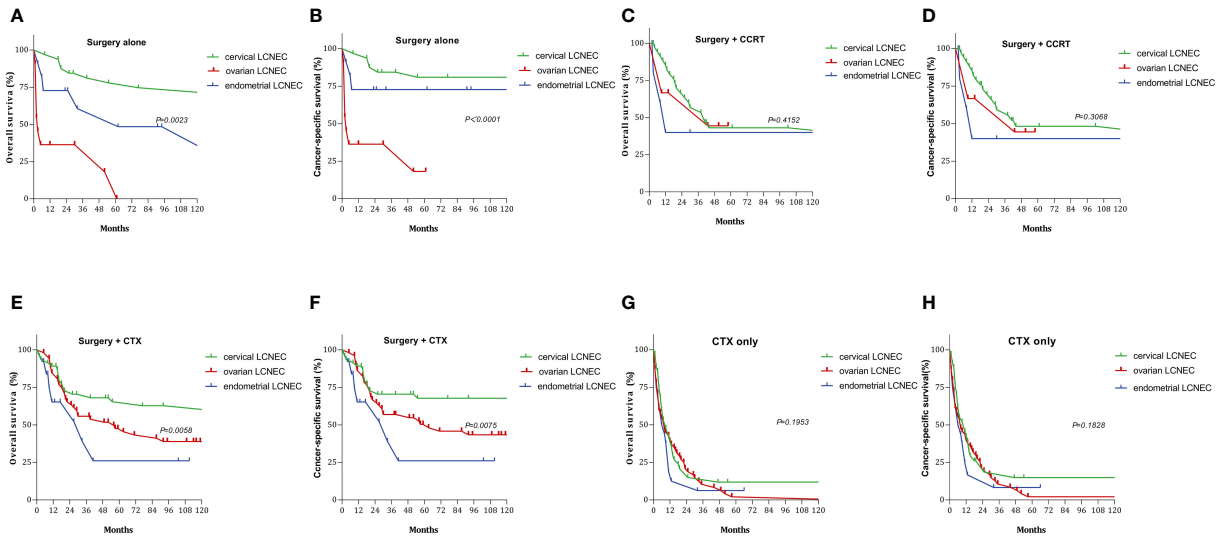

FIGURE 5
Survival curves for gynecologic LCNEC patients with different treatments: **(A)** overall survival (OS) in surgery alone with gynecologic LCNEC; **(B** cancer-specific survival (CSS) in surgery alone with gynecologic LCNEC; **(C)** overall survival (OS) in survery+CCRT with gynecologic LCNEC; **(D)** cancer-specific survival (CSS) in survery+CCRT with gynecologic LCNEC; **(E)** overall survival (OS) in surgery+CTX with gynecologic LCNEC **(F)** cancer-specific survival (CSS) in surgery+CTX with gynecologic LCNEC; **(G)** overall survival (OS) in CTX only with gynecologic LCNEC **(H)** cancer-specific survival (CSS) in CTX only with gynecologic LCNEC.

TABLE 3 Multivariate-Prognostic factors for gynecologic large-cell neuroendocrine carcinoma (LCNEC).

Subject Characteristics	Overall survival						Cancer-specific survival					
	Cervical LCNEC		Ovarian LCNEC		Endometrial LCNEC		Cervical LCNEC		Ovarian LCNEC		Endometrial LCNEC	
	HR (95% CI)	*P*-value	HR (95% CI)	*P*-value	HR (95% CI)	*P*-value	HR (95% CI)	*P*-value	HR (95% CI)	*P*-value	HR (95% CI)	*P*-value
Age												
<45	1	0.948	1	0.598	1	0.441	1	0.517	1	0.459		0.314
45-64	0.945 (0.309-2.892)	0.922	0.71 (0.313-1.608)	0.411	0.411 (0.134-1.258)	0.119	0.908 (0.290-2.843)	0.868	0.686 (0.301-1.563)	0.37	0.338 (0.108-1.056)	0.062
65-84	0.798 (0.200-3.186)	0.749	0.756 (0.343-1.665)	0.488	0.463 (0.156-1.373)	0.165	0.368 (0.063-2.151)	0.267	0.659 (0.298-1.457)	0.303	0.385 (0.127-1.169)	0.092
≥85			0.959 (0.397-2.318)	0.927	0.347 (0.073-1.652)	0.184			0.896 (0.369-2.177)	0.808	0.447 (0.095-2.091)	0.306
AJCC stsge												
I	1	**0.010**	–	–	–	–	1	**0.01**	–	–	–	–
II	6.799 (0.232-28.884	0.266	–	–	–	–	8.208 (0.304-21.489)	0.211	–	–	–	–
III	10.898 (5.802-48.739)	0.003	–	–	–	–	12.820 (9.807-25.969)	0.002	–	–	–	–
IV	17.619 (5.125-68.660)	0.006	–	–	–	–	15.503 (5.120-52.590)	0.006	–	–	–	–
Unknown	NA		NA				NA					
Lymph nodes status												
Negative	1	**0.003**		**0.004**		**0.008**		**0**		**0.003**		**0.028**
Positive	1.177 (0.115-12.071)	0.891	2.425 (0.967-6.081)	0.059	9.321 (2.079-41.797)	0.004	0 (0-0.054)	0.002	3.607 (1.173-11.093)	0.025	8.432 (1.709-41.602)	0.009
No examined	0.001 (0.001-0.059)	0.001	3.748 (1.646-8.534)	0.002	4.845 (1.528-15.358)	0.007	0.896 (0.080-10.046)	0.929	5.502 (1.935-15.650)	0.001	4.348 (1.149-16.457)	0.03
Unknown	NA		NA		NA		NA		NA		NA	
Surgery performed												
Surgery	1		1		1		1		1		1	
No surgery	6.4 (0.487-84.182)	0.158	2.157 (1.406-3.310)	**<0.001**	2.672 (1.336-5.347)	**0.005**	0.132 (0.009-1.961)	0.141	2.158 (1.389-3.350)	**0.001**	2.659 (1.229-5.754)	**0.013**
Unknown	NA		NA		NA		NA		NA		NA	
Chemotherapy												
Yes	1		1		1		1		1		1	
No	20.2 (3.848-106.034)	**<0.001**	3.165 (2.207-4.539)	**<0.001**	1.898 (1.053-3.422)	**0.033**	46.514 (5.804-372.76)	**<0.001**	2.984 (2.058-4.327)	**<0.001**	1.476 (0.780-2.974)	0.232
Distant metastasis												
Yes	1		–	–	–	–	1		–	–	–	–
No	0.806 (0.236-2.758)	0.731	–	–	–	–	0.888 (0.254-3.11)	0.853	–	–	–	–
Unknown	NA						NA					

AJCC, American Joint Commission on Cancer; LCNEC, large-cell neuroendocrine; HR, hazard ratio; CI, confidence interval; NA, Not available; black bold means p<0.05.

etoposide treatment were also associated with improved survival. Nonetheless, recurrence was observed in 70% (38/54) of patients, and 40% (25/62) of cases were classified as stage IV. In their study of 45 patients with cervical LCNEC, Burkeen et al. (12) reported a median age of 36 years and a median OS duration of 16 months, with early cases (I/II) accounting for 73%. Lee and Ji (13) reported a case of cervical LCNEC treated with radical surgery and CCRT. After a disease-free period of 18 months, the patient experienced three consecutive recurrences in the kidney, breast, and adrenal gland, respectively, and survived for a total of 63 months. Habeeb and Habeeb (14) reported a case in which a patient with stage IIA2 disease died 21 months postoperatively despite treatment with CTX and palliative RT. In the current study, the median age of patients with cervical LCNEC was 48.48

(n=169). The median durations of OS and CSS in the cervical group were 26 and 41 months, respectively, which are longer than those reported in the two largest studies mentioned above. However, the OS and CSS rates for cervical LCNEC were still only 35.98% and 45.23% at 5 years.

The principles of surgical treatment for cervical LCNEC are the same as those used for cervical squamous cell carcinoma. Strategies involving postoperative adjuvant systemic CTX combined with RT have been developed primarily based on data from patients with LCNEC of the lung (1, 6, 7, 11, 12). Our results suggest that surgery alone can improve OS and CSS for early-stage cervical LCNEC, while surgery+CCRT can improve survival for advanced-stage LCNEC, highlighting the need for a targeted treatment approach. Some somatostatin receptor binding is commonly observed in patients with high-grade NETs. Therefore, Shahabi et al. (15) suggested exploring targeted therapy with octreotide, a somatostatin analog, while Kajiwara et al. proposed a somatostatin type 2A analog for the treatment of tumor cells expressing somatostatin type 2A receptors (16). However, this strategy has not been standardized and requires further study.

The metastatic epidemiology of cervical LCNEC remains unclear, as only a few relevant case reports have been published (17, 18). Given the aggressive nature of the disease, early metastases to the peripheral lymph nodes, lung, liver, bone, and brain have been reported (19, 20). Our study included 12 cases of lung metastasis, nine of bone metastasis, six of liver metastasis, and three of brain metastasis. Treatment data in cases of recurrence are limited in the SEER database. Tempfer et al. (21) demonstrated the potential value of immune checkpoint inhibitors, while other studies have noted that nivolumab and the MEK inhibitor trametinib can be considered (22, 23). In their study, Carroll et al. (24) demonstrated that pure high-grade neuroendocrine cervical cancer is microsatellite stable, with most patients exhibiting negative PD-L1 expression. Since most of the tumors tested expressed PARP-1, future clinical trials may wish to include PARP inhibitors for patients with recurrent high-grade neuroendocrine cervical cancer.

The largest case series for ovarian LCNEC included 58 patients, although only 15 cases were classified as pure ovarian LCNEC, and the median survival time was only 10 months. These results emphasize that even patients with stage I disease are likely to experience a very poor prognosis (25). In their study of 45 patients with ovarian LCNEC, Burkeen et al. reported that the majority of patients had advanced stage (III/IV) disease (12). Among the 33 cases reported by Oshita et al., the 5-year OS rate was only 34.9% (26). Lin et al. also reported a case in which a patient with stage IV primary pure ovarian LCNEC with liver metastases was treated with three cycles of postoperative paclitaxel + carboplatin, noting that she experienced disease progression with pulmonary metastases and died 3 months after surgery (27). Ki et al. reported three cases of stage I LCNEC characterized by poor survival due to biological invasiveness, despite extensive surgery and CTX (28). Among the 219 cases of ovarian LCNEC in our study, median OS and CSS durations were 11 and 12 months, and the 5-year OS and CSS rates were only 17.84% and 19.23%, respectively. Among these patients, 113 had advanced disease, accounting for 51.7% of cases. The 5-year OS and CSS rates were lower for ovarian LCNEC than for cervical or endometrial LCNEC, and liver metastasis was noted in 10 cases of ovarian LCNEC. These results highlight the need to examine factors that place patients at high risk for poor prognosis following a diagnosis of ovarian LCNEC, as well as those associated with prognosis.

A previous study reported that the overexpression of synaptophysin is an independent contributor to poor prognosis, based on a multivariate analysis that included age, FIGO stage, and postoperative residual tumors (29). Our multivariate results indicated that lymph node metastasis, surgery, and CTX are independent prognostic factors for OS and CSS in patients with ovarian LCNEC, emphasizing the need to focus on surgery and postoperative adjuvant CTX in these patients. In principle, surgery for ovarian LCNEC is equivalent to that for epithelial ovarian cancer. Our research shows that surgery+CTX should be recommended for early-stage ovarian LCNEC, while surgery+CCRT should be recommended for advanced cases. As the SEER database does not include data regarding sites of recurrence for ovarian LCNEC, further studies are required to clarify this issue and identify effective treatments for recurrent ovarian LCNEC.

Endometrial LCNEC is a rare malignancy that appears to exhibit an aggressive course even in early stages, with a strong tendency for distant metastasis and rapid recurrence (6, 7, 30). Over 19 years, 18 Japanese medical institutions have accumulated only 14 cases of endometrial LCNEC, including seven each of the mixed and pure types (31), highlighting the extremely low incidence of the disease. The prognosis appears to be significantly worse for pure cases than that for mixed cases but significantly better for cases treated with surgery than without and for those in which surgery is incomplete. Radical surgery should therefore be considered for endometrial LCNEC. Tu et al. (32) reported that cytoreductive surgery was suboptimal in a patient with stage IV disease. Despite receiving platinum-based adjuvant chemotherapy after surgery, the patient developed obstructive ileus developed 2 months later, and he died 8 days after ileus surgery. Suh et al. (33) reported a case in which stage IIIB endometrial LCNEC demonstrated a progressive course even after surgery, multiple postoperative CTX and RT regimens (etoposide-cisplatin, irinotecan-cisplatin), and FOLFIRI (fluorouracil, leucovorin, irinotecan) treatment. In their case, lymph node metastasis was identified 12 months after surgery, and the patient died 23 months after surgery. Nguyen et al. (30) reported a stage IVB endometrial LCNEC in a 71-year-old patient who underwent surgical

debulking, who survived for only 32 days after surgery. Both studies described the disease as exhibiting a rapidly progressive course.

Among the 79 patients with endometrial LCNEC in our study, 48 had advanced-stage disease, accounting for 60.9% of cases, and the median age at onset was 55.37 years. In these patients, the median OS and CSS durations were both 11 months, and the 5-year OS and CSS rates were 23.21% and 31.39%, respectively. Among patients with endometrial LCNEC, we observed 10 cases of lung metastasis, seven of liver metastasis, five of bone metastasis, and two of brain metastasis. These results suggest that endometrial LCNEC often occurs in the advanced stage, highlighting its strong invasiveness and risk of poor prognosis. Standard surgical procedures for endometrial cancer include total hysterectomy, bilateral salpingo-oophorectomy, and lymph node dissection, although omentectomy is performed in the absence of endometrioid histology. Similar surgical procedures have been used in most patients with endometrial LCNEC. However, given its low incidence and the apparent risk of metastasis, it seems that a multimodal treatment approach should be utilized for endometrial LCNEC. Our results suggest that surgery+RT can improve OS and CSS in patients with early-stage endometrial LCNEC, while surgery+CCRT should be considered for advanced cases. In addition to histologic subtype, only complete surgery was an important prognostic factor in our multivariate analysis. In accordance with this finding, Matsumoto et al. (7) also reported that complete surgery can improve the prognosis of early to advanced endometrial LCNEC. Our multivariate analysis for endometrial LCNEC indicated that lymph node metastasis, surgery, and CTX were independent prognostic factors for OS, while lymph node metastasis and surgery were independent prognostic factors for CSS.

Adjuvant chemotherapy options for gynecologic LCNEC are similar to those for primary pulmonary LCNEC, including platinum-based chemotherapy and paclitaxel-carboplatin-based chemotherapy (34). Several strategies have been employed, including cisplatin+cyclophosphamide, etoposide+cisplatin, paclitaxel+carboplatin (12, 35). Cisplatin+vinorelbine and other regimens have been used for tumors that have failed to respond to first-line therapy (12). Irinotecanplatin or topotecan can be considered as second-line therapy for gynecologic LCNEC (34–37), while octreotide, a synthetic somatostatin analog, represents a therapeutic option for combination CTX (16).

Establishing the diagnosis of gynecologic LCNEC can be challenging. LCNECs are characterized by the presence of large polygonal cells as well as a low nucleocytoplasmic ratio and thick nuclear chromatin, with prominent peripheral palisades and frequent glandular differentiation. Gynecologic LCNEC must therefore be assessed *via* immunohistochemical analysis, as these tumors exhibit a positive immune response to at least one neuroendocrine marker such as synaptophysin, chromogranin A, neuron-specific alkene-positive immunostaining for alcoholase or CD56, or p63 (38). Such immune responses are therefore used to confirm the diagnosis.

Our study had some limitations. Because LCNEC is high-grade by definition, no variable analyses were performed for grade. In addition, although the SEER database separates reports of simple LCNEC and mixed LCNEC, we performed analyses for simple LCNEC only, which is less common than mixed LCNEC. Furthermore, specific information on CTX, RT, and disease recurrence is not included in the SEER database, highlighting the need to accumulate data from additional cases to guide future clinical work. Because the incidence rate of cervical LCNEC is higher than that of ovarian or endometrial LCNEC, a relatively higher number of cervical LCNEC cases were included in the current study, and methods for surgical intervention and postoperative adjuvant treatment are more standardized for cervical LCNEC than for the other two disease entities. Indeed, data are largely lacking for recurrent ovarian and endometrial LCNEC at present. This limitation underscores the importance of accumulating additional cases to aid in the development of targeted treatment strategies for cases for ovarian and endometrial LCNEC, such as immunotherapy or gene detection. Such data may in turn help to improve survival among patients with rarer forms of LCNEC.

Conclusion

The current study, which represents the largest analysis of gynecologic LCNEC thus far, demonstrates that surgery should be used for initial treatment. Surgery+CTX or RT can be used in early-stage cases, while both CTX and RT should be used for advanced cases. Additional studies involving larger numbers of cases are required to determine the most appropriate strategies for treating these aggressive tumors. Establishing a global database of gynecologic LCNEC may aid in designing retrospective and prospective studies of such strategies. Furthermore, future studies may wish to focus on the molecular and genetic aspects of targeting NETs to improve survival in patients with gynecologic LCNEC.

Data availability statement

The original contributions presented in the study are included in the article/supplementary material. Further inquiries can be directed to the corresponding author.

Author contributions

LP: clinical data collection, conceptualization, data curation, formal analysis, and writing - original draft. JC: clinical data collection and conceptualization. XC: data curation and writing -

review and editing. All authors significantly contributed to the study and approved the submitted version.

Conflict of interest

The authors declare that the research was conducted in the absence of any commercial or financial relationships that could be construed as a potential conflict of interest.

Publisher's note

References

1. Travis WD, Linnoila RI, Tsokos MG, Hitchcock CL, Cutler GB, Nieman L, et al. Neuroendocrine tumors of the lung with proposed criteria for large-cell neuroendocrine carcinoma. an ultrastructural, immunohistochemical, and flow cytometric study of 35 cases. *Am J Surg Pathol* (1991) 15:529–53. doi: 10.1097/00000478-199106000-00003

2. Walenkamp AM, Sonke GS, Sleijfer DT. Clinical and therapeutic aspects of extrapulmonary small cell carcinoma. *Cancer Treat Rev* (2009) 35:228–36. doi: 10.1016/j.ctrv.2008.10.007

3. Brennan SM, Gregory DL, Stillie A, Herschtal A, Mac Manus M, Ball DL. Should extrapulmonary small cell cancer be managed like small cell lung cancer? *Cancer* (2010) 116:888–95. doi: 10.1002/cncr.24858

4. van Meerbeeck JP, Fennell DA, De Ruysscher DK. Small-cell lung cancer. *Lancet* (2011) 378:1741–55. doi: 10.1016/S0140-6736(11)60165-7

5. Frazier SR, Kaplan PA, Loy TS. The pathology of extrapulmonary small cell carcinoma. *Semin Oncol* (2007) 34:30–8. doi: 10.1053/j.seminoncol.2006.11.017

6. Winer I, Kim C, Gehrig P. Neuroendocrine tumors of the gynecologic tract update. *Gynecol Oncol* (2021) 162:210–19. doi: 10.1016/j.ygyno.2021.04.039

7. Gardner GJ, Reidy-Lagunes D, Gehrig PA. Neuroendocrine tumors of the gynecologic tract: A society of gynecologic oncology (SGO) clinical document. *Gynecol Oncol* (2011) 122:190–8. doi: 10.1016/j.ygyno.2011.04.011

8. Crowder S, Tuller E. Small cell carcinoma of the female genital tract. *Semin Oncol* (2007) 34:57–63. doi: 10.1053/j.seminoncol.2006.10.028

9. Wang KL, Wang TY, Huang YC, Lai JC, Chang TC, Yen MS. Human papillomavirus type and clinical manifestation in seven cases of large-cell neuroendocrine cervical carcinoma. *J Formos Med Assoc* (2009) 108:428–32. doi: 10.1016/S0929-6646(09)60088-7

10. Albores-Saavedra J, Gersell D, Gilks CB, Henson DE, Lindberg G, Santiago H, et al. Terminology of endocrine tumors of the uterine cervix: Results of a workshop sponsored by the college of American pathologists and the national cancer institute. *Arch Pathol Lab Med* (1997) 121:34–9.

11. Embry JR, Kelly MG, Post MD, Spillman MA. Large Cell neuroendocrine carcinoma of the cervix: Prognostic factors and survival advantage with platinum chemotherapy. *Gynecol Oncol* (2011) 120:444–8. doi: 10.1016/j.ygyno.2010.11.007

12. Burkeen G, Chauhan A, Agrawal R, Raiker R, Kolesar J, Anthony L, et al. Gynecologic large cell neuroendocrine carcinoma: A review. *Rare Tumors* (2020) 12:2036361320968401. doi: 10.1177/2036361320968401

13. Lee E, Ji YI. Large Cell neuroendocrine carcinoma of the cervix with sequential metastasis to different sites: A case report. *Case Rep Oncol* (2018) 11:665–70. doi: 10.1159/000493912

14. Habeeb A, Habeeb H. Large Cell neuroendocrine carcinoma of the uterine cervix. *BMJ Case Rep* (2019) 12:bcr–2018. doi: 10.1136/bcr-2018-225880

15. Shahabi S, Pellicciotta I, Hou J, Graceffa S, Huang GS, Samuelson RN, et al. Clinical utility of chromogranin a and octreotide in large cell neuro endocrine carcinoma of the uterine corpus. *Rare Tumors* (2011) 3:e41. doi: 10.4081/rt.2011.e41

16. Kajiwara H, Hirabayashi K, Miyazawa M, Nakamura N, Hirasawa T, Muramatsu T, et al. Immunohistochemical expression of somatostatin type 2A receptor in neuroendocrine carcinoma of uterine cervix. *Arch Gynecol Obstet* (2009) 279:521–5. doi: 10.1007/s00404-008-0760-y

17. Hooker N, Mohanan S, Burks RT. A rare presentation of stage IV large cell neuroendocrine carcinoma of the cervix with metastasis to the cranium. *Case Rep Obstet Gynecol* (2018) 2018:2812306. doi: 10.1155/2018/2812306

18. Ono K, Yokota NR, Yoshioka E, Noguchi A, Washimi K, Kawachi K, et al. Metastatic large cell neuroendocrine carcinoma of the lung arising from the uterus: A pitfall in lung cancer diagnosis. *Pathol Res Pract* (2016) 212:654–7. doi: 10.1016/j.prp.2016.03.009

19. Nagao S, Miwa M, Maeda N, Kogiku A, Yamamoto K, Morimoto A, et al. Clinical features of neuroendocrine carcinoma of the uterine cervix: A single-institution retrospective review. *Int J Gynecol Cancer* (2015) 25:1300–5. doi: 10.1097/IGC.0000000000000495

20. Sato Y, Shimamoto T, Amada S, Asada Y, Hayashi T. Large Cell neuroendocrine carcinoma of the uterine cervix: A clinicopathological study of six cases. *Int J Gynecol Pathol* (2003) 22:226–30. doi: 10.1097/01.PGP.0000071046.12278.D1

21. Tempfer CB, Tischoff I, Dogan A, Hilal Z, Schultheis B, Kern P, et al. Neuroendocrine carcinoma of the cervix: A systematic review of the literature. *BMC Cancer* (2018) 18:530. doi: 10.1186/s12885-018-4447-x

22. Sharabi A, Kim SS, Kato S, Sanders PD, Patel SP, Sanghvi P, et al. Exceptional response to nivolumab and stereotactic body radiation therapy (SBRT) in neuroendocrine cervical carcinoma with high tumor mutational burden: Management considerations from the center for personalized cancer therapy at UC San Diego moores cancer center. *Oncologist* (2017) 22:631–7. doi: 10.1634/theoncologist.2016-0517

23. Lyons YA, Frumovitz M, Soliman PT. Response to MEK inhibitor in small cell neuroendocrine carcinoma of the cervix with a KRAS mutation. *Gynecol Oncol Rep* (2014) 10:28–9. doi: 10.1016/j.gore.2014.09.003

24. Carroll MR, Ramalingam P, Salvo G, Fujimoto J, Solis Soto LM, Phoolcharoen N, et al. Evaluation of PARP and PDL-1 as potential therapeutic targets for women with high-grade neuroendocrine carcinomas of the cervix. *Int J Gynecol Cancer* (2020) 30:1303–7. doi: 10.1136/ijgc-2020-001649

25. Yang X, Chen J, Dong R. Pathological features, clinical presentations and prognostic factors of ovarian large cell neuroendocrine carcinoma: A case report and review of published literature. *J Ovarian Res* (2019) 12:69. doi: 10.1186/s13048-019-0543-z

26. Oshita T, Yamazaki T, Akimoto Y, Tanimoto H, Nagai N, Mitao M, et al. Clinical features of ovarian large-cell neuroendocrine carcinoma: Four case reports and review of the literature. *Exp Ther Med* (2011) 2:1083–90. doi: 10.3892/etm.2011.325

27. Lin CH, Lin YC, Yu MH, Su HY. Primary pure large cell neuroendocrine carcinoma of the ovary. *Taiwan J Obstet Gynecol* (2014) 53:413–6. doi: 10.1016/j.tjog.2013.06.017

28. Ki EY, Park JS, Lee KH, Bae SN, Hur SY. Large Cell neuroendocrine carcinoma of the ovary: A case report and a brief review of the literature. *World J Surg Oncol* (2014) 12:314. doi: 10.1186/1477-7819-12-314

29. Shakuntala PN, Uma Devi K, Shobha K, Bafna UD, Geetashree M. Pure large cell neuroendocrine carcinoma of ovary: A rare clinical entity and review of literature. *Case Rep Oncol Med* (2012) 2012:120727. doi: 10.1155/2012/120727

30. Nguyen ML, Han L, Minors AM, Bentley-Hibbert S, Pradhan TS, Pua TL, et al. Rare large cell neuroendocrine tumor of the endometrium: A case report and review of the literature. *Int J Surg Case Rep* (2013) 4:651–5. doi: 10.1016/j.ijscr.2013.04.027

31. Matsumoto H, Shimokawa M, Nasu K, Shikama A, Shiozaki T, Futagami M, et al. Clinicopathologic features, treatment, prognosis and prognostic factors of neuroendocrine carcinoma of the endometrium: A retrospective analysis of 42 cases from the Kansai clinical oncology Group/Intergroup study in Japan. *J Gynecol Oncol* (2019) 30:e103. doi: 10.3802/jgo.2019.30.e103

32. Tu YA, Chen YL, Lin MC, Chen CA, Cheng WF. Large Cell neuroendocrine carcinoma of the endometrium: A case report and literature review. *Taiwan J Obstet Gynecol* (2018) 57:144–9. doi: 10.1016/j.tjog.2017.12.025

33. Suh DS, Kwon BS, Hwang SY, Lee NK, Choi KU, Song YJ, et al. Large Cell neuroendocrine carcinoma arising from uterine endometrium with rapidly progressive course: Report of a case and review of literature. *Int J Clin Exp Pathol* (2019) 12:1412–7.

34. Matsumoto H, Nasu K, Kai K, Nishida M, Narahara H, Nishida H. Combined large-cell neuroendocrine carcinoma and endometrioid adenocarcinoma of the endometrium: A case report and survey of related literature. *J Obstet Gynaecol Res* (2016) 42(2):206–10. doi: 10.1111/jog.12881

35. Shepherd FA, Evans WK, MacCormick R, Feld R, Yau JC. Cyclophosphamide, doxorubicin, and vincristine in etoposide- and cisplatin-resistant small cell lung cancer. *Cancer Treat Rep* (1987) 71:941–4.

36. Makihara N, Maeda T, Nishimura M, Deguchi M, Sonoyama A, Nakabayashi K, et al. Large Cell neuroendocrine carcinoma originating from the uterine endometrium: A report on magnetic resonance features of 2 cases with very rare and aggressive tumor. *Rare Tumors* (2012) 4:e37. doi: 10.4081/rt.2012.e37

37. O'Brien ME, Ciuleanu TE, Tsekov H, Shparyk Y, Cuceviá B, Juhasz G, et al. Phase III trial comparing supportive care alone with supportive care with oral topotecan in patients with relapsed small-cell lung cancer. *J Clin Oncol* (2006) 24:5441–7. doi: 10.1200/JCO.2006.06.5821

38. Pocrnich CE, Ramalingam P, Euscher ED, Malpica A. Neuroendocrine carcinoma of the endometrium: A clinicopathologic study of 25 cases. *Am J Surg Pathol* (2016) 40:577–86. doi: 10.1097/PAS.0000000000000633

frontiers | Frontiers in Oncology

TYPE Original Research
PUBLISHED 05 December 2022
DOI 10.3389/fonc.2022.978123

OPEN ACCESS

EDITED BY
Federica Perelli,
Santa Maria Annunziata Hospital, Italy

REVIEWED BY
Zezhong Ye,
Harvard Medical School, United States
Filippo Ferrari,
University of Verona, Italy
Yong Lu,
Shanghai Jiao Tong University, China

*CORRESPONDENCE
Xiaoli Song
sharp80501@126.com

†These authors have contributed equally to this work

SPECIALTY SECTION
This article was submitted to Gynecological Oncology, a section of the journal Frontiers in Oncology

RECEIVED 25 June 2022
ACCEPTED 16 November 2022
PUBLISHED 05 December 2022

CITATION
Xu Y, Luo H-J, Ren J, Guo L-m, Niu J and Song X (2022) Diffusion-weighted imaging-based radiomics in epithelial ovarian tumors: Assessment of histologic subtype.
Front. Oncol. 12:978123.
doi: 10.3389/fonc.2022.978123

Diffusion-weighted imaging-based radiomics in epithelial ovarian tumors: Assessment of histologic subtype

Yi Xu[1†], Hong-Jian Luo[2†], Jialiang Ren[3], Li-mei Guo[1], Jinliang Niu[1] and Xiaoli Song[1*]

[1]Department of Radiology, Second Hospital of Shanxi Medical University, Taiyuan, Shanxi, China, [2]Department of Radiology, The Third Affiliated Hospital of Zunyi Medical University (The First People's Hospital of Zunyi), Zunyi, Guizhou, China, [3]GE Healthcare, Beijing, China

Background: Epithelial ovarian tumors (EOTs) are a group of heterogeneous neoplasms. It is importance to preoperatively differentiate the histologic subtypes of EOTs. Our study aims to investigate the potential of radiomics signatures based on diffusion-weighted imaging (DWI) and apparent diffusion coefficient (ADC) maps for categorizing EOTs.

Methods: This retrospectively enrolled 146 EOTs patients [34 with borderline EOT(BEOT), 30 with type I and 82 with type II epithelial ovarian cancer (EOC)]. A total of 390 radiomics features were extracted from DWI and ADC maps. Subsequently, the LASSO algorithm was used to reduce the feature dimensions. A radiomics signature was established using multivariable logistic regression method with 3-fold cross-validation and repeated 50 times. Patients with bilateral lesions were included in the validation cohort and a heuristic selection method was established to select the tumor with maximum probability for final consideration. A nomogram incorporating the radiomics signature and clinical characteristics was also developed. Receiver operator characteristic, decision curve analysis (DCA), and net reclassification index (NRI) were applied to compare the diagnostic performance and clinical net benefit of predictive model.

Results: For distinguishing BEOT from EOC, the radiomics signature and nomogram showed more favorable discrimination than the clinical model (0.915 vs. 0.852 and 0.954 vs. 0.852, respectively) in the training cohort. In classifying early-stage type I and type II EOC, the radiomics signature exhibited superior diagnostic performance over the clinical model (AUC

0.905 vs. 0.735). The diagnostic efficacy of the nomogram was the same as that of the radiomics model with NRI value of -0.1591 (P = 0.7268). DCA also showed that the radiomics model and combined model had higher net benefits than the clinical model.

Conclusion: Radiomics analysis based on DWI, and ADC maps serve as an effective quantitative approach to categorize EOTs.

KEYWORDS

epithelial ovarian tumors, diffusion weighted imaging, apparent diffusion coefficient, radiomics, nomogram

Introduction

Epithelial ovarian tumors (EOTs) are a group of heterogeneous neoplasms and are subdivided into three subtypes: benign, borderline, and malignant tumors (1–3). The importance of the preoperative differentiation of these subtypes has been gradually recognized due to their differences in lifestyle and genetic risk factors, patterns of spread, responses to chemotherapy, and prognoses. Borderline epithelial ovarian tumor (BEOT) with low malignant potential constitute a special histological type of EOT. Due to the younger age of onset, fertility-sparing surgery is a very important topic for consideration in BEOT patients (4, 5). In addition, adjuvant chemotherapy or radiotherapy is not recommended even in patients with advanced BEOT (6, 7). Differing from BEOT, epithelial ovarian cancer (EOC) accounts for the highest tumor-related mortality among women diagnosed with gynecological malignancy (2, 8). The dualistic model further classifies EOC into type I and type II, referring to the pathways of tumorigenesis (9, 10). Type I EOC develops in a stepwise fashion from well-established precursor lesions and has a good prognosis but low responsiveness to standard treatments such as platinum chemotherapy and hormonal treatments due to *KRAS* and *BRAF* mutations and high expression levels of c-Fos (11, 12). In contrast, type II EOC tends to present in advanced stages and has poorer outcomes. The reliable early identification of these subtypes contributes to the rational choice of treatment strategies and prognosis prediction (13).

Magnetic resonance imaging (MRI) is now widely applied in assessment of adnexal masses. As a functional imaging technique, diffusion weighted imaging (DWI) and the corresponding apparent diffusion coefficient (ADC) maps hold promise as additional tools for differentiating between the benign and malignant conditions of a particular disease and monitoring the course of therapy (14, 15). Previous studies have shown great capability of DWI sequences with ADC map for categorizing ovarian tumors (16, 17). However, no consensus has been reached regarding ADC measurements for the characterization of ovarian tumors. Radiomics has recently emerged as a powerful approach for non-invasively capturing the inter-lesion heterogeneity that can be used to build an objective and accurate decision support systems for cancer at low cost (18, 19). Innumerable quantitative features extracted using high-dimensional data from DWI and ADC map could reflect the underlying pathophysiology of tissue (20, 21). Previous studies have demonstrated the usefulness of histograms analysis based on ADC for the differential diagnosis of ovarian cancer (22, 23). Compared to the first-order features, the higher-order statistical features in DWI and ADC maps could better describe the diffusion pattern and heterogeneous distribution of tumor tissues. The present investigation used imaging features based on DWI and ADC maps to quantitatively characterize the properties of complex adnexal masses with the goal of improving the capability of diagnosing subtypes of EOT and providing guidance for clinicians to design specialized treatment plans. The complex ovarian masses often present cystic-solid characteristics. Most radiomics studies in EOTs have delineated regions of interest (ROIs) that cover all voxels, including hemorrhagic, necrotic, and cystic areas within the tumor (24, 25). The cystic components were relatively homogeneous when compare with the solid components. Thus, the ADC differences of the solid components might be compromised by a larger proportion of cystic components in the whole tumor (26). Therefore, whole-tumor ROI analysis with a prior ROI focused on the solid components of the lesion was conducted.

In the present study, a radiomics signature based on DWI and ADC maps was developed preoperatively to noninvasively classify EOTs into subtypes. Moreover, a comprehensive nomogram that incorporated the radiomics signature and clinical characteristics was established for the preoperative subtype differentiation of EOTs.

Material and methods

Patients

A total of 146 patients with surgically confirmed BEOT or EOC who underwent preoperative magnetic resonance imaging (MRI) examination between March 2016 and January 2021 were included. The exclusion criteria were as follows: (1) patients who received preoperative treatment; (2) MRI performed more than 1 month before surgery; and (3) poor image quality or maximum diameter of lesions < 1 cm.

Clinical data, including age, menopausal status, and CA-125 level, were obtained from the medical records. Two radiologists (with 4 and 8 years of experience in MRI interpretation) without knowledge of the clinical and histologic information evaluated the MRI data, and discrepancies were resolved by consensus. Information on tumor configuration, pelvic fluid, and peritoneal involvement were obtained. Tumor configuration was characterized as mainly cystic, mixed cystic-solid, and mainly solid. The institutional ethics committee approved this retrospective study and the informed consents were waived.

MRI acquisition and tumor segmentation

MRI was performed using a 3.0T MR system (GE, Discovery 750W) with a phased-array coil. The scanning parameters of axial DWI were as follows: TE 70.5 msec; TR 4000 ms; FOV 34 cm; slice thickness (mm)/gap (mm) 5/1; flip angle 90; acquisition matrix 128 × 128; and b value 0 and 1000 s/mm^2. The DWI sequence images were transferred to the workstation, and ADC maps were automatically calculated by a commercially available software package (Functool, GE Medical Systems). More details of MR image acquisition are provided in Appendices A. ROIs were manually segmented along the lesion on the largest slice using ITK-SNAP software (version 3.8.0, www.itksnap.org). Two different ROIs were positioned on the slice (Figure 1): (a) an ROI encompassing the whole tumor area; and (b) an ROI encompassing the solid part of the tumor area while avoiding hemorrhagic, necrotic, or cystic regions on the axial DWI images (b value of 1000 s/mm^2) by referring to the T2-weighted images. ROIs were copied to the ADC map automatically.

Feature extraction and selection

Before radiomics feature extraction, several preprocessing techniques were applied to standardized images to improve texture recognition. Radiomics features were extracted from ROI_{whole} and ROI_{solid} on DWI and ADC maps, respectively, using PyRadiomics (27). For each ROI, 9 shape features, 18 histogram features, and 75 texture features (24 gray level co-occurrence matrix (GLCM) features, 16 gray level run-length matrix (GLRLM) features, 16 gray level size-zone matrix (GLSZM) features, 14 gray level dependence matrix (GLDM) features, and 5 neighborhood gray tone difference matrix (NGTDM) features were calculated. Therefore, a total of 390 features were extracted for each lesion from both DWI and ADC maps. Detailed descriptions of the image preprocessing and feature extraction processes are provided in Appendices B.

The interobserver reproducibility was initially analyzed using 30 randomly chosen images for ROI segmentation. The Dice coefficient and Hausdorff distance were applied to estimate the similarity of ROIs. The features selection procedure included 4 steps. First, the radiomics features with poor reproducibility were removed. Second, univariate analysis was performed to select important features by using the Wilcoxon rank-sum test with a P value less than 0.05; third, the most significant predictive features were selected by using the least absolute shrinkage and selection operator (LASSO) logistic regression algorithm. Fourth, in multivariate logistic regression, backward stepwise selection was applied using a likelihood ratio test with Akaike's information criterion as the stopping rule.

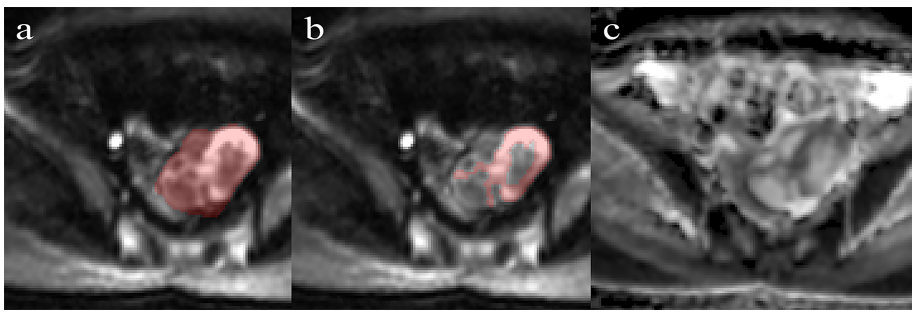

FIGURE 1
Performance of region of interest on the DWI (b = 1000 s/mm^2) by referring to T2WI. **(A)** Whole-tumor ROIs are manually drawn along the edge of the tumor on the DWI. **(B)** Solid-tumor ROIs are drawn along the solid components of the tumor. **(C)** The corresponding ADC map.

Model construction

The shape features, first-order, and high-order image features from DWI and ADC maps were selected, and their performance in the discrimination of EOTs was evaluated separately. Then, all the important radiomics features were included in stepwise multivariate logistic regression analysis to construct a radiomics signature. For each patient, a score named as the radscore, was calculated Model construction was followed by 3-fold cross-validation repeated 50 times. A clinical model based on clinical characteristics and a nomogram with the Radscore and clinical risk characteristics were also established.

Two classification tasks were assessed and shown in Figure 2: 1) BEOT vs. EOC and 2) early-stage (I-II) type I vs. type II EOC. For the classification of BEOT and EOC, patients with a single lesion were included in the training cohort, and patients with

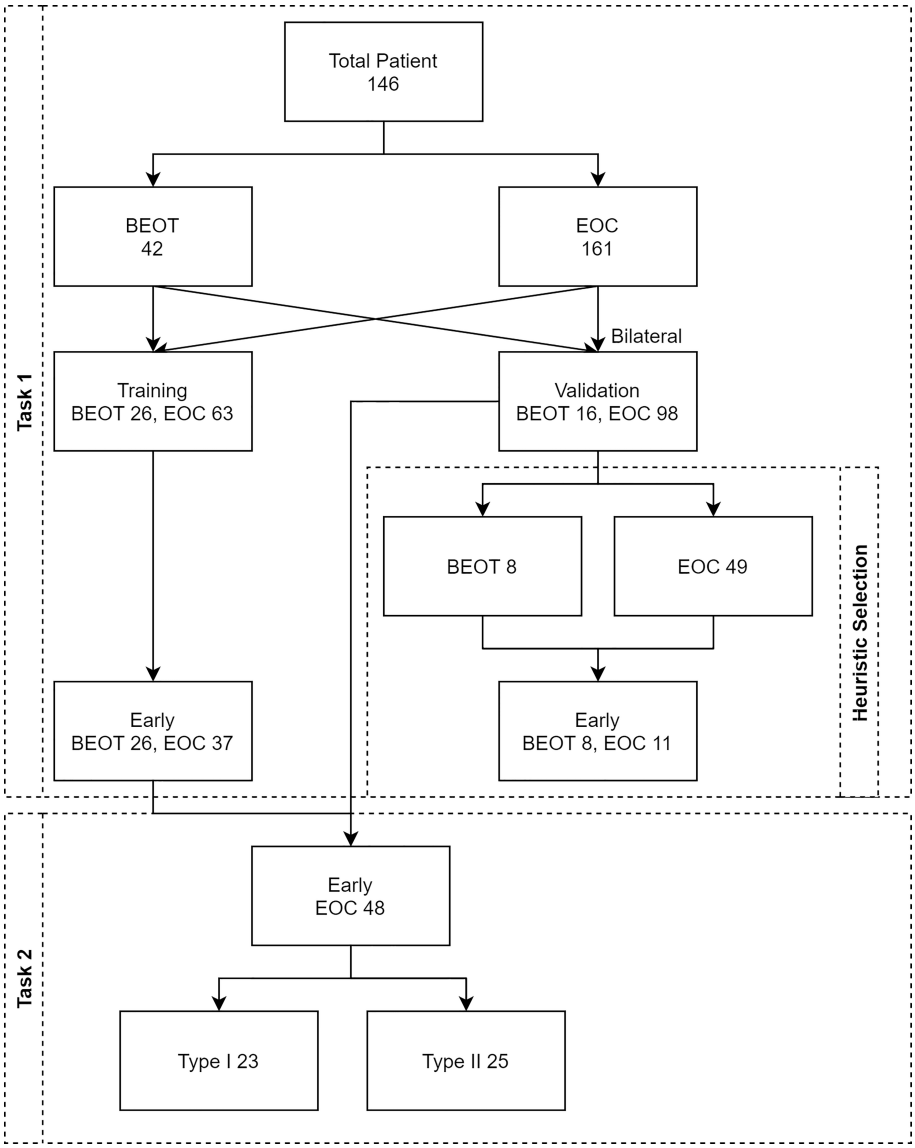

FIGURE 2
Flow diagram illustrating the two classification tasks. Task 1 was established for distinguishing BEOT from EOC, and task 2 was established from early-stage type I from II EOC. A total of 146 patients with 203 epithelial ovarian tumors, including 34 patients with 46 BEOT and 112 patients with 161 EOC.

bilateral lesions were included in the validation cohort. Three distinct strategies were applied for the validation cohort: 1) both tumors were taken as independent samples; 2) the more complex tumor based on image features identified by radiologists; and 3) computer-assisted screening was established to select the tumor with maximum probability for final consideration. In addition, the diagnostic performance in differentiating between BEOT and early-stage EOC was also assessed. For the classification of early-stage type I and type II EOCs, all single and bilateral tumors were used as independent samples because of the small sample size.

Statistical analysis

The Mann-Whitney *U* test and Pearson's chi-square test were applied to assess the differences in the clinical characteristics of the patients. The interobserver reproducibility was evaluated using intraclass correlation coefficients (ICCs), and an ICC value less than 0.75 was considered poor reproducibility. The area under the receiver operating characteristic (ROC) curve (AUC), accuracy, sensitivity, and specificity were employed to quantitatively measure the discrimination capability of all the models. The 95% CI are computed with 2000 stratified bootstrap replicates. The Hosmer–Lemeshow test was performed to quantitatively assess the calibration and agreement between the predicted and observed results of all models. The DeLong test was used to determine whether significant differences existed in terms of the AUC values among these models. Decision curve analysis (DCA) was applied to compare the net benefits of the different models at different threshold probabilities. The net reclassification index (NRI) was applied to measure the prediction increment of the radiomics signature (28). All statistical analyses were performed in R software (version 3.6.3; https://www.rproject.org). Two-tailed *p* values less than 0.05 were considered statistically significant.

Results

Patients characteristics

The patients' clinical characteristics are presented in Table 1. In terms of distinguishing BEOT from EOC, patient age, menopausal status, CA-125 level, bilaterality, MR-reported pelvic fluid, tumor configuration, and peritoneal involvement were significantly different (all $P < 0.05$), whereas no significant differences were detected in the bilaterality ($P > 0.05$). In terms of distinguishing early-stage type I and type II EOCs, patient age, CA-125 level, MR-reported pelvic fluid, tumor configuration and peritoneal involvement were significantly different (all $P < 0.05$), whereas no significant differences were detected in the menopausal status of the patients ($P > 0.05$). Then, the clinical model and radiomics nomogram were constructed by using the significant clinical characteristics.

Feature selection and performance of the radiomics signature for distinguishing BEOT from EOC

The mean Dice coefficient and Hausdorff distance were 0.810 and 6.750 for DWI and 0.935 and 9.149 for ADC, respectively. Detailed information regarding the ICCs is shown in Appendices C. Among 390 radiomics features, 2 shape features, 4 features from DWI, and 3 features from ADC were selected using the multivariate LASSO method, and the prediction performance outcomes of the shape features, DWI

TABLE 1 Patients characteristics.

	BEOT (n=34)	EOC (n=112)	*P* value	Type I EOC (n=30)	Type II EOC (n=82)	*P* value
Age (year)	38.5 (27.0;47.0)	57.0 (50.0;64.0)	< 0.001	55.0 (47.0;60.0)	58.0 (51.0;66.8)	0.047
CA125 level	18.1 (8.46;40.8)	54.2 (20.2;204)	0.001	36.0 (16.3;76.4)	94.2 (21.5;250)	0.018
Menopausal (%)	7/34 (20.6%)	74/112 (66.1%)	< 0.001	18/30 (60.0%)	56/82 (68.3%)	0.551
Early-stage (%)	34/34 (100%)	48/112 (42.9%)	–	23/30 (76.7%)	25/82(30.5%)	< 0.001
Bilaterality (%)	8/34 (23.5%)	49/112 (43.8%)	0.055	4/30 (13.3%)	45/82 (54.9%)	< 0.001
MRI reported fluid (%)	8/34 (23.5%)	68/112 (60.7%)	< 0.001	11/30 (36.7%)	57/82 (69.5%)	0.003
MRI reported peritoneal metastasis (%)	2/34(5.9%)	45/112 (40.2%)	< 0.001	3/30 (10.0%)	42/82 (51.2%)	< 0.001
MRI reported tumor configuration (%)						
Mainly cystic	28/42 (66.7%)	52/161 (32.3%)		16/34 (47.1%)	36/127 (28.3%)	
Mixed cystic-solid	5/42 (11.9%)	47/161 (29.2%)	0.001	13/34 (38.2%)	34/127 (26.8%)	0.002
Mainly solid	9/42 (21.4%)	62/161 (38.5%)		5/34 (14.7%)	57/127 (44.9%)	

BEOT, borderline epithelial ovarian tumor; EOC, epithelial ovarian cancer.

features, and ADC map features were separately evaluated, and the result are shown in Appendices D. Then, a stepwise multivariable logistic regression algorithm was applied to build the radiomics signature by using the selected features. Finally, 3 features, namely, ADC_solid_glszm_LowGrayLevelZone Emphasis, ADC_solid_glcm_lmc1, and ADC_solid_Skewness, were included in the radiomics signature. The distribution of features is shown in Appendices E. Rad-score, menopausal status, and CA-125 level were identified as independent factors for discriminating between BEOT and EOC.

Compared with the clinical model, the radiomics signature and nomogram showed better performance for distinguishing BEOT from EOC in the training cohort (0.915 vs. 0.852, P = 0.21; 0.954 vs. 0.852, P = 0.01) and in the validation cohort (0.974 vs. 0.736, P = 0.01; 0.954 vs. 0.736, P = 0.004) by tumor. The accuracy, sensitivity, specificity, positive predictive value, negative predictive value and their 95% CI were shown in Table 2. For the validation cohort by patients, the maximum probability selection method achieved a higher diagnostic performance than the two methods mentioned above (more detailed information is shown in Appendices F). NRI with value of 0.5791 (95% CI: 0.2162 - 0.942, P = 0.00176) in comparing between maximum probability selection method and radiologist selection method. The diagnostic performance for distinguishing BEOT from EOC in the training and validation cohorts was presented by ROC curves. DCA showed that using either the radiomics signature or nomogram adds more benefit than using the clinical model. Good calibration was observed, and the Hosmer-Lemeshow test showed the goodness-of-fit of the radiomics signature (P = 0.074 and 0.663) and nomogram (P = 0.175 and 0.207) (more detailed information regarding the calibration curves and DCA are shown in Appendices G). Figure 3 illustrates the ROC curve and the nomogram for preoperatively distinguishing BEOT from EOC. In addition, the predictive performance for distinguishing BEOT from early-stage EOC was also determined. As shown in Figure 4, the radiomics signature and nomogram showed better performance than the clinical model in distinguishing BEOT from early-stage EOC in the training cohort (AUC: 0.904 vs. 0827, P = 0.23; AUC: 0.955 vs. 0.827, P = 0.013) and in the validation cohort (AUC: 0.948 vs. 0.766, P = 0.15; AUC: 0.936 vs. 0.766, P = 0.08). More detailed information regarding the results is provided in Appendices H.

Feature selection and performance of the radiomics signature for distinguishing early-stage type I from II EOC

Among 390 radiomics features, 10 potential features were selected using the LASSO method. The selected features were then applied to build the radiomics signature by using a stepwise multivariable logistic regression algorithm. Finally, 4 radiomics features (whole_MinorAxisLength, DWI_whole_glrlm_GrayLevelVariance, DWI_solid_gldm_ LargeDependence HighGrayLevelEmphasis, and ADC_whole_glrlm_ ShortRunLow GrayLevelEmphasis) were identified for inclusion in the radiomics signature. The distribution of features is shown in Appendices I. Table 3 summarizes the diagnostic performance of the clinical model, radiomics signature, and nomogram. The radiomics signature showed favorable discrimination, with an AUC of 0.905 with accuracy, sensitivity, and specificity of 88.1%, 94.3% and 79.2%, respectively. Rad-score, pelvic fluid, and tumor configuration were identified as independent factors for discriminating between early-stage type I and type II EOC through univariate and multivariable analyses. The radiomics signature performed significantly better than the clinical model (0.905 vs. 0.735, P = 0.007) in distinguishing early-stage type I EOC from type II EOC. The diagnostic efficacy of the nomogram was the same as that of the radiomics model with a NRI of -0.1591 (95% CI: -1.0516 - 0.7334, P = 0.7268). Good calibration was observed, and the Hosmer-Lemeshow test showed the goodness-of-fit of the data (P = 0.062). DCA showed that using the radiomics signature adds more benefit than using the clinical model. More detailed information regarding the calibration curves and DCA are shown in Appendices J. Figure 5 shows the ROC for preoperatively classifying early-stage type I and type II EOCs.

TABLE 2 Diagnostic performance of clinical model, radiomics, and nomogram in differentiating BEOT from EOC.

	Training cohort			Validation cohort		
	Clinical model	Radiomics	Nomogram	Clinical model	Radiomics	Nomogram
AUC (95% CI)	0.852(0.776-0.928)	0.915(0.845-0.986)	0.954(0.901-1.000)	0.736(0.603-0.869)	0.974(0.937-1.000)	0.954(0.896-1.000)
Accuracy (95% CI)	0.753(0.650-0.838)	0.865(0.776-0.928)	0.921(0.845-0.968)	0.596(0.501-0.687)	0.930(0.830-0.981)	0.842(0.721-0.925)
Sensitivity (95% CI)	0.730(0.546-0.864)	0.873(0.698-0.968)	0.937(0.738-1.000)	0.571(0.342-0.778)	0.918(0.898-1.000)	0.837(0.694-1.000)
Specificity (95% CI)	0.808(0.630-0.923)	0.846(0.615-0.962)	0.885(0.731-1.000)	0.750(0.524-0.938)	1.000(0.497-1.000)	0.875(0.625-1.000)
PPV (95% CI)	0.902(0.873-0.916)	0.932(0.917-0.938)	0.952(0.939-0.955)	0.933(0.894-0.950)	1.000(1.000-1.000)	0.976(0.971-0.980)
NPV (95% CI)	0.553(0.491-0.585)	0.733(0.667-0.758)	0.852(0.826-0.867)	0.222(0.167-0.263)	0.667(0.498-0.667)	0.467(0.385-0.500)

BEOT, borderline epithelial ovarian tumor; EOC, epithelial ovarian cancer; AUC, area under curve; PPV, positive predictive value; NPV, negative predictive value; 95% CI, 95% confidence interval.

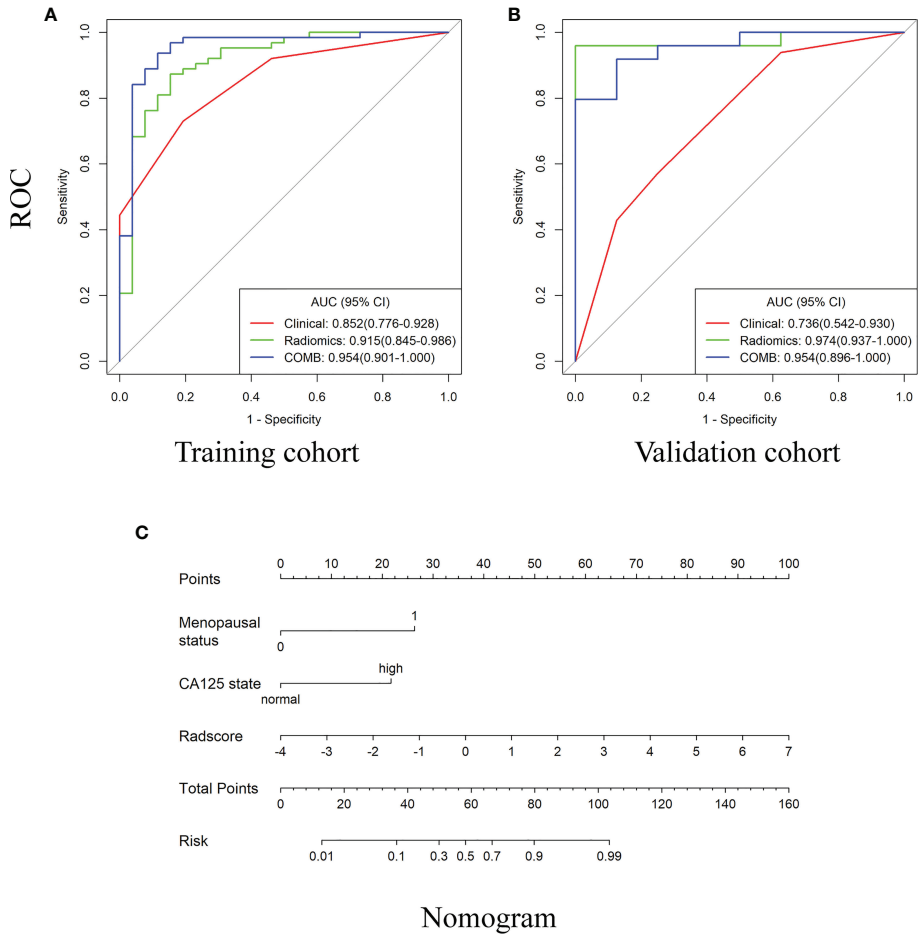

FIGURE 3
The receiver operating characteristic (ROC) curves and the nomogram for preoperatively distinguishing borderline epithelial ovarian tumor from epithelial ovarian cancer. **(A–B)** The ROC curves of clinical, radiomics and nomogram in training and validations cohorts. **(C)** The DWI-based radiomics nomogram.

Discussion

EOTs are a group of tumors consisting of dissimilar cell types with different biological behaviors. Subtype differentiation is beneficial for the individualized treatment of EOTs because of the different disease courses. BEOT is characterized by mild nuclear atypia and a lack of stromal invasion, whereas EOC is characterized by high cellularity and abundant stromal invasion. According to the concept of radiomics, these differences could be reflected by quantitative analysis and radiomics methods. Our results demonstrated that the radiomics signature and the nomogram showed higher performance than the clinical model in differentiating BEOT and EOC and in classifying type I and type II EOCs. In addition, the maximum probability selection method achieved excellent diagnostic performance for distinguishing BEOT from EOC. Therefore,

TABLE 3 Diagnostic performance of clinical model, radiomics, and nomogram in classification between early-stage type I and II EOC.

	AUC (95% CI)	Accuracy (95% CI)	Sensitivity (95% CI)	Specificity (95% CI)	PPV (95% CI)	NPV (95% CI)
Clinical model	0.735(0.615-0.854)	0.712(0.579-0.822)	0.743(0.486-0.873)	0.667(0.375-0.834)	0.765(0.680-0.793)	0.640(0.500-0.690)
Radiomics	0.905(0.818-0.991)	0.881(0.771-0.951)	0.943(0.457-1.000)	0.792(0.542-0.958)	0.868(0.762-0.875)	0.905(0.867-0.920)
Nomogram	0.905(0.818-0.991)	0.881(0.771-0.951)	0.943(0.485-1.000)	0.792(0.500-0.958)	0.868(0.772-0.875)	0.905(0.857-0.920)

EOC, epithelial ovarian cancer; AUC, area under curve; PPV, positive predictive value; NPV, negative predictive value; 95% CI, 95% confidence interval.

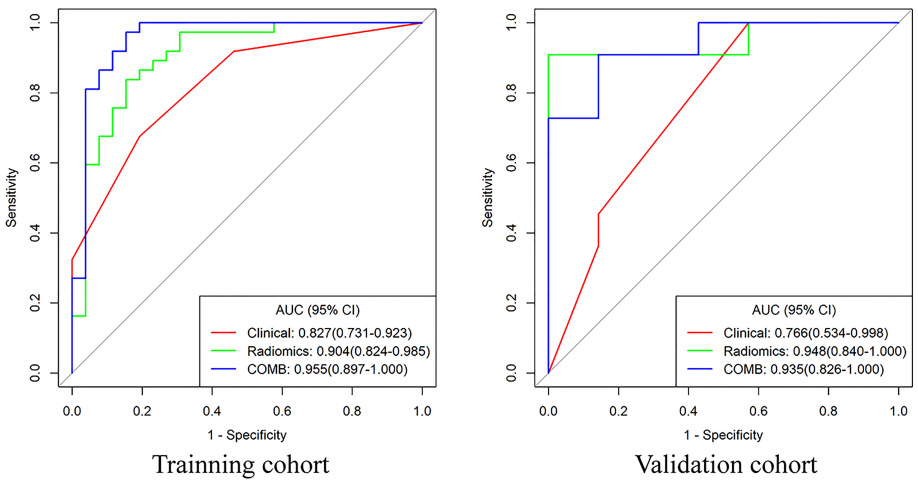

FIGURE 4
The receiver operating characteristic curves of clinical model, radiomics and nomogram for distinguishing BEOT from early-stage EOC.

radiomics signatures derived from DWI and ADC maps may be powerful noninvasive imaging biomarkers for the subtype differentiation of EOTs.

Morphological changes in EOT can be observed by conventional ultrasound and MRI examination. However, it remains a challenge for differentiation diagnosis of EOT due to morphological complexity and overlap.The Assessment of Different NEoplasias in the adneXa model and Ovarian-Adnexal Reporting and Data System based on ultrasound appearances achieved good performance for the discrimination between benign and malignant adnexal tumor, but depending on an experienced examiner and high-end ultrasound equipment (29). The reproducible and noninvasive nature of radiomics provides clinician with a favorable approach to predict clinicopathological variables. Theoretically, radiomics features morphological and features decode subtype of EOTs differently. Several radiomics

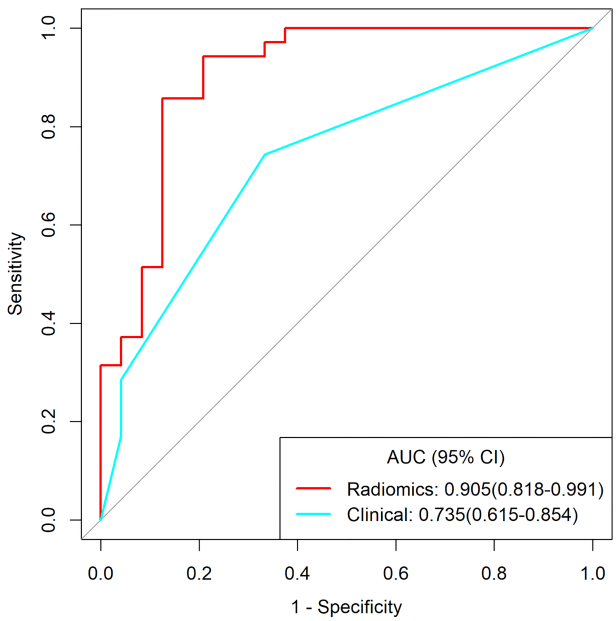

FIGURE 5
The receiver operating characteristic curves of clinical model and radiomics for distinguishing early-stage type I and type II EOC.

studies based on DWI have been established for ovarian cancer classification and histological grade evaluation. Mimura et al. (28) found that the 10th percentile of ADC values had the highest AUC for differentiating borderline ovarian tumors from malignant ovarian tumors. Li et al. (22) studied the potential of histogram features in the ADC map for grading serous ovarian carcinoma. Their results showed that all ADC histogram features except kurtosis are effective in distinguishing high-grade serous ovarian carcinoma from low-grade serous ovarian carcinoma. In contrast to previous studies that focused on histogram features, we extracted a large number of quantitative and minable imaging features to find more valuable information related to the subtype differentiation of EOTs. Our results showed that the features of Skewness, GLCM_lmc1 and GLSZM_LowGrayLevel ZoneEmphasis were the key features for categorizing EOTs. The skewness features revealed that malignant EOT exhibited greater asymmetry with respect to value distributions about the mean as compared with borderline EOT. The high-order features of GLCM and GLSZM could quantify the spatial relationships and interactions between pixel intensities to capture the distinctive intratumour heterogeneity and subtle alterations in subtypes of EOTs. Our results demonstrated that radiomics presents a clinically applicable and cost-effective decision-making tool for personalized medicine in EOTs. The radiomics signature and nomogram showed better performance than the clinical model in discriminating BEOT from EOC, indicating that radiomics may help improve the diagnostic accuracy before invasive procedures. For patients with bilateral tumors, maximum probability selection was established and achieved excellent diagnostic performance for distinguishing BEOT from EOC. It is worth noting that the radiomics signature performed better than the nomogram, but without a significant difference. This discrepancy, however, may be due to the instability of clinical characteristics. In clinical practice, it is more difficult to distinguish between BEOT and early-stage EOC with limited tumor spread because advanced EOC tends to show more aggressive characteristics, such as peritoneal involvement, distant metastases, and ascites. Therefore, a subtask of distinguishing between BEOT and early-stage EOC was also performed and achieved a high overall classification performance, with an AUC value of 0.904 in the training cohort.

A dualistic model classifies EOC into two broad categories designated type I and type II based on the pathogenesis and origin. Zhang et al. (25) reported that radiomics features extracted from MRI yielded excellent performance in classifying type I and type II ovarian cancers. However, only intensity information in the ADC map was analyzed. Jian et al. (24) constructed a multiparametric MRI model for differentiating between type I and type II EOC. Although some algorithms have been proposed for the classification of type I and type II EOC, clinical characteristics were not incorporated. In this study, a radiomics signature achieved better performance than the clinical model in discriminating early-stage type I EOC from type II EOC. However, the nomogram comprising radiomics features and clinical characteristics showed same diagnostic efficacy as the radiomics with NRI value of -0.1591. These results indicate that clinical factors have little effect on the nomogram for distinguishing the early-stage type I EOC from type II EOC and the radiomics features could be an effective quantitative approach to categorize EOTs. Radiomics provides a more objective and accurate way for gynecologists to develop a customized process to maximize the success of preventive and therapeutic interventions with minimum side effects in patients with EOT.

In addition, the ROI methods have varied between ovarian radiomics studies and have not achieved consensus. The accuracy of EOT classification often depends on the feature expression of the ROI. As a complex mass comprising solid and cystic components, the features from the whole tumor or the solid components alone may not be sufficiently accurate to distinguish the subtypes of EOTs. In this study, whole-tumor ROI analysis with a prior ROI focused on the solid components of ovarian lesions was performed. The present results demonstrate that ROIs reflect the different characteristics of tumors, and their combination can more comprehensively reflect the internal heterogeneity of ovarian tumors.

Several limitations should be noted. First, for a radiomics study, the sample size of a single center, such as ours, is arguably somewhat small. A multicenter, large-scale trial should be performed to validate our preliminary results. Second, lesion segmentation was manually outlined on a single slice. Undoubtedly, volumetric tumor delineation could provide a more comprehensive evaluation of the underlying spatial heterogeneity, but the analysis is time-consuming for clinical application. A two-dimensional analysis may be more highly recommended for clinical application (30). More studies are warranted to explore the optimal tumor segmentation approach for clinical application. Finally, the ADC values used in this study were derived from a monoexponential diffusion model, and features of other parameter maps derived from DWI images using the biexponential or stretched-exponential diffusion mode will be considered in our future work for ovarian tumors.

In this present study, imaging features were extracted from DWI scans of ovarian tumors. The results demonstrated that the subtype of EOTs could be predicted based on imaging features from DWI and the nomogram. Future studies with larger sample sizes and more radiomic features should be conducted to refine our findings.

Data availability statement

The original contributions presented in the study are included in the article/Supplementary Material. Further inquiries can be directed to the corresponding authors.

Ethics statement

The studies involving human participants were reviewed and approved by The institutional ethics committee of the Shanxi Medical University Second Hospital. Written informed consent for participation was not required for this study in accordance with the national legislation and the institutional requirements.

Author contributions

YX: methodology, resources, and data curation. H-JL: methodology, conceptualization, and investigation. L-MG: conceptualization and supervision. YX and H-JL: writing - original draft and data curation. JR: resources and data curation. XS and JN: project administration, supervision, and funding acquisition. All authors contributed to the article and approved the submitted version.

Funding

This work is supported by the Applied Basic Research Programs of Shanxi Province (grant number 20210302123290).

Conflict of interest

The author, JR, was employed by GE Healthcare.

The remaining authors declare that the research was conducted in the absence of any commercial or financial relationships that could be construed as a potential conflict of interest.

Publisher's note

All claims expressed in this article are solely those of the authors and do not necessarily represent those of their affiliated organizations, or those of the publisher, the editors and the reviewers. Any product that may be evaluated in this article, or claim that may be made by its manufacturer, is not guaranteed or endorsed by the publisher.

Supplementary material

The Supplementary Material for this article can be found online at: https://www.frontiersin.org/articles/10.3389/fonc.2022.978123/full#supplementary-material

References

1. Narod S. Can advanced-stage ovarian cancer be cured? *Nat Rev Clin Oncol* (2016) 13(4):255–61. doi: 10.1038/nrclinonc.2015.224

2. Lheureux S, Gourley C, Vergote I, Oza AM. Epithelial ovarian cancer. *Lancet* (2019) 393(10177):1240–53. doi: 10.1016/s0140-6736(18)32552-2

3. Siegel RL, Miller KD, Jemal A. Cancer statistics, 2019. *CA Cancer J Clin* (2019) 69(1):7–34. doi: 10.3322/caac.21551

4. Bentivegna E, Gouy S, Maulard A, Pautier P, Leary A, Colombo N, et al. Fertility-sparing surgery in epithelial ovarian cancer: A systematic review of oncological issues. *Ann Oncol* (2016) 27(11):1994–2004. doi: 10.1093/annonc/mdw311

5. Sherman ME, Mink PJ, Curtis R, Cote TR, Brooks S, Hartge P, et al. Survival among women with borderline ovarian tumors and ovarian carcinoma: A population-based analysis. *Cancer* (2004) 100(5):1045–52. doi: 10.1002/cncr.20080

6. Gershenson DM. Management of borderline ovarian tumours. *Best Pract Res Clin Obstet Gynaecol* (2017) 41:49–59. doi: 10.1016/j.bpobgyn.2016.09.012

7. du Bois A, Trillsch F, Mahner S, Heitz F, Harter P. Management of borderline ovarian tumors. *Ann Oncol* (2016) 27(Suppl 1):i20–2. doi: 10.1093/annonc/mdw090

8. Jiang X, Tang H, Chen T. Epidemiology of gynecologic cancers in China. *J Gynecol Oncol* (2018) 29(1):e7. doi: 10.3802/jgo.2018.29.e7

9. Karnezis AN, Cho KR, Gilks CB, Pearce CL, Huntsman DG. The disparate origins of ovarian cancers: Pathogenesis and prevention strategies. *Nat Rev Cancer* (2017) 17(1):65–74. doi: 10.1038/nrc.2016.113

10. Shih Ie M, Kurman RJ. Ovarian tumorigenesis: A proposed model based on morphological and molecular genetic analysis. *Am J Pathol* (2004) 164(5):1511–8. doi: 10.1016/s0002-9440(10)63708-x

11. Meinhold-Heerlein I, Bauerschlag D, Hilpert F, Dimitrov P, Sapinoso LM, Orlowska-Volk M, et al. Molecular and prognostic distinction between serous ovarian carcinomas of varying grade and malignant potential. *Oncogene* (2005) 24 (6):1053–65. doi: 10.1038/sj.onc.1208298

12. Tothill RW, Tinker AV, George J, Brown R, Fox SB, Lade S, et al. Novel molecular subtypes of serous and endometrioid ovarian cancer linked to clinical outcome. *Clin Cancer Res* (2008) 14(16):5198–208. doi: 10.1158/1078-0432.Ccr-08-0196

13. Bamias A, Sotiropoulou M, Zagouri F, Trachana P, Sakellariou K, Kostouros E, et al. Prognostic evaluation of tumour type and other histopathological characteristics in advanced epithelial ovarian cancer, treated with surgery and paclitaxel/carboplatin chemotherapy: Cell type is the most useful prognostic factor. *Eur J Cancer* (2012) 48(10):1476–83. doi: 10.1016/j.ejca.2011.09.023

14. Messina C, Bignone R, Bruno A, Bruno A, Bruno F, Calandri M, et al. Diffusion-weighted imaging in oncology: An update. *Cancers (Basel)* (2020) 12 (6):1493. doi: 10.3390/cancers12061493

15. Wang Y, Miller FH, Chen ZE, Merrick L, Mortele KJ, Hoff FL, et al. Diffusion-weighted MR imaging of solid and cystic lesions of the pancreas. *Radiographics* (2011) 31(3):E47–64. doi: 10.1148/rg.313105174

16. Zhang G, Yao W, Sun T, Liu X, Zhang P, Jin J, et al. Magnetic resonance imaging in categorization of ovarian epithelial cancer and survival analysis with focus on apparent diffusion coefficient value: correlation with ki-67 expression and serum cancer antigen-125 level. *J Ovarian Res* (2019) 12(1):59. doi: 10.1186/s13048-019-0534-0

17. Mukuda N, Fujii S, Inoue C, Fukunaga T, Tanabe Y, Itamochi H, et al. Apparent diffusion coefficient (ADC) measurement in ovarian tumor: Effect of region-of-interest methods on ADC values and diagnostic ability. *J Magn Reson Imaging* (2016) 43(3):720–5. doi: 10.1002/jmri.25011

18. Lambin P, Leijenaar RTH, Deist TM, Peerlings J, de Jong EEC, van Timmeren J, et al. Radiomics: The bridge between medical imaging and personalized medicine. *Nat Rev Clin Oncol* (2017) 14(12):749–62. doi: 10.1038/nrclinonc.2017.141

19. Mayerhoefer ME, Materka A, Langs G, Häggström I, Szczypiński P, Gibbs P, et al. Introduction to radiomics. *J Nucl Med* (2020) 61(4):488–95. doi: 10.2967/jnumed.118.222893

20. Hu Q, Wang G, Song X, Wan J, Li M, Zhang F, et al. Machine learning based on MRI DWI radiomics features for prognostic prediction in nasopharyngeal carcinoma. *Cancers (Basel)* (2022) 14(13):3201. doi: 10.3390/cancers14133201

21. Xu S, Yao Q, Liu G, Jin D, Chen H, Xu J, et al. Combining DWI radiomics features with transurethral resection promotes the differentiation between muscle-invasive bladder cancer and non-muscle-invasive bladder cancer. *Eur Radiol* (2020) 30(3):1804–12. doi: 10.1007/s00330-019-06484-2

22. Li HM, Zhang R, Gu WY, Zhao SH, Lu N, Zhang GF, et al. Whole solid tumour volume histogram analysis of the apparent diffusion coefficient for differentiating high-grade from low-grade serous ovarian carcinoma: correlation with ki-67 proliferation status. *Clin Radiol* (2019) 74(12):918–25. doi: 10.1016/j.crad.2019.07.019

23. He M, Song Y, Li H, Lu J, Li Y, Duan S, et al. Histogram analysis comparison of monoexponential, advanced diffusion-weighted imaging, and dynamic contrast-enhanced MRI for differentiating borderline from malignant epithelial ovarian tumors. *J Magn Reson Imaging* (2020) 52(1):257–68. doi: 10.1002/jmri.27037

24. Jian J, Li Y, Pickhardt PJ, Xia W, He Z, Zhang R, et al. MR image-based radiomics to differentiate type I and type II epithelial ovarian cancers. *Eur Radiol* (2021) 31(1):403–10. doi: 10.1007/s00330-020-07091-2

25. Zhang H, Mao Y, Chen X, Wu G, Liu X, Zhang P, et al. Magnetic resonance imaging radiomics in categorizing ovarian masses and predicting clinical outcome: A preliminary study. *Eur Radiol* (2019) 29(7):3358–71. doi: 10.1007/s00330-019-06124-9

26. Lu J, Li HM, Cai SQ, Zhao SH, Ma FH, Li YA, et al. Prediction of platinum-based chemotherapy response in advanced high-grade serous ovarian cancer: ADC histogram analysis of primary tumors. *Acad Radiol* (2021) 28(3):e77–85. doi: 10.1016/j.acra.2020.01.024

27. van Griethuysen JJM, Fedorov A, Parmar C, Hosny A, Aucoin N, Narayan V, et al. Computational radiomics system to decode the radiographic phenotype. *Cancer Res* (2017) 77(21):e104–7. doi: 10.1158/0008-5472.Can-17-0339

28. Mimura R, Kato F, Tha KK, Kudo K, Konno Y, Oyama-Manabe N, et al. Comparison between borderline ovarian tumors and carcinomas using semi-automated histogram analysis of diffusion-weighted imaging: focusing on solid components. *Jpn J Radiol* (2016) 34(3):229–37. doi: 10.1007/s11604-016-0518-6

29. Moro F, Esposito R, Landolfo C, Froyman W, Timmerman D, Bourne T, et al. Ultrasound evaluation of ovarian masses and assessment of the extension of ovarian malignancy. *Br J Radiol* (2021) 94(1125):20201375. doi: 10.1259/bjr.20201375

30. Zhao H, Li W, Lyu P, Zhang X, Liu H, Liang P, et al. TCGA-TCIA-Based CT radiomics study for noninvasively predicting Epstein-Barr virus status in gastric cancer. *AJR Am J Roentgenol* (2021) 217(1):1–11. doi: 10.2214/ajr.20.23534

Frontiers in Oncology

Advances knowledge of carcinogenesis and tumor progression for better treatment and management

The third most-cited oncology journal, which highlights research in carcinogenesis and tumor progression, bridging the gap between basic research and applications to imrpove diagnosis, therapeutics and management strategies.

Discover the latest Research Topics

See more →

Frontiers

Avenue du Tribunal-Fédéral 34
1005 Lausanne, Switzerland
frontiersin.org

Contact us

+41 (0)21 510 17 00
frontiersin.org/about/contact